



12-1990

Dynamic Modeling of a Pressurized Water Reactor Plant for Diagnostics and Control

Masoud Naghedolfeizi
University of Tennessee - Knoxville

Follow this and additional works at: https://trace.tennessee.edu/utk_gradthes

 Part of the [Nuclear Engineering Commons](#)

Recommended Citation

Naghedolfeizi, Masoud, "Dynamic Modeling of a Pressurized Water Reactor Plant for Diagnostics and Control. " Master's Thesis, University of Tennessee, 1990.
https://trace.tennessee.edu/utk_gradthes/2667

This Thesis is brought to you for free and open access by the Graduate School at TRACE: Tennessee Research and Creative Exchange. It has been accepted for inclusion in Masters Theses by an authorized administrator of TRACE: Tennessee Research and Creative Exchange. For more information, please contact trace@utk.edu.

To the Graduate Council:

I am submitting herewith a thesis written by Masoud Naghedolfeizi entitled "Dynamic Modeling of a Pressurized Water Reactor Plant for Diagnostics and Control." I have examined the final electronic copy of this thesis for form and content and recommend that it be accepted in partial fulfillment of the requirements for the degree of Master of Science, with a major in Nuclear Engineering.

B. R. Upadhyaya, Major Professor

We have read this thesis and recommend its acceptance:

R. E. Uhrig, L. F. Miller

Accepted for the Council:

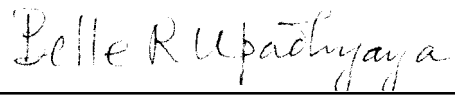
Carolyn R. Hodges

Vice Provost and Dean of the Graduate School

(Original signatures are on file with official student records.)



To the Graduate Council:

I am submitting herewith a thesis written by Masoud Naghedolfeizi entitled "Dynamic Modeling of a Pressurized Water Reactor Plant for Diagnostics and Control." I have examined the final copy of this thesis for form and content and recommend that it be accepted in partial fulfillment of the requirements for the degree of Master of Science, with a major in Nuclear Engineering.

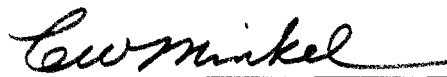


B. R. Upadhyaya, Major Professor

We have read this thesis
and recommend its acceptance:

Accepted for the Council:



Vice Provost
and Dean of The Graduate School

STATEMENT OF PERMISSION TO USE

In presenting this thesis in partial fulfillment of the requirements for a Master's degree at The University of Tennessee, Knoxville, I agree that the Library shall make it available to borrowers under rules of the Library. Brief quotations from this thesis are allowable without special permission, provided that accurate acknowledgment of the source is made.

Permission for extensive quotation from or reproduction of this thesis may be granted by my major professor, or in his absence, by the Head of Interlibrary Services when, in the opinion of either, the proposed use of the material is for scholarly purposes. Any copying or use of the material in this thesis for financial gain shall not be allowed without my written permission.

Signature Mersoudi Zeynepold Leizi

Date 11/13/1990

**DYNAMIC MODELING OF A
PRESSURIZED WATER REACTOR PLANT
FOR DIAGNOSTICS AND CONTROL**

A Thesis

Presented for the

Master of Science

Degree

The University of Tennessee, Knoxville

Masoud Naghedolfeizi

December 1990

ACKNOWLEDGMENTS

The author wishes to express his gratitude to Dr. B. R. Upadhyaya for his guidance, advice, inspiration, and valuable suggestions during the course of this study while serving as a major professor. Appreciation is also expressed to the other committee members: Dr. R. E. Uhrig and Dr. L. F. Miller for their comments and assistance.

The author also wishes to express his sincere gratitude to Dr. R. E. Uhrig and the department head Dr. T. W. Kerlin for the financial support of this research. Appreciation is also expressed to graduate students A. L. Hurst, L. J. Nugent, M. Abdelhai, and N. Hajji for their assistance.

Special thanks to my family members who offered love, encouragement, and support from far away.

ABSTRACT

A nonlinear model, based on lumped parameter approach, has been developed for computer simulation of a typical Westinghouse Pressurized Water Reactor (PWR) system. The model predicts dynamic behavior of system variables under steady-state and transient conditions. Nonlinear simulation has been applied to study the control systems of the PWR plant. This includes the design of proper actuators and control systems for reactor, steam generator, pressurizer, and turbine models. This model has also been used to identify the responses of plant variables to anomalies in the PWR subsystems at 85% power.

Linear models of the PWR primary loop components have been developed to compare linear simulation results with nonlinear simulation results. The results of this study are used to specify a region where a linear simulation can be utilized. A linear analysis has also been carried out to evaluate the performance of the reactor and steam generator models in the frequency domain.

The dynamic response characteristics derived from the overall plant model may be used to train diagnostic neural networks. This study will be useful in identifying plant variables that are sensitive to incipient anomalies in plant components.

TABLE OF CONTENTS

CHAPTER	PAGE
1. INTRODUCTION	1
1.1 Statement of the Problem and Objectives	1
1.2 Simulation Procedure	3
1.3 Simulation Software Systems	5
1.4 Review of Prior Work	6
1.5 Significance of the Proposed Work	7
1.6 Organization of the Thesis	8
2. METHODOLOGY	9
2.1 Pressurized Water Reactor (PWR) Plants	9
2.2 Modeling Procedure	12
2.2.1 Assumptions	13
2.2.2 Governing Equations	14
2.3 Linearized Models	19
2.4 Design of Control Systems	19
2.4.1 Control Block Diagram	20
2.4.2 Control Elements	21
3. MODEL DEVELOPMENT OF THE PRIMARY SIDE COM- PONENTS	24

CHAPTER	PAGE
3.1 Reactor	24
3.1.1 Reactor Model	26
3.1.2 Comparison between Linear and Nonlinear Models	31
3.1.3 Reactor Power Control System	36
3.2 Steam Generator	42
3.2.1 Steam Generator Model	45
3.2.2 Steam Generator Control System	47
3.2.3 Comparison between Linear and Nonlinear Models	50
3.3 Pressurizer System	60
3.3.1 Pressurizer Model	63
3.3.2 Pressurizer Control System	65
3.4 Reactor Coolant Pump	68
3.4.1 Model Development of the Coolant Pump	70
3.5 Summary	75
4. MODEL DEVELOPMENT OF THE SECONDARY LOOP .	77
4.1 Steam Turbine System	77
4.1.1 Turbine Model	80
4.1.2 Main Condenser	81
4.1.3 Condenser Model Development	82
4.1.4 Turbine Speed Control System	86
4.2 Balance of Plant Simulation Model	91
4.3 Summary	91

CHAPTER	PAGE
5. PRIMARY LOOP AND OVERALL SYSTEM SIMULATION	96
5.1 Primary Side Simulation Model	96
5.2 PWR Plant Simulation	102
5.3 System Anomalies	110
6. FREQUENCY-DOMAIN ANALYSIS	114
6.1 Introduction	114
6.2 Frequency-Response Analysis	116
7. CONCLUSIONS AND FUTURE WORK	120
7.1 Conclusions	120
7.2 Future Work	122
BIBLIOGRAPHY	124
APPENDICES	127
A. DESIGN PARAMETERS OF A PWR SYSTEM	128
B. U-TUBE STEAM GENERATOR MODEL FORMULATION . . .	133
C. PRESSURIZER MODEL FORMULATION	142
D. STEAM TURBINE MODEL FORMULATION	147
E. COMPUTER PROGRAMS	154
VITA	177

LIST OF TABLES

TABLE	PAGE
3.1 Reactor Model Variables	30
3.2 Design Parameters of the Reactor Control System	43
3.3 Three-Element Controller Variables	51
3.4 Design Parameters of the Three-element Controller	51
3.5 Reactor Coolant Pump Variables	76
4.1 Design Parameters of the Turbine Speed Control System	90
A.1 Reactor Design Parameters	129
A.2 Steam Generator Design Parameters	130
A.3 Pressurizer Design Parameters	131
A.4 Coolant Pump Design Parameters	131
A.5 Turbine Cycle Design Parameters	132
B.1 Steam Generator Model Variables	140
C.1 Pressurizer Model Variables.	146
D.1 Turbine Model Variables	152

LIST OF FIGURES

FIGURE	PAGE
1.1 Schematic diagram of a typical PWR system [23].	2
2.1 Schematic diagram of a Westinghouse PWR plant	10
2.2 Typical block diagram representation of a feedback control system [11].	20
3.1 Schematic diagram of a Westinghouse reactor [15].	25
3.2 Schematic diagram of the reactor model (including the primary loop piping).	27
3.3 Dynamic responses of the reactor model to 10 cents external reac- tivity.	32
3.4 Dynamic responses of the reactor model to a 10 °F step increase in the cold leg temperature (core inlet coolant).	33
3.5 Responses of the reactor linear model to 10 and 20 cents step in- creases in the external reactivity.	34
3.6 Responses of the reactor nonlinear model to 10 and 20 cents step increases in the external reactivity.	35
3.7 Schematic diagram of the Westinghouse average temperature coolant program [15].	37
3.8 Block diagram representation of the reactor control system.	38
3.9 Reactor control rod speed program [15].	41

FIGURE	PAGE
3.10 Schematic diagram of a typical Westinghouse U-tube steam generator [15].	44
3.11 Block diagram representation of the three-element controller [15].	48
3.12 Typical responses of the steam generator nonlinear model, including the three-element controller, to a 10% step increase in the steam valve coefficient.	52
3.13 Dynamic responses of the linear and nonlinear simulation models of the steam generator to a 10% step decrease in the steam valve coefficient.	54
3.14 Dynamic responses of the linear and nonlinear simulation models of the steam generator to a 15% step decrease in the steam valve coefficient.	56
3.15 Dynamic responses of the linear and nonlinear simulation models of the steam generator to a 25% step decrease in the steam valve coefficient.	58
3.16 A general view of a typical pressurizer used in Westinghouse PWR systems [15].	62
3.17 Pressurizer pressure control diagram [15].	67
3.18 Block diagram representation of pressurizer pressure control system.	67
3.19 Response of the pressurizer nonlinear model to 1 <i>lbm/sec</i> surge flow.	69
3.20 Response of the pressurizer nonlinear model to 50 <i>lbm/sec</i> surge flow.	69
3.21 Response of the pressurizer linear model to -1 <i>lbm/sec</i> surge flow.	69

FIGURE	PAGE
3.22 Reactor coolant pump characteristic curve [15].	71
3.23 Dynamic response of the reactor coolant pump to a 100% step decrease in the supplied power.	74
4.1 Flow diagram representation of a turbine cycle [6].	79
4.2 Schematic diagram of the turbine condenser model.	83
4.3 Generalized block diagram of a typical speed control system [15]. .	87
4.4 Block diagram representation of a turbine speed control system. .	88
4.5 Typical responses of the secondary loop of the PWR system to a 15% step decrease in the power demand signal.	92
5.1 Typical responses of the PWR primary side to a 15% step decrease in steam valve coefficient.	98
5.2 Typical responses of the overall PWR system to a 15% step decrease in power demand signal.	104
5.3 Typical responses of the PWR system to anomalies at 85% of the full power operating conditions of the plant.	112
6.1 Frequency responses of the reactor core linear model.	117
6.2 Frequency responses of the steam generator linear model.	118
B.1 Schematic diagram of the steam generator model [3]	139
C.1 Schematic diagram of the pressurizer model.	145

CHAPTER 1

INTRODUCTION

1.1 Statement of the Problem and Objectives

The study of dynamic behavior of complex Pressurized Water Reactor (PWR) systems is helpful in predicting the transient operating conditions of these plants. The knowledge of transient behavior is useful in application to process control and safety assessments. Since it is not practical to examine the performance of a PWR system by experiments, dynamic modeling and simulation are used as an alternative for studying the PWR system performance. These studies are also useful in identifying the process variables that are sensitive to certain malfunctions in the system and in developing diagnostic neural networks.

A typical PWR plant, illustrated in Fig. 1.1, consists of two major loops; the primary loop and the secondary loop. The primary loop includes reactor core, pressurizer, steam generator, and reactor coolant pump. This loop supplies steam as a working fluid for the secondary loop. The secondary loop often called the “Balance of Plant” (BOP), consists of turbine, moisture separators, steam reheaters, condenser, and feedwater pump and feedwater heaters. It produces useful energy by converting heat contained within the working fluid to work.

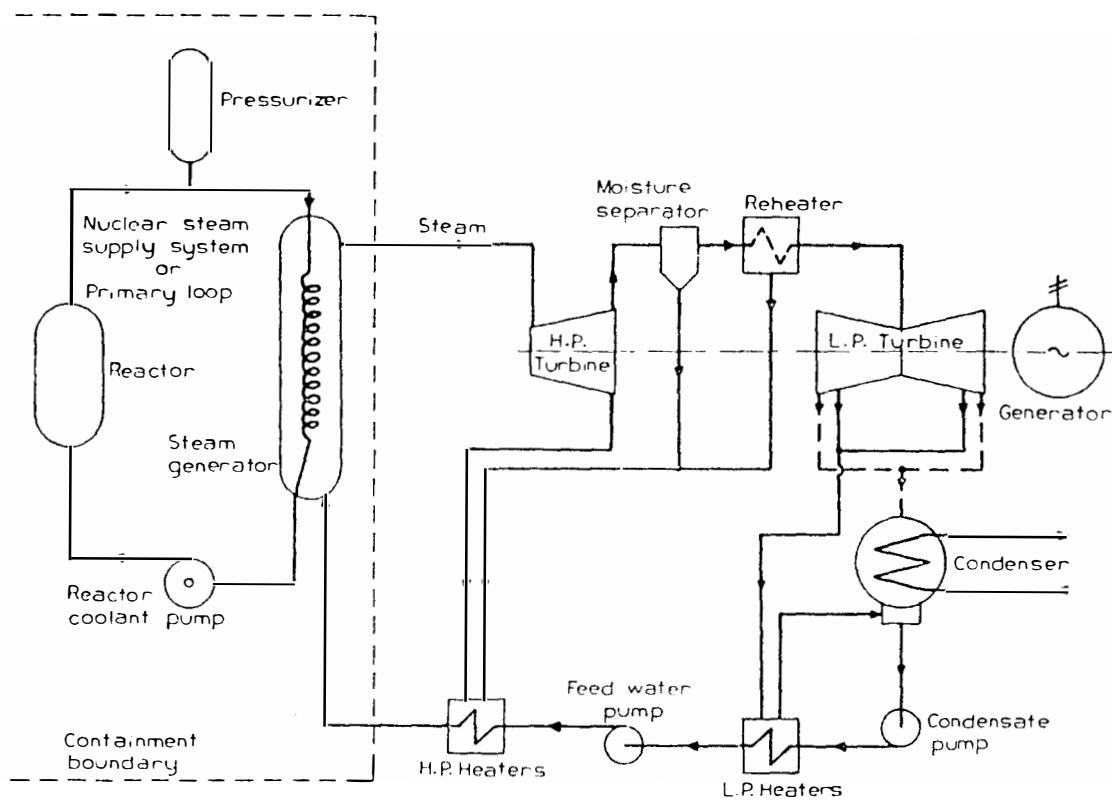


Figure 1.1: Schematic diagram of a typical PWR system [23].

Many studies of PWR simulation are available. The authors [1-6] were mainly concerned with either linear simulations of a PWR system or model development of individual subsystems (for example, primary loop, pressurizer, and steam generator). A complete nonlinear simulation of a PWR system is necessary for a realistic analysis of the system performance. Therefore, it is imperative to develop a nonlinear model of an overall PWR system which can evaluate the performance of the system under normal and abnormal conditions.

In this thesis, a complete nonlinear simulation of a typical Westinghouse PWR system, which can predict the system performance under steady-state and transient conditions of the plant, is developed. Moreover, a linear simulation of the primary side components is developed to perform both time- and frequency-domain analyses of the system. These simulations are also used to satisfy the following objectives:

- Specifying a region where a linear simulation can be utilized.
- Investigating the overall behavior and performance of the plant due to perturbations and anomalies in one or more components.
- Designing proper actuators and controllers for process control in the plant.

1.2 Simulation Procedure

The modular modeling of the plant components is used to develop a system model and perform the simulation. A lumped-parameter model is used as the basis for the modular modeling technique. The detailed model is derived from

first principles. Linear and nonlinear simulations have been applied to the study of a typical Westinghouse PWR. The dynamic models of all important components of this PWR, shown in Fig. 1.1, are developed for nonlinear analysis. Theoretical models of the components are obtained by formulating the describing differential or algebraic equations, usually derived from conservation of mass, energy, and momentum relationships. Accurate design and measurement data are used to determine the model parameters and inputs. The development of these models requires various assumptions. These assumptions and their limits of applicability are identified in the description of subsystem models.

The dynamic performance of each component is studied individually in the time domain using nonlinear simulation. The individual component models are integrated into an overall nonlinear plant simulation program. This is utilized to study the plant dynamic performance under normal and abnormal conditions. Since system nonlinearities are considered in the model, transients causing large departures from normal system operating conditions will be satisfactorily analyzed. A linear analysis is carried out for the primary loop components. The results of this analysis are compared with the results of the nonlinear simulation analysis. This comparison is valuable for specifying a region where a linear simulation can be utilized. Moreover, the linear simulation can be used for determining stability margin and evaluating the system performance in the frequency domain.

Component models are used in the simulation of the plant control systems. The overall system integrates the reactor core, steam generator, pressurizer, and turbine systems. The performance of the control systems are evaluated by study-

ing the behavior of their related systems in the time- and frequency-domains. However, Some of these control systems (pressurizer and reactor core) have piece-wise characteristic functions and can be analyzed only in the time domain.

Two different computer software systems are developed for linear and nonlinear analyses of the overall plant and its subsystems. A software system called “NSPWR” is developed for analyzing nonlinear models. This incorporates codes for the reactor core, pressurizer, steam generator, reactor coolant pump, primary side system, turbine cycle, and the complete PWR plant. NSPWR will be used both for plant diagnostic analysis and as a training simulator in the time-domain. Another package called “LSPWR” is developed for linear system modeling of the primary side components. This package is utilized for both frequency analysis of each component model under steady state and for transient time-domain analysis.

1.3 Simulation Software Systems

Two advanced computer software systems (ACSL [19] and MATRIXx [20]) have been used for developing the modeling codes. ACSL (Advanced Continuous Simulation Language) [19] software has been used for the NSPWR codes and supports many good features for the dynamic analysis of complex systems. These include integration routines, a run time executive, free form inputs, and graphical plots. It also provides a simple method of representing mathematical models on a digital computer. The MATRIXx software has been utilized for LSPWR codes and provides excellent features for time- and frequency-domain analyses of linear systems. These include standard functions, arithmetic operators, control system

functions, and graphical plots. MATRIXx solves a complex linear system and can handle and manage large systems rapidly and accurately.

These two commercial codes are available on a Vax Workstation at the University of Tennessee Nuclear Engineering Department.

1.4 Review of Prior Work

Research in modular modeling of a PWR was performed in the past for many different applications [1-6]. Freels [1] had presented a complete linear simulation of a typical PWR. He utilized the modular modeling technique to develop a model of the PWR plant incorporating reactor core, pressurizer, steam generator, piping, turbine, and feedwater flow control. Mneimneh [2] developed a nonlinear model of the primary loop of a PWR including reactor core, piping, pressurizer, and steam generator. The other authors [3-6] were primarily concerned with model development of only one of the components of a PWR system and they validated them in connection with other components in the system. The review of previous work showed that relatively little attention was given to the validation of a linear simulation in comparison with a nonlinear simulation of a PWR. The literature review also revealed that no studies were made to identify the behavior of a PWR plant due to anomalies in the plant components. Computer codes which were previously developed for analyzing a PWR system are not sufficient or practical for today's applications. These codes were written in old computer software languages which are not suitable for fast simulation and interactive analysis with graphical displays.

1.5 Significance of the Proposed Work

A complete nonlinear simulation model of a typical PWR system has been developed in this research. The study of this model is important for observing effects of nonlinear processes (for example, two-phase flow) in the dynamic behavior of a PWR system which can not be achieved by studying a linear model. The behavior of plant variables in the nonlinear model can also be identified by introducing artificial anomalies in the plant components. A linear simulation has been performed to define a linear operating range for the primary loop components, and is compared to the nonlinear simulation for the same components. This is valuable for determining the limits of applicability of linear simulation methods. Some of the subsystem models (steam generator, pressurizer, and turbine) that are developed for this work, can be applied to other areas; for example, the simulation of fossil power plant components, and for developing diagnostic neural networks. Computer codes have also been developed in a “self-contained” fashion. They have been written in advanced simulation software languages (ACSL [19] and MATRIXx [20]). They can be easily modified for new plant data or additional system development. This work can also be extended to accident and safety analyses of the plant, and for identification of plant variables which are sensitive to anomalies in components.

1.6 Organization of the Thesis

This thesis is organized in seven chapters and five appendices. Following this introductory chapter, modeling procedures and design methodology of control systems are presented in Chapter 2. A brief description of a PWR is also provided in this Chapter. Chapter 3 focuses on the development of mathematical models of the primary loop system components. It describes models of the reactor core, pressurizer, steam generator, reactor coolant pump, and their related control systems. A comparison between linear and nonlinear simulation of the reactor core and steam generator models are also discussed. Chapter 4 deals with model development of the secondary loop system. It describes models for steam turbine, steam separator, reheater, condenser, and feedwater heaters. Time response characteristics of the primary side and overall PWR plant are considered in Chapter 5. The responses of the combined PWR plant due to anomalies in the control systems or plant components are also analyzed in this chapter. Chapter 6 deals with frequency response analysis of the reactor and steam generator linear models. Concluding remarks and suggestions for future work are stated in Chapter 7. Appendix A shows typical design parameters used for this study. Mathematical models of steam generator, pressurizer, and turbine are presented in Appendices B, C, and D, respectively. Appendix E shows the overall plant computer program developed in this research project.

CHAPTER 2

METHODOLOGY

This chapter presents a brief description of a typical PWR plant (Westinghouse type) and a methodology for developing accurate models of the plant components. Moreover, it contains fundamental design procedures of the control systems employed in a typical PWR system. A detailed discussion of the PWR models and control systems are presented in Chapters 3-5.

2.1 Pressurized Water Reactor (PWR) Plants

A PWR plant basically consists of two separate main systems; primary loop and secondary loop (see Fig. 2.1).

The primary system called “the Nuclear Steam Supply System” includes a reactor core, pressurizer, and three or four loops, each having a vertical steam generator and a coolant pump. In each loop, the water is circulated through the reactor and steam generator by a large coolant pump. The high flow rate of circulating water removes fission heat generated in the reactor core. The heat is transferred to the secondary fluid in the steam generator as the coolant flows throughout the steam generator U-tubes. To prevent boiling in the core, the primary system pressure is maintained at a sufficiently high level and is controlled by a pressurizer.

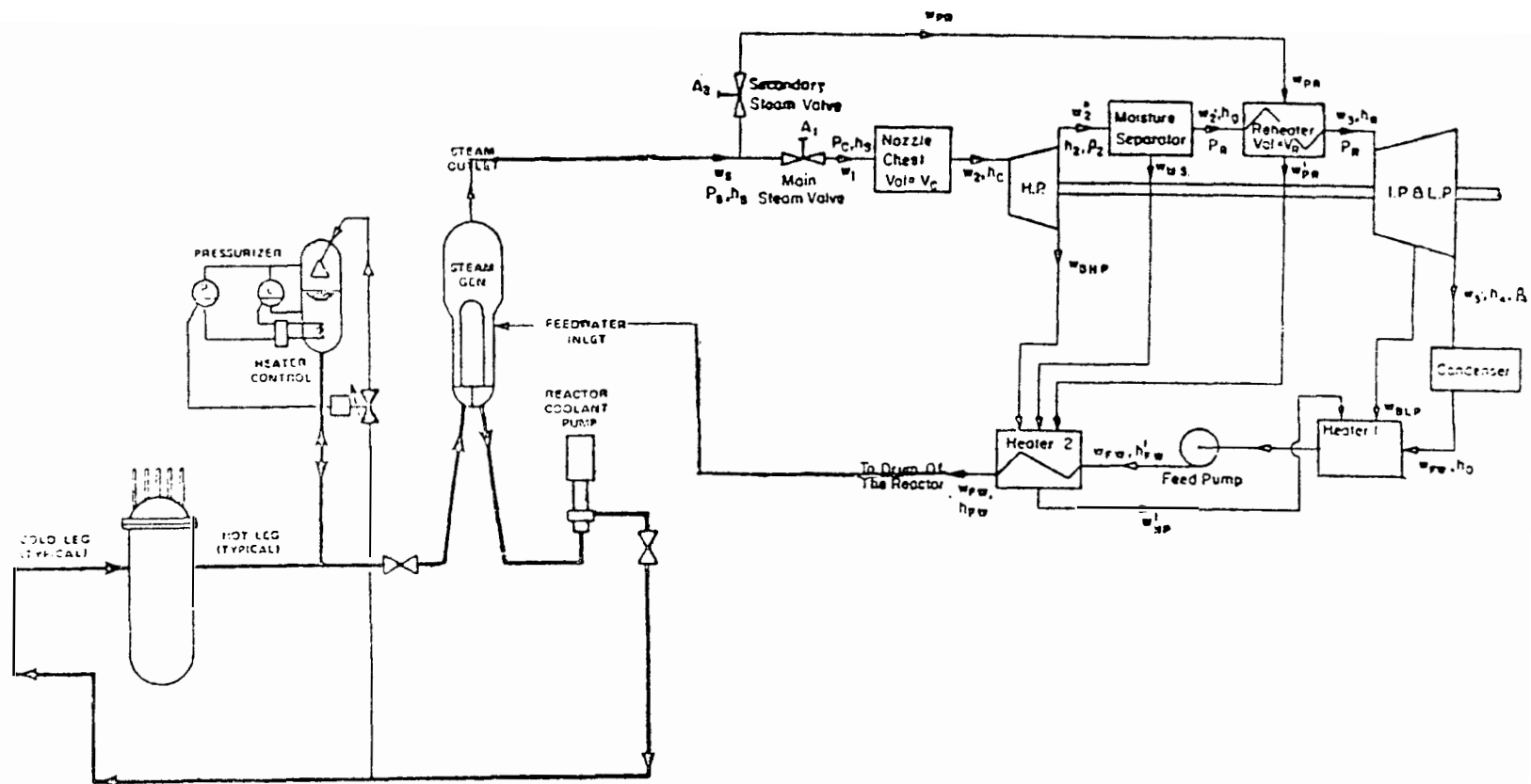


Figure 2.1: Schematic diagram of a Westinghouse PWR plant

The secondary system frequently called “the Balance of Plant ” includes a turbine, main condenser, feedwater pumps, and feedwater heaters. The high pressure and temperature steam leaving the steam generator is delivered to the turbine nozzles. The steam expands in the high and low pressure turbine stages and in doing so, produces useful work. During the expansion from one stage to the other, a moisture separator device removes water from the steam and transfers it to a high pressure feedwater heater. Then, the steam is superheated in a reheater device before it enters the low pressure turbine. The low pressure steam leaves the turbine and enters the main condenser where the steam is condensed by cooling water. The condensate leaving the condenser is passed through low and high pressure feedwater heaters by a feedwater pump. There, water is heated with the steam extracted from the high and intermediate stages of the main turbine (which results in an improvement of the cycle efficiency). The flow leaving the high pressure feedwater heater is transferred to the steam generator through a feedwater valve system.

A schematic diagram of a typical Westinghouse PWR system is shown in Fig 2.1. The net electrical generation capacity of the plant is 1200 *MW* based on a 3436 *MW* thermal energy in the reactor. The primary loop side operates at 2250 *psia* and at an average temperature of 547 °*F*. The secondary side, or turbine cycle admits steam at 1.4924×10^7 *lbm/hr* with a turbine inlet steam temperature of 521.9 °*F* at 850 *psia*. The main condenser operates at 1 *psia* at saturation conditions. The feedwater temperature entering the steam generator is 432 °*F*. Note that the primary side of this PWR system includes four loops, each having

a steam generator and a coolant pump.

2.2 Modeling Procedure

A lumped-parameter modeling approach has been used as the basis for system modeling. In the lumped-parameter approach, the average behavior of a model is evaluated by assuming the average properties over the lumped region. Since the model properties are not spatially dependent, the describing equations can be formulated in terms of ordinary differential equations. The describing equations are derived from physical laws as well as pertinent empirical and constitutive relations. Model development of a physical system based on lumped-parameter model consists of the following steps:

- Choose the component to be modeled.
- Specify the nodal structure of the model.
- Make appropriate assumptions and constraints.
- Derive proper governing equation for the model.
- Validate the model.

The above steps are applied for model development of a typical PWR plant components. Since the assumptions and the method of deriving the governing equations are important steps in model development of a PWR plant, they are discussed in more details.

2.2.1 Assumptions

One of the most important steps in model development of a PWR system is to make appropriate assumptions. The assumptions define a framework for operating domain of the system. Because PWR systems consist of a large number of components, a wide range of assumptions will be involved in the model development of such complex systems. These assumptions are defined to reduce model complexity and to facilitate computational requirements. They are mainly concerned with physical processes and geometrical configurations of the models. Due to existence of similarities in physical processes describing the dynamics of PWR components, there is a set of basic assumptions which are common in the models. The basic assumptions on which the models are constructed are:

- A one-dimensional model exists for heat transfer, thermal-hydraulics, and point kinetic equations. This assumption reduces the order and complexity of these equations.
- The PWR system and its subsystems are well-isolated from their surrounding environment. This assumption disregards the effect of external disturbances to the models.
- Water is an incompressible fluid. This allows us to consider a constant density for water.
- Saturated equilibrium condition exists between water and steam phases in two-phase flow models (for example, pressurizer and condenser).

- Heat transfer coefficients used in the models are constant parameters. This assumption neglects the small variations of these parameters due to changes in flow rate and temperature.
- Fluid friction factors are defined to be constant for turbulent flows through pipes and the steam generator downcomer region.

Individual assumptions of each component with their limits of applicability will be identified in the model documentations (see Chapters 3 and 4).

2.2.2 Governing Equations

The model governing equations are derived from conservation of mass, energy, and momentum relations as well as constitutive equations. The conservation relations usually describe the dynamics of a system while, the constitutive equations define physical quantities or characteristics (for example, water/steam properties or pump performance). they are important for supporting and complementing the concepts provided by the conservation relations. The operational forms of these equations are introduced below.

Conservation of Mass

The conservation of mass for a thermodynamic system is defined by

$$\frac{dM_{lm}}{dt} = \sum \dot{m}_i - \sum \dot{m}_e \quad (2.1)$$

where

M_{lm} = Mass instantaneously stored in the system.

\dot{m}_i, \dot{m}_e = Mass flow rates associated with into and out
of the system, respectively.

The preceding equation is commonly called the continuity equation. Equation (2.1) in this form has been used for the majority of PWR component models such as reactor core, steam generator, pressurizer, reactor coolant pump, and turbine cycle.

Conservation of Energy

Conservation of energy is a statement of the first law of thermodynamics which is defined in the following form:

The rate of energy accumulation in a system is equal to the difference between rates of entering and exiting energies plus rate of heat input to the system minus rate of output work from the system.

The above expression can be formulated for a lumped model as follows.

$$\frac{d}{dt}(Mu)_{lm} = \sum (\dot{m}h)_i - \sum (\dot{m}h)_e + Q - W \quad (2.2)$$

where

h_i, h_e = Inlet and outlet enthalpy values.

Q = Heat input to the node.

u_{lm} = Stored internal energy of the lumped model.

W = Work extracted from the system.

Equation (2.2) has been applied to the reactor core, pressurizer, steam generator, turbine reheater, feedwater heaters, and condenser models.

Conservation of Linear Momentum

From Newton's second law, the conservation of linear momentum relationship for a lumped model is derived as follows.

$$\frac{d}{dt}(Mv)_{lm} = \sum (\dot{m}v)_i - \sum (\dot{m}v)_e + \sum F_i \quad (2.3)$$

where

F_i = External forces.

v_{lm} = Velocity of stored mass in the lumped model.

v_i = Velocity of fluid entering the mass.

v_e = Velocity of fluid exiting the mass.

The above equation has been utilized for reactor coolant pump and steam generator downcomer region.

Constitutive Equations:

1. Water and Steam Properties

Thermodynamic properties of water and steam are generally available in the form of tables or graphical plots. The direct use of such tables or curves is not convenient for dynamic simulations. Therefore, they should be expressed in mathematical forms which can be applicable for simulation purposes.

In this study, water and steam properties have been expressed using first order algebraic equations which are linear functions (within a certain range) of system pressure in a postulated model. The general functional relationship is given by

$$F(p) = X_p + K_p P_s \quad (2.4)$$

where

$F(p)$ = Thermodynamic properties of water or steam in a system.

X_p = Constant of equation.

K_p = $\frac{\partial F(p)}{\partial P_s}$

P_s = Absolute pressure of the system.

2. Pump Performance Characteristics

The performance characteristics (for example, efficiency and head) of pumps are given in the form of general operating curves. Usually such curves are determined experimentally, and it would be quite tedious and difficult to apply them for simulation purposes. Thus, the use of mathematical relationships of these curves are used for dynamic simulations.

In this research, The reactor coolant pump head curve has been simulated as a quadratic function of the pump flow rate. The functional relationship of the curve is shown in Chapter 3.

3. Heat Transfer Equations

An overall heat transfer equation has been considered for determining all major heat transfer processes in the reactor core, steam generator, and turbine cycle models. This equation is given by

$$Q = UA\Delta T \quad (2.5)$$

where

- A = Effective heat transfer area.
 U = Overall heat transfer coefficient.
 ΔT = Temperature difference.

The overall heat transfer coefficient in the preceding equation is an equivalent parameter obtained by combining convection and conduction heat transfer coefficients. Generally, it is given as a design parameter (for simulation purposes) or determined by

$$U = \frac{1}{1/h_1 + \Delta x/k + 1/h_2} \quad (2.6)$$

where

- h_1, h_2 = Convection heat transfer coefficients in the first and
 the second fluid nodes.
 k = Conduction heat transfer coefficient in the intermediate material.
 Δx = Thickness of material.

4. Empirical Equations

The only empirical relation that is used for the PWR simulation is Callender's equation. This equation has been developed for determining the isentropic end point enthalpy of a high pressure turbine for a nuclear power plant. Callender's equation is shown in Appendix D.

2.3 Linearized Models

A linearized model of a physical system can be obtained from its nonlinear form by using the perturbation method. In this method, the model variables are perturbed about their steady-state operating values and the reference condition is subtracted after neglecting higher-order (cross product) terms. For instance, the linearized representation of a postulated equation is obtained as follows.

$$S = LW \quad (2.7)$$

Perturbing the variables:

$$S + \delta S = (L_0 + \delta L)(W_0 + \delta W) \quad (2.8)$$

Subtracting the preceding equation from its reference points and neglecting the higher-order terms yields

$$\delta S = W_0 \delta L + L_0 \delta W \quad (2.9)$$

The perturbation technique has been applied for obtaining the linearized representations of reactor core, steam generator, pressurizer, and reactor coolant pump models.

2.4 Design of Control Systems

Control systems are used extensively in PWR plants. They are employed to ensure safe and reliable operating conditions in the plant during normal and abnormal modes. The effectiveness of the control systems is mainly based on their design methods. A design procedure is outlined as follows.

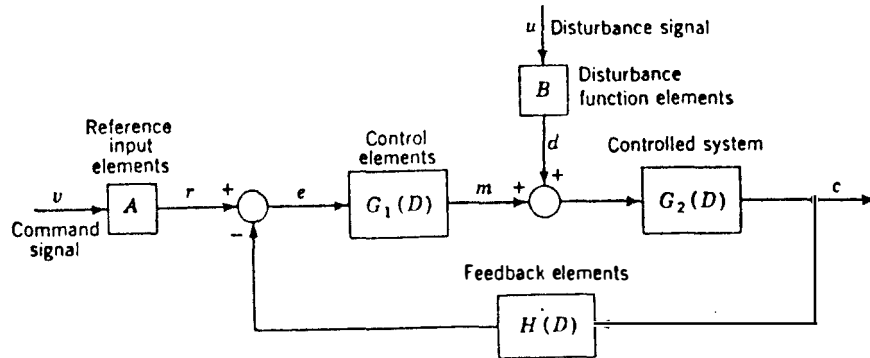


Figure 2.2: Typical block diagram representation of a feedback control system [11].

- Define all variables.
- Derive the transfer function of the controlled system.
- Specify constraints and limitations.
- Construct a control block diagram representation.
- Analyze the system performance.

All information pertinent to a control system should be integrated in a typical control block diagram representation. This is helpful in gaining a better understanding from the system operating conditions.

2.4.1 Control Block Diagram

A typical block diagram of a feedback control system is shown in Fig. 2.2. A signal obtained through feedback element, which is a function of the output response,

is compared with the reference input in a comparator element. Any difference between these two signals results in an error signal which actuates the control elements. The control elements in turn change the conditions in the controlled system in a way that reduces the original (steady-state) error. The amount of error can be regulated by using a proper control element.

2.4.2 Control Elements

Many types of control elements are used in control systems. Examples of these are: on-off, proportional, integral, proportional plus integral, proportional plus derivative, and proportional-integral-derivative. Depending upon application requirements (for example, a zero steady-state error or a fast response) for controlling a given process in a system, an appropriate control element is identified. Proportional plus integral (PI) and Proportional plus integral plus derivative (PID) controllers are used in this work. They are briefly discussed below.

1. Proportional plus Integral (PI)

A PI controller incorporates the desirable transient characteristic of a proportional controller and the zero steady-state error feature of an integral controller. The transfer function of a PI controller is described by

$$\frac{R(s)}{I(s)} = K_p + \frac{1}{\tau_i s} \quad (2.10)$$

where

$R(s)$ = Output response.

$I(s)$ = Input signal.

K_p = Proportional gain.

τ_i = Integral time constant.

s = Laplace operator.

2. Proportional plus Integral plus Derivative (PID)

A PID controller combines the action of a PI controller and the fast response feature of a derivative element. The transfer function of a PID controller is given by

$$\frac{R(s)}{I(s)} = K_p + \frac{1}{\tau_i s} + \tau_d s \quad (2.11)$$

where τ_d is the derivative time constant.

The time constants and gain factors are computed on the basis of design indices or performance criteria. For example, overshoot, phase margin, gain margin, settling time, and rise time are some of the performance indices. The design indices which are used for this study are:

- A maximum amount of 10% overshoot or undershoot from the nominal values.
- A minimum phase margin of 30 degrees.
- A reasonable settling time characterized by time response analysis of the controlled system.

The strategy described in this section is applied for designing the following plant control systems:

- reactivity,
- pressurizer pressure,
- steam generator water level(three-element controller), and
- turbine speed.

The performance of the control systems are investigated in their individual models as well as in the combined PWR plant. This is accomplished by employing time- and frequency-domain analyses of the dynamic models. The results are used to evaluate and optimize their design parameters. Note that due to the nonlinear gain factors of the reactivity and pressurizer pressure control systems, they are analyzed only in the time-domain.

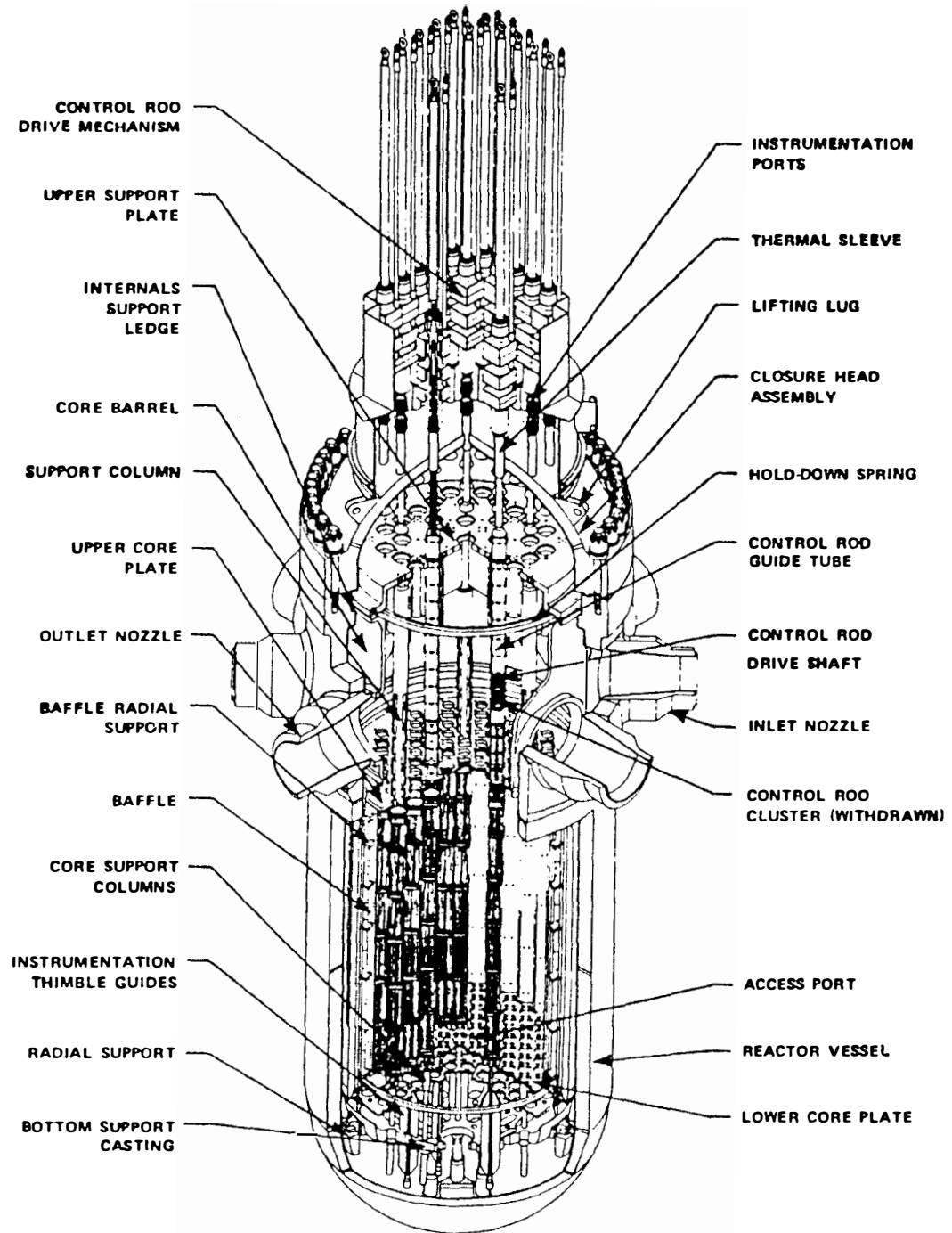
CHAPTER 3

MODEL DEVELOPMENT OF THE PRIMARY SIDE COMPONENTS

This chapter deals with model development of the primary side components of a Westinghouse PWR plant. It includes theoretical models of the reactor core, steam generator, pressurizer, and reactor coolant pump. Moreover, it describes control systems of the reactor core, steam generator, and the pressurizer. A comparison of the simulation results of linear and nonlinear model responses of reactor core and steam generator systems is also presented.

3.1 Reactor

Figure 3.1 shows the internals of a Westinghouse reactor vessel. The reactor coolant enters the vessel through nozzles above the top of the core. It flows through an annulus between the vessel and the core wall into the bottom of the core. The water then flows up through the core and out of the exit nozzles to the steam generator. The coolant leaving the steam generator is circulated in the primary loop by a large coolant pump. Typical design parameters of the reactor (Westinghouse type) are listed in Table A.1 of Appendix A.



Reactor Vessel Internals

Figure 3.1: Schematic diagram of a Westinghouse reactor [15].

3.1.1 Reactor Model

The reactor dynamic model used in this study incorporates the reactor core, the upper and lower plenums, and the connecting piping between the reactor core and the steam generator. The lumped-parameter approach is used to develop the reactor model from the first principles.

The reactor vessel is simulated as a cylindrical tank with one effective fuel element at the center. The fuel element generates heat from fission and the surrounding coolant removes the heat with an average overall heat transfer coefficient. The heat transfer model of this process is similar to Mann's model for heat exchangers (see Fig. 3.2).

The model is nodalized according to the Fig. 3.2. The fuel element and the coolant are divided into three and six nodes respectively. The remaining reactor coolant system nodes used in this model are: upper plenum, lower plenum, hot leg, and cold leg. A point kinetics model with the average of six delayed-neutron precursor groups is used to predict the average fission power in the reactor core. The power is assumed to be constant along the axial direction in the reactor core.

The mathematical simulation model of the reactor core consists of a set of 15 ordinary differential equations. These equations are derived from the physical model and describe the reactor core kinetics and thermal-hydraulics under transient and steady-state conditions. The model equations are expressed as follows:

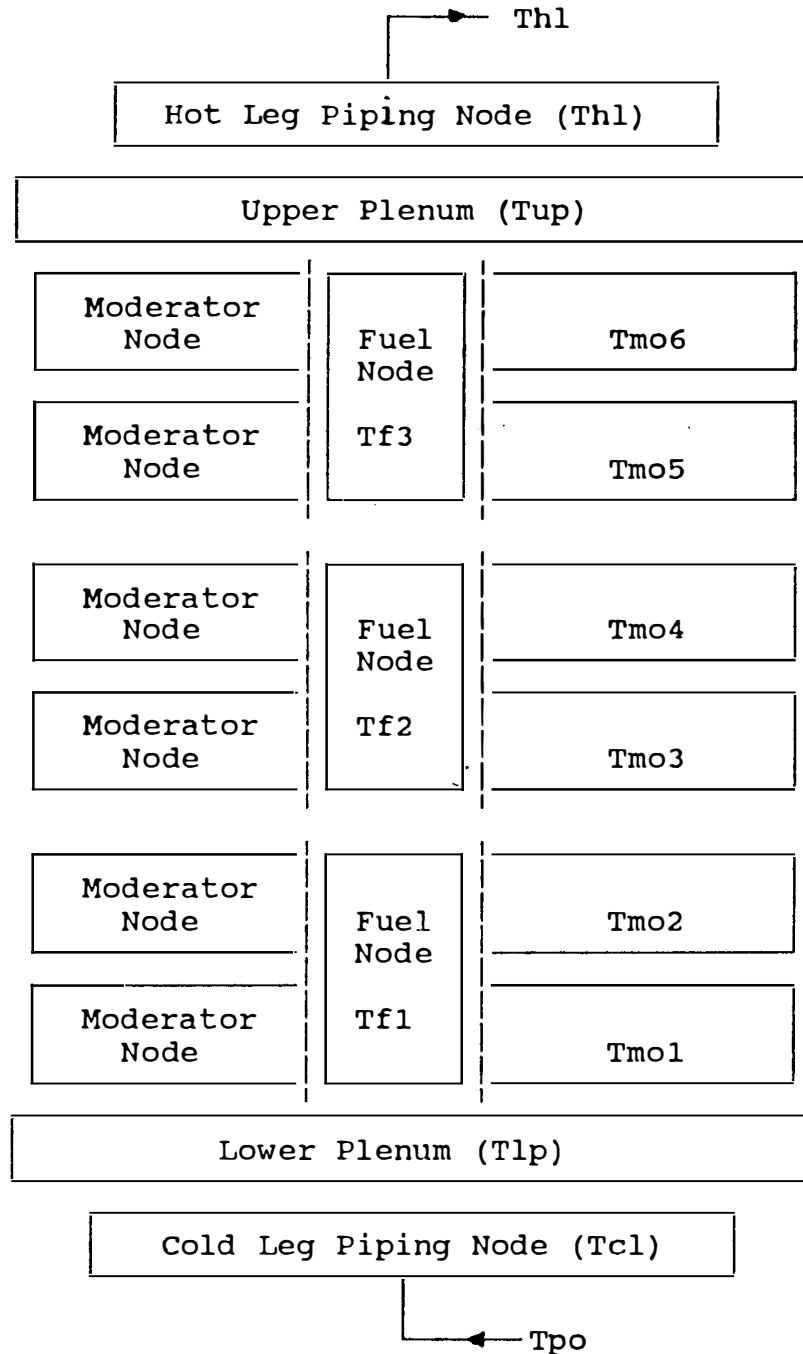


Figure 3.2: Schematic diagram of the reactor model (including the primary loop piping).

Point Reactor Kinetics Equations

$$\frac{d(P/P_0)}{dt} = \frac{\rho - \beta_t}{\Lambda} \frac{P}{P_0} + \lambda C \quad (3.1)$$

$$\frac{dC}{dt} = \frac{\beta}{\Lambda} \frac{P}{P_0} - \lambda C \quad (3.2)$$

Reactor Core Heat Transfer Equations

First node:

$$\frac{dT_{f1}}{dt} = \frac{F_r P_0}{(MC_p)_F} \frac{P}{P_0} + \frac{hA}{(MC_p)_F} (T_{mo1} - T_{f1}) \quad (3.3)$$

$$\frac{dT_{mo1}}{dt} = \frac{(1 - F_r) P_0}{(MC_p)_C} \frac{P}{P_0} + \frac{hA}{(MC_p)_C} (T_{f1} - T_{mo1}) + \frac{(T_{lp} - T_{mo1})}{\tau_C} \quad (3.4)$$

$$\frac{dT_{mo2}}{dt} = \frac{(1 - F_r) P_0}{(MC_p)_C} \frac{P}{P_0} + \frac{hA}{(MC_p)_C} (T_{f1} - T_{mo1}) + \frac{(T_{mo1} - T_{mo2})}{\tau_C} \quad (3.5)$$

Second node:

$$\frac{dT_{f2}}{dt} = \frac{F_r P_0}{(MC_p)_F} \frac{P}{P_0} + \frac{hA}{(MC_p)_F} (T_{mo3} - T_{f2}) \quad (3.6)$$

$$\frac{dT_{mo3}}{dt} = \frac{(1 - F_r) P_0}{(MC_p)_C} \frac{P}{P_0} + \frac{hA}{(MC_p)_C} (T_{f2} - T_{mo3}) + \frac{(T_{mo2} - T_{mo3})}{\tau_C} \quad (3.7)$$

$$\frac{dT_{mo4}}{dt} = \frac{(1 - F_r) P_0}{(MC_p)_C} \frac{P}{P_0} + \frac{hA}{(MC_p)_C} (T_{f2} - T_{mo3}) + \frac{(T_{mo3} - T_{mo4})}{\tau_C} \quad (3.8)$$

Third node:

$$\frac{dT_{f3}}{dt} = \frac{F_r P_0}{(MC_p)_F} \frac{P}{P_0} + \frac{hA}{(MC_p)_F} (T_{mo5} - T_{f3}) \quad (3.9)$$

$$\frac{dT_{mo5}}{dt} = \frac{(1 - F_r) P_0}{(MC_p)_C} \frac{P}{P_0} + \frac{hA}{(MC_p)_C} (T_{f3} - T_{mo5}) + \frac{(T_{mo4} - T_{mo5})}{\tau_C} \quad (3.10)$$

$$\frac{dT_{mo6}}{dt} = \frac{(1 - F_r) P_0}{(MC_p)_C} \frac{P}{P_0} + \frac{hA}{(MC_p)_C} (T_{f3} - T_{mo5}) + \frac{(T_{mo5} - T_{mo6})}{\tau_C} \quad (3.11)$$

Cold Leg Temperature

$$\frac{dT_{cl}}{dt} = \frac{(T_{po} - T_{cl})}{\tau_{cl}} \quad (3.12)$$

Lower Plenum Temperature

$$\frac{dT_{lp}}{dt} = \frac{(T_{cl} - T_{lp})}{\tau_{lp}} \quad (3.13)$$

Upper Plenum Temperature

$$\frac{dT_{up}}{dt} = \frac{(T_{mo6} - T_{up})}{\tau_{up}} \quad (3.14)$$

Hot Leg Temperature

$$\frac{dT_{hl}}{dt} = \frac{(T_{up} - T_{hl})}{\tau_{hl}} \quad (3.15)$$

Constitutive Equations

$$\begin{aligned} \rho = \rho_{ex} + \frac{\alpha_f}{3} [(T_{f1} + \dots + T_{f3}) - (T_{f1_0} + \dots + T_{f3_0})] + \\ \frac{\alpha_c}{6} [(T_{mo1} + \dots + T_{mo6}) - (T_{mo1_0} + \dots + T_{mo6_0})] \end{aligned} \quad (3.16)$$

$$\lambda = \frac{\beta_t}{\sum_{i=1}^6 \frac{\beta_i}{\lambda_i}} \quad (3.17)$$

$$\tau_C = \frac{M_C}{2\dot{M}} \quad (3.18)$$

$$\tau_{cl} = \frac{M_{cl}}{\dot{M}} \quad (3.19)$$

$$\tau_{lp} = \frac{M_{lp}}{\dot{M}} \quad (3.20)$$

$$\tau_{up} = \frac{M_{up}}{\dot{M}} \quad (3.21)$$

$$\tau_{hl} = \frac{M_{hl}}{\dot{M}} \quad (3.22)$$

The definitions of the model variables are listed in Table 3.1.

The preceding equations represent the mathematical model of the reactor system. The forcing functions to the isolated model will be external reactivity and the steam generator outlet temperature.

Table 3.1: Reactor Model Variables

<i>Variable</i>	<i>Definition</i>
1. A	Effective heat transfer area between fuel and coolant
2. C	Precursor concentration
3. C_{PC}	Coolant heat capacity
4. C_{PF}	Fuel heat capacity
5. F_r	Fraction of the total power generated in fuel elements
6. h	Average overall heat transfer coefficient
7. \dot{M}	Coolant mass flow rate
8. M_c	Coolant mass in two fluid nodes
9. M_{cl}	Cold leg water mass
10. M_F	Fuel mass in each node
11. M_{hl}	Hot leg water mass
12. M_{lp}	Lower plenum water mass
13. M_{mo}	Coolant node mass
14. M_{up}	Upper plenum water mass
15. P	Reactor core power in each node
16. T_{cl}	Cold leg temperature
17. T_{f1-3}	Fuel temperatures in nodes (1-3)
18. T_{hl}	Hot leg temperature
19. T_{lp}	Fluid temperature in lower plenum
20. $T_{m\bullet 1-6}$	Moderator temperatures in nodes (1-6)
21. T_{up}	Fluid temperature in Upper plenum
22. T_{po}	Outlet temperature of the primary water leaving steam generator U-tubes
23. α_c	Coolant coefficient of reactivity
24. α_f	Fuel coefficient of reactivity
25. β_t	Total delayed neutron group fraction
26. λ	Average of six group decay constant
27. Λ	Neutron generation time
28. ρ	Total reactivity
29. ρ_{ex}	External reactivity
30. $\tau_{cl}, \tau_{hl}, \tau_C, \tau_{lp}, \tau_{up}$	Time constants of cold leg, hot leg, moderator nodes, lower plenum, and upper plenum

Figure 3.3 shows the dynamic responses of normalized core power, fuel temperature, and hot leg temperature for a 10 cent step increase in the external reactivity. Figure 3.4 gives the responses of the above variables for a $10^{\circ}F$ step increase in the inlet temperature of the cold leg piping. The simulation responses of the reactor core normalized power and hot leg temperature are similar to those obtained by Freels [1] and Mneimneh [2].

3.1.2 Comparison between Linear and Nonlinear Models

A comparison is made between the results obtained from the linear and nonlinear simulations of the reactor model for both 10 and 20 cents step increases in external reactivity (see Figs. 3.5 and 3.6). In both cases, the responses of normalized reactor power in the linear model are similar to those of the nonlinear model. However, small differences exist between the linear and nonlinear simulation responses of reactor power when the reactivity insertion is 20 cents. In the linear model, the core power has a peak value of 13% in the transient and a constant value of 8% at steady-state. Whereas, in the nonlinear model, these values are 12% and 7% respectively. In general, the results show that the linear model agrees with the nonlinear one. This is due to the fact that the majority of the core model equations are linear. The only nonlinear equation is the reactor core power equation. Therefore, one expects the results of both simulations will be nearly the same even for large perturbations in the forcing terms.

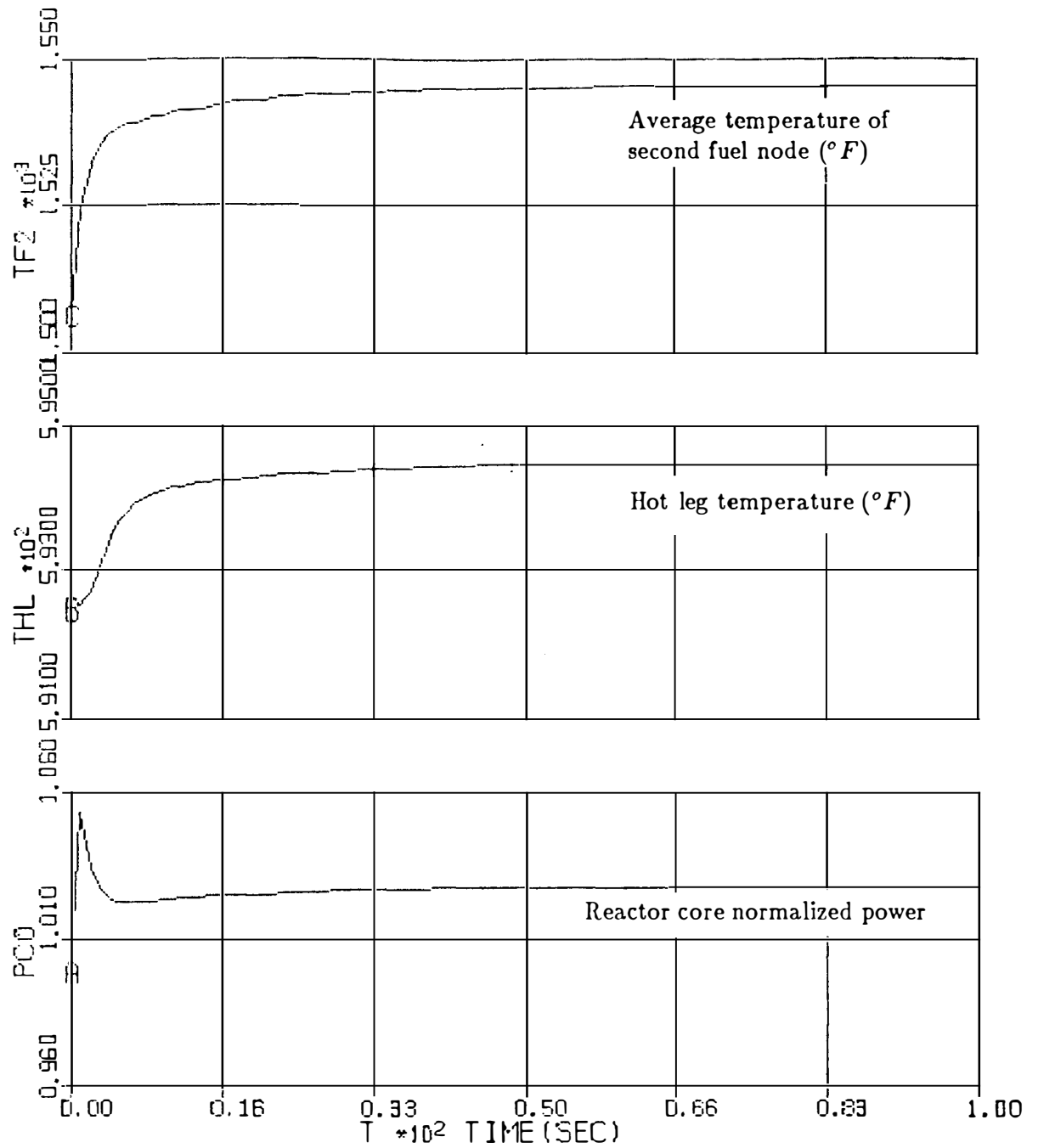


Figure 3.3: Dynamic responses of the reactor model to 10 cents external reactivity.

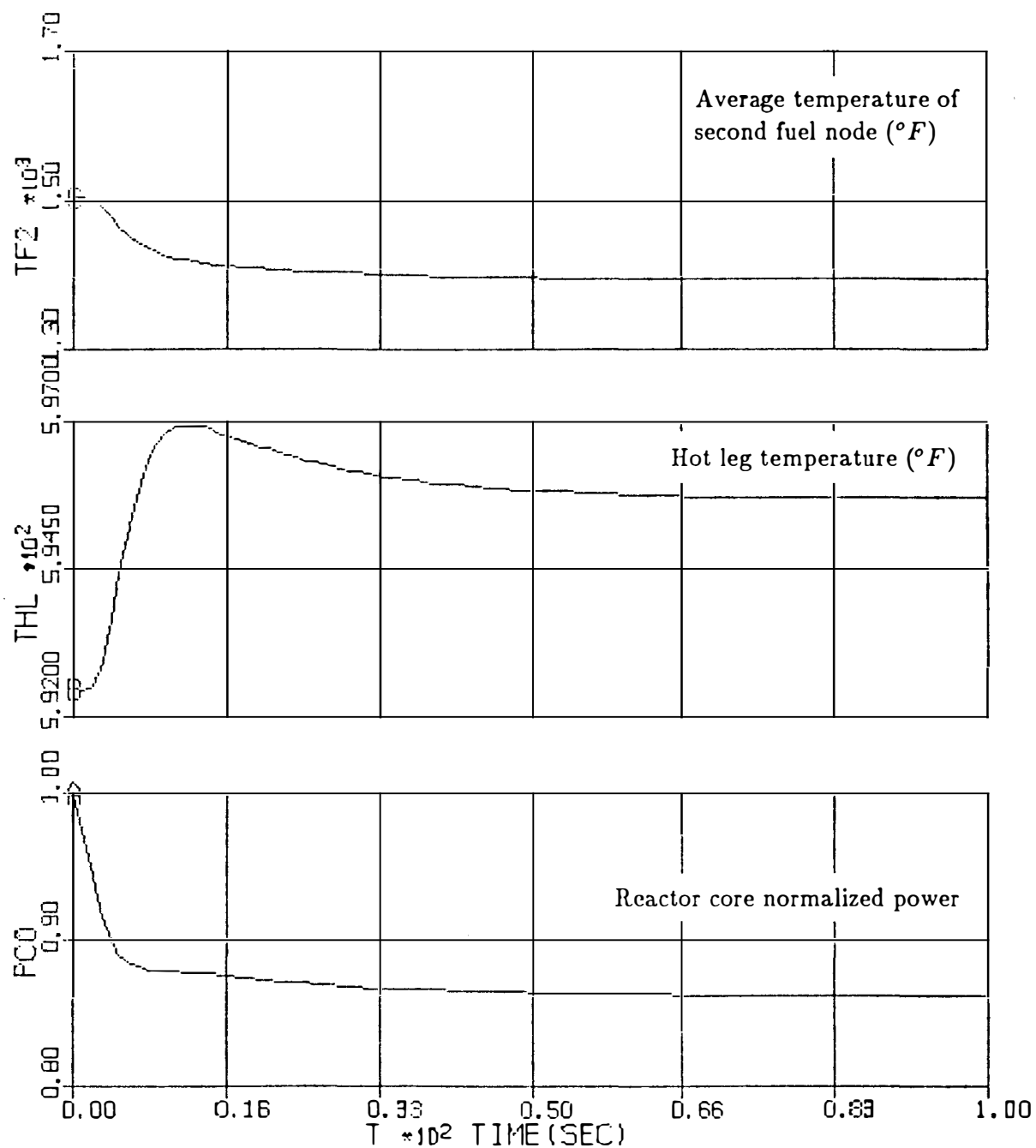


Figure 3.4: Dynamic responses of the reactor model to a $10 \text{ }^{\circ}\text{F}$ step increase in the cold leg temperature (core inlet coolant).

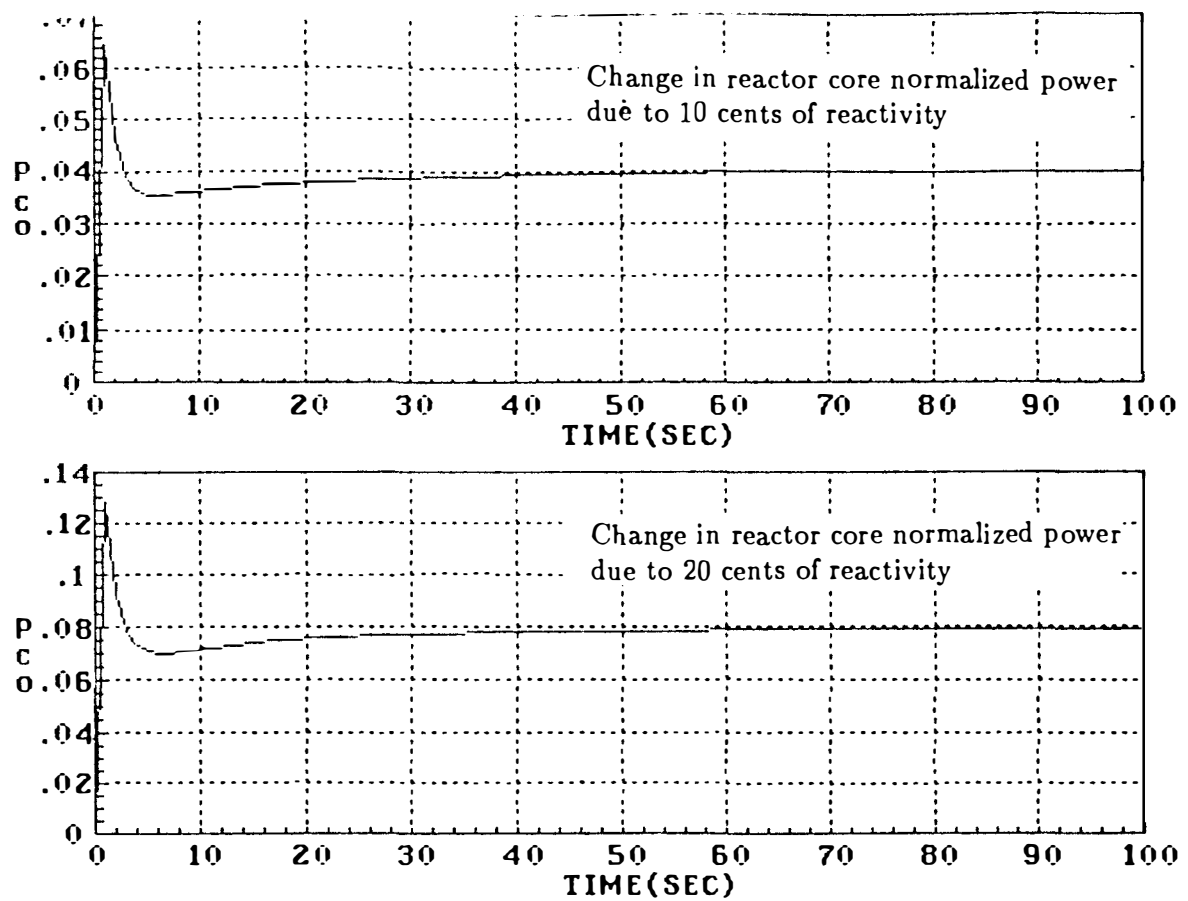


Figure 3.5: Responses of the reactor linear model to 10 and 20 cents step increases in the external reactivity.

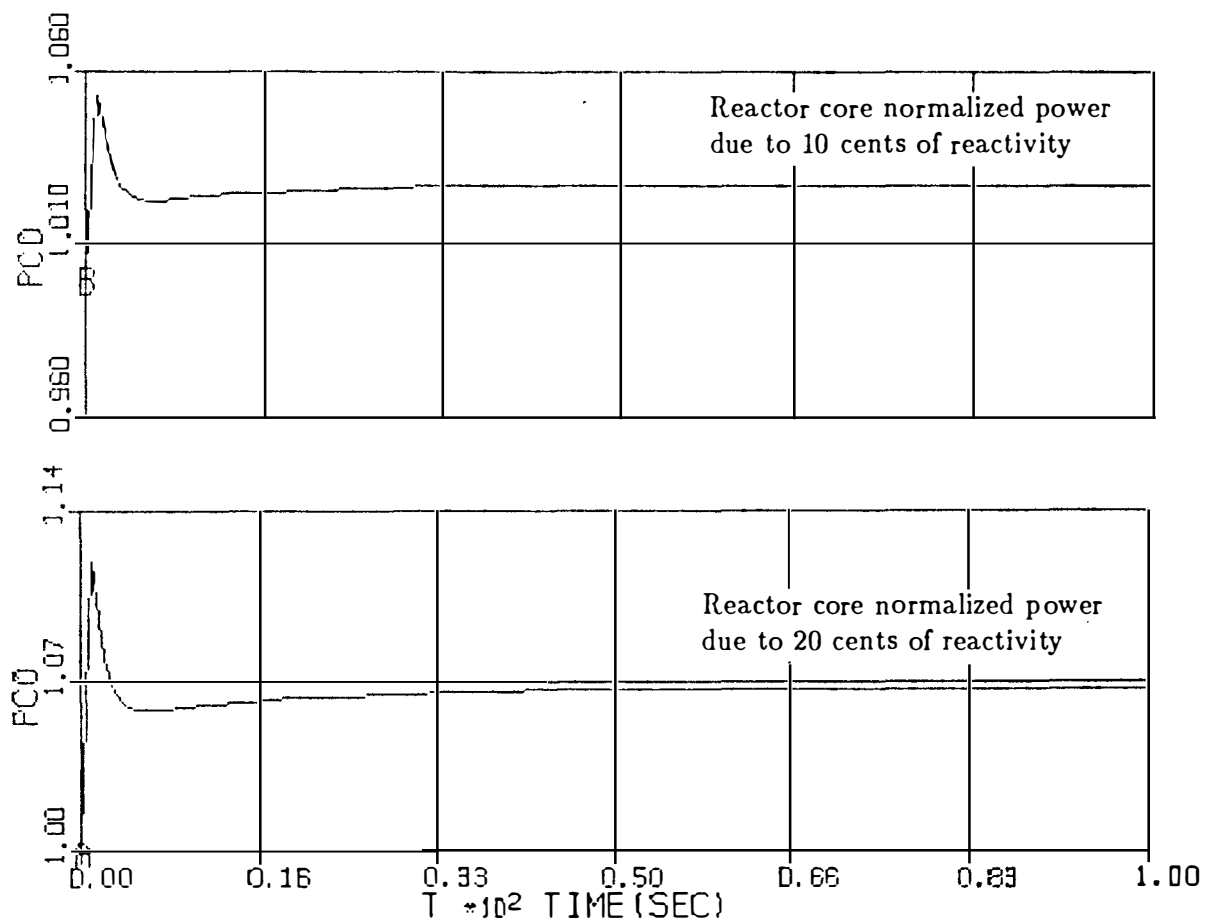


Figure 3.6: Responses of the reactor nonlinear model to 10 and 20 cents step increases in the external reactivity.

3.1.3 Reactor Power Control System

The purpose of the reactor control system is to regulate the power level in the reactor when a change in power demand occurs, and to ensure a safe and reliable operation in the core during transient and steady-state conditions. The control system must be able to handle sudden changes in the load demand without scrambling the reactor.

The negative feedback of reactivity due to changes in fuel and moderator temperatures is an inherent control system in a PWR. However, this control system is not sufficient for normal operating range in a PWR system. Therefore, the need for an external control system is crucial. The control system shown in this study is based on the steady-state program (average coolant temperature program) given in Westinghouse documentations [15] (see Fig. 3.7). The control system initiates the movement of the control rods by taking two major signals. These two signals are the average temperature set point and the lead-lag average temperature. The negative lead-lag temperature signal is compared to the positive set point signal in a comparator device. Any difference between these two signals constitutes a temperature error signal which ultimately determines the rate and direction of control rod movement. The steady-state program requires that the sign of error signal be consistent with the sign of induced reactivity. For example, a positive error signal results in a positive change of reactivity in the system which indicates an increase in reactor power. The block diagram representation of the control system is shown in Fig. 3.8. The mathematical relations of the control signals are given as follows:

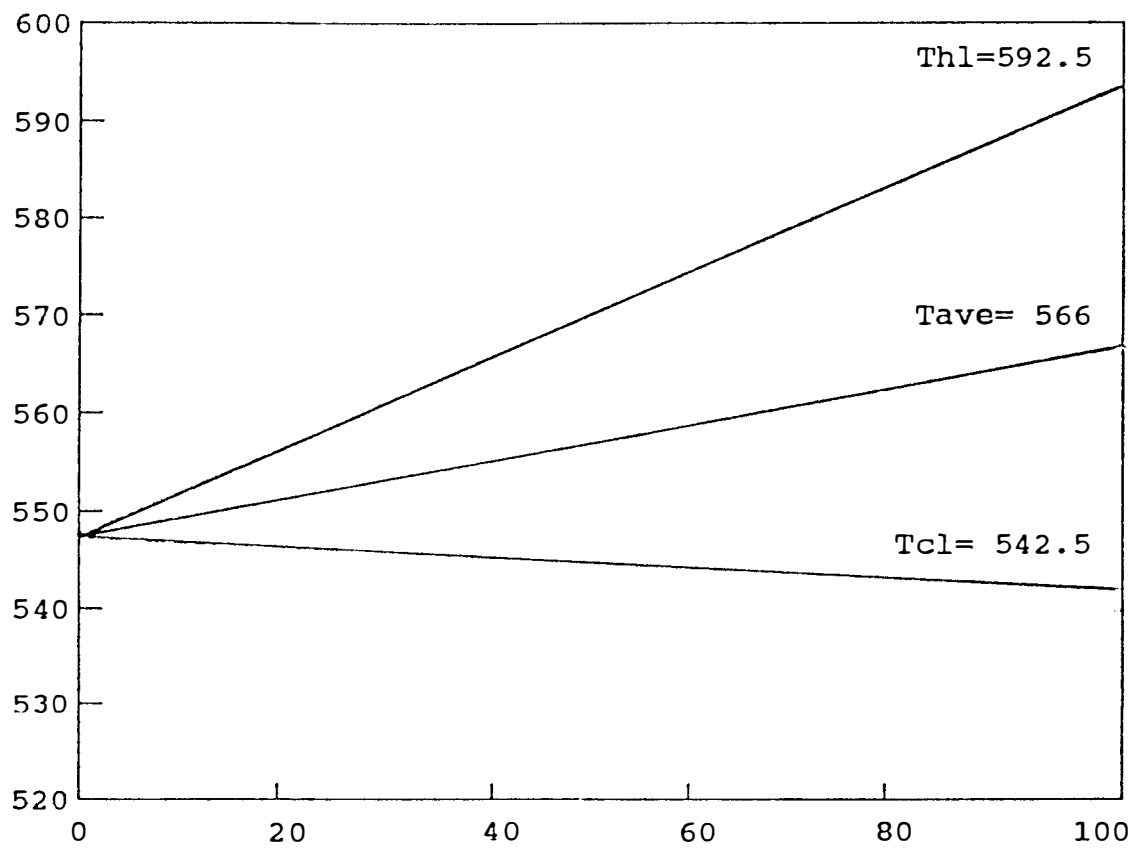


Figure 3.7: Schematic diagram of the Westinghouse average temperature coolant program [15].

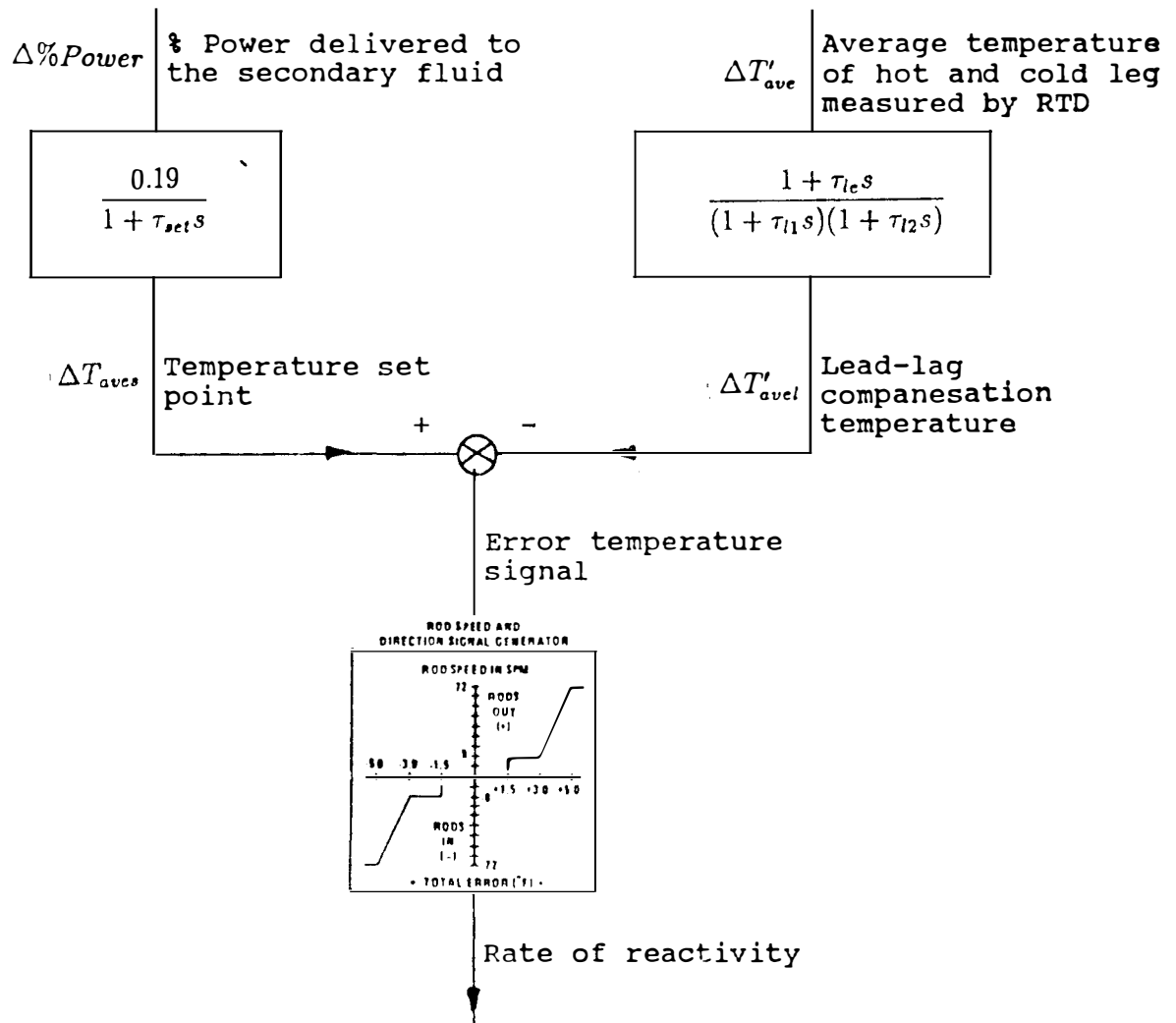


Figure 3.8: Block diagram representation of the reactor control system.

The reactor coolant average temperature is defined as:

$$T_{ave} = \frac{T_{cl} + T_{hl}}{2} \quad (3.23)$$

where

T_{cl} = Cold leg temperature.

T_{hl} = Hot leg temperature.

The average set point temperature at the steady-state condition can be expressed from Fig. 3.7 as:

$$T_{aves} = 0.19Power\% + 547 \quad (3.24)$$

where

$Power\%$ = the percent of power delivered to the secondary side.

The temperature signals to the reactor core control system are obtained from the transfer functions given in Westinghouse documentations [15]. The time domain representation of these transfer functions are:

1. The average temperature set point:

$$\frac{dT_{aves}}{dt} = \frac{0.19Power\% + 547 - T_{aves}}{\tau_{set}} \quad (3.25)$$

where

τ_{set} = Time constant of the average temperature set point.

2. The hot and cold leg temperatures measured by the RTDs¹ :

$$\frac{dT'_{cl}}{dt} = \frac{T_{cl} - T'_{cl}}{\tau_{RTD}} \quad (3.26)$$

¹RTD refers to “ Resistance Temperature Detector ” and it is a temperature measuring device

$$\frac{dT'_{hl}}{dt} = \frac{T_{hl} - T'_{hl}}{\tau_{RTD}} \quad (3.27)$$

where

T'_{cl} = Cold leg temperature measured by RTD.

T'_{hl} = Hot leg temperature measured by RTD.

τ_{RTD} = Time constant of RTD.

3. The lead-lag average temperature:

$$\frac{d^2 T_{avel}}{dt^2} = \frac{T'_{ave} - T_{avel} - (\tau_{l1} + \tau_{l2}) \frac{dT_{avel}}{dt} + \frac{\tau_{le}}{2} \left(\frac{dT'_{cl}}{dt} + \frac{dT'_{hl}}{dt} \right)}{\tau_{l1} \tau_{l2}} \quad (3.28)$$

where

$$T'_{ave} = \frac{T'_{cl} + T'_{hl}}{2} \quad (3.29)$$

τ_{l1} = The first lag time constant.

τ_{l2} = The second lag time constant.

τ_{le} = The lead-lag time constant.

4. The error temperature signal:

$$e = T_{aves} - T_{avel} \quad (3.30)$$

The error signal will actuate the control rod system according to the control rod speed program shown in Fig 3.9. The rod speed is a nonlinear function of the error temperature signal. It is simulated as a piecewise function by a set of logical statements in a computer program to compute the rod speed for different amount

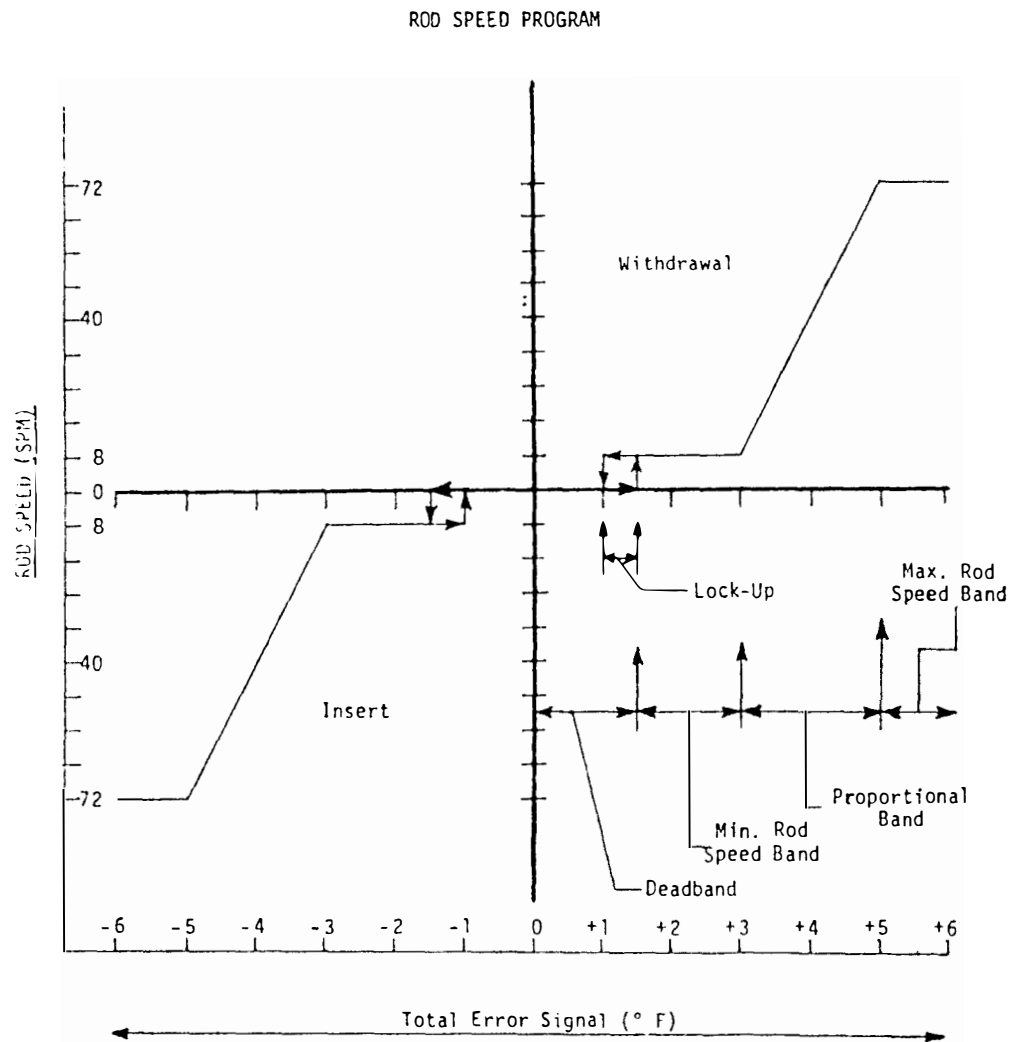


Figure 3.9: Reactor control rod speed program [15].

of the error signal. The speed program and the error signal will determine the rate of induced reactivity as follows:

$$\frac{d\rho_{ex}}{dt} = R_s V_s e \quad (3.31)$$

where

ρ_{ex} = External reactivity.

R_s = Amount of reactivity at each step (which is a constant value).

V_s = Rods speed (which varies as a function of error signal).

Table 3.2 shows design parameters of the reactor control system. These parameters are mainly taken from Westinghouse documentations [15].

Since the average temperature variations depend on the steam generator and turbine operating conditions, the control system performance should be examined in the primary loop or the overall plant system. This is presented in Chapter 5 where the overall plant system model is discussed.

3.2 Steam Generator

A type of steam generator widely used in PWR systems is the recirculation U-tube steam generator (UTSG). The general arrangement of a typical Westinghouse UTSG is given in Fig. 3.10.

The primary coolant enters the steam generator through an inlet nozzle on the left bottom of the inlet plenum. The coolant flows inside the U-tubes first upward

Table 3.2: Design Parameters of the Reactor Control System

1.	The first lag time constant, $\tau_{l1}(sec)$	10.0
2.	The second lag time constant, $\tau_{l2}(sec)$	5.0
3.	The lead-lag time constant, $\tau_{le}(sec)$	80.0
4.	Time constant of RTD, $\tau_{RTD}(sec)$	4.0
5.	Time constant of the average temperature set point, $\tau_{set}(sec)$	30.0
6.	Induced reactivity at each step, $R_s(cent/step)$	0.325

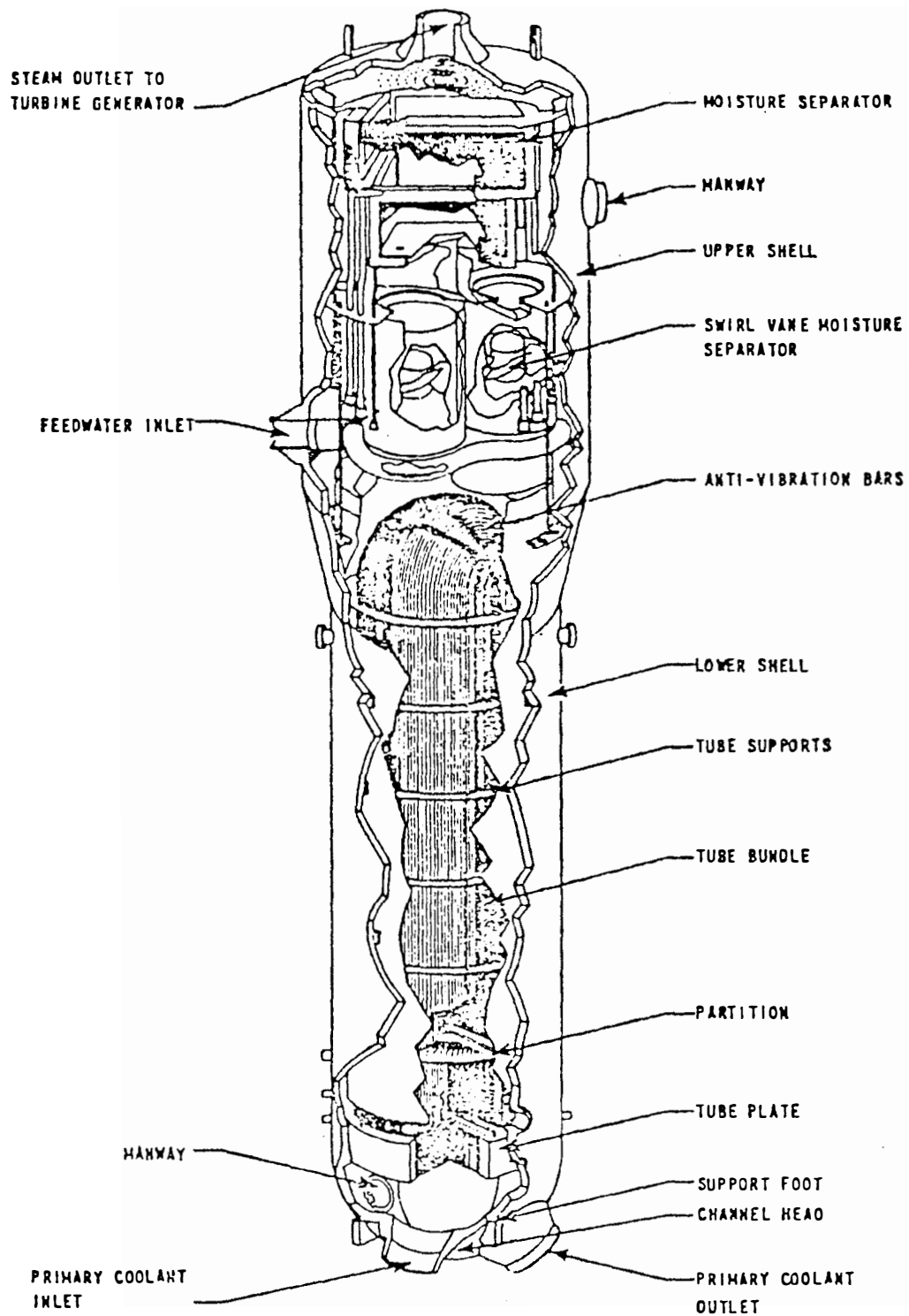


Figure 3.10: Schematic diagram of a typical Westinghouse U-tube steam generator [15].

and then downward, and thus transfers heat to the secondary fluid in the shell side of the steam generator. The primary fluid leaves the outlet plenum through an on outlet nozzle connected to the cold leg pipings.

Feedwater enters inside the downcomer shell at a level just above the U-tubes region. It flows down through an annulus inside the shell and mixes with water coming from the drum section. The water enters the tube bundle region where heat is transferred to the fluid. As it flows over the outside of the U-tubes, a mixture of steam and water is formed. The mixture enters the riser region where the nozzle effect increases the natural driving force. As the flow passes through the separator region, water is removed from the steam and returned to the drum section. The steam leaving the separator passes through steam dryers and exits the steam generator with a quality of approximately 99.75%. Typical design parameters of a Westinghouse UTSG are listed in Table A.2 of Appendix A.

3.2.1 Steam Generator Model

The steam generator is one of the most important components of a PWR system. It provides a dynamic link between the reactor and turbine-generator systems. Therefore, a good understanding of steam generator behavior is essential for the study of a PWR system. This goal can be achieved by a dynamic simulation model of the steam generator.

Many theoretical models of the UTSG have been developed by Ali [3]. Ali's detailed model (model D) is utilized in this work. The model can be used to predict dynamic behavior of thermal and hydraulic processes in a UTSG system. The

theoretical simulation model has been developed based on the conservation equations (mass, energy, and momentum) and constitutive relations with the following assumptions:

- Both water and steam are considered to be saturated.
- Density and specific heat of the feedwater, subcooled region, and the primary side are assumed to be constant.
- Heat transfer coefficients are constants.
- Steam leaving the UTSG is assumed to be 100% saturated.
- Heat transfer between the downcomer and tube bundle regions is negligible.

The thermodynamic properties of the saturated water and steam are assumed to be linear functions of the steam pressure for a range of ± 100 *psi* from the normal operating point. Equation (3.32) shows the mathematical expression of this assumption.

$$F_p = X_m + K_n P \quad (3.32)$$

where

F_p = Saturated water or steam property.

X_m = Constant of the equation.

K_n = $\frac{\partial F_p}{\partial P}$

P = Steam pressure.

The steam flow leaving the UTSG is considered to be a critical flow. The flow is defined in terms of steam pressure and steam valve coefficient as follows:

$$W_s = C_l P \quad (3.33)$$

where

W_s = Steam flow rate.

C_l = Steam valve coefficient.

P = Steam pressure.

A set of 18 state variables define the nonlinear mathematical model of the UTSG. The forcing functions of the isolated UTSG model are: primary inlet temperature, steam valve coefficient, feedwater temperature, and feedwater flow rate. The feedwater flow rate will be a new state variable when the three-element controller model is coupled to the system. The mathematical formulations of the steam generator model are shown in Appendix B.

3.2.2 Steam Generator Control System

A three-element controller is considered as the only UTSG control system in this study. The three-element controller is used to regulate the water level in the steam generator and utilizes three signals, namely, feedwater flow rate, steam flow rate, and steam generator water level. It maintains the level at a desired set point by controlling the feedwater flow rate to the system.

The block diagram representation of a typical three-element controller designed by Westinghouse Corporation is shown in Fig. 3.11. It includes a filter, two

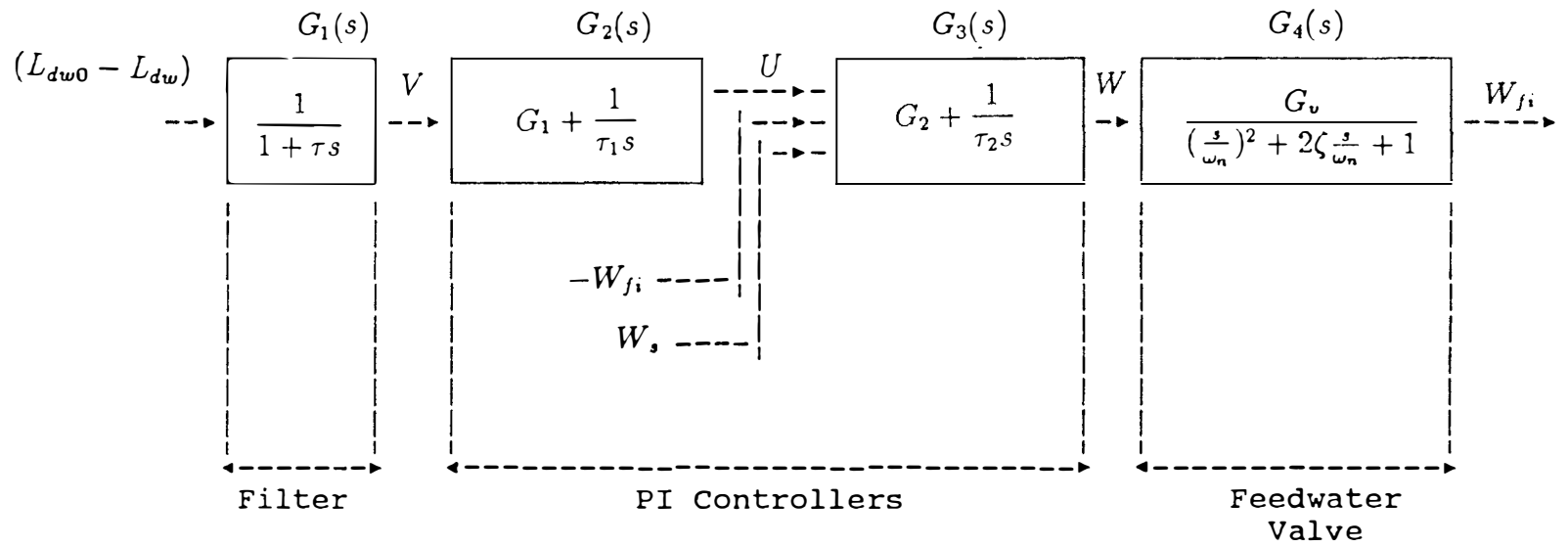


Figure 3.11: Block diagram representation of the three-element controller [15].

proportional and integral (PI) controllers, and feedwater valve dynamics. The actuating level signal e is preprocessed using a low-pass filter before entering the first PI control element $G_1(S)$. This helps to diminish the effect of faulty extraneous noise in the signal. The positive feedwater and negative steam flow signals are summed with the output signal of $G_1(S)$ and passed through the second PI control element $G_2(S)$. The resulting signal leaving $G_2(S)$ governs the feedwater positioner which has a second order system characteristic.

The mathematical form of the differential equations relating the valve motion to the level signal are derived from Fig. 3.11 as follows:

Filter Equation

$$\frac{dV}{dt} = \frac{L_{dw} - L_{dw0} - V}{\tau} \quad (3.34)$$

First PI Controller Equation

$$\frac{dU}{dt} = \frac{G_1(L_{dw} - L_{dw0} - V)}{\tau} + \frac{V}{\tau_1} \quad (3.35)$$

Second PI Controller Equation

$$\frac{dW}{dt} = G_2V\left(\frac{1}{\tau_1} - \frac{G_1}{\tau}\right) + \frac{U}{\tau_2} + \frac{G_1G_2(L_{dw} - L_{dw0})}{\tau} \quad (3.36)$$

Flow Signal Equation

$$\frac{dZ}{dt} = C_lP - W_{fi} \quad (3.37)$$

Feedwater Valve Equation

$$\frac{d^2W_{fi}}{dt^2} + 2\zeta\omega_n \frac{dW_{fi}}{dt} + \omega_n^2(W_{fi} - W_{fi0}) - G_vG_2\omega_n^2(C_lP - W_{fi}) - G_v\omega_n^2\left(W + \frac{Z}{\tau_2}\right) = 0 \quad (3.38)$$

The definitions of the variables used in the three-element controller are shown in Table 3.3. The design parameters for the filter element and the feedwater valve system are the same as those given by the Westinghouse Corporation. The controller element parameters such as proportional gains and integral time constants are optimized by a computer program in the nonlinear model of the UTSG. The optimization is accomplished by using a computer code with 15% perturbation in the steam valve coefficient. The control parameters are chosen and then optimized by minimizing the error in the UTSG water level during transient, limiting overshoot or undershoot of the system to 10% of its initial values, and selecting a proper settling time (at 5% steady-state value) for the system (approximately 160 sec). A trial and error procedure is used to perform this optimization. The optimized parameters along with the other parameters of the three-element controller are shown in Table 3.4.

Typical responses of the nonlinear coupled system (UTSG and Three-element controller) due to a 10% step increase in the steam valve coefficient are shown in Fig. 3.12. The steady-state values of the responses are similar to those obtained by Freels [1] and Cherng [4].

3.2.3 Comparison between Linear and Nonlinear Models

The dynamic responses of the linear and nonlinear simulations of the steam generator system, including the three-element controller, are shown in Figs. 3.13-3.15 for the three cases of 10%, 15%, and 25% step decreases in the steam valve coefficient. The responses include steam pressure, water level, and feedwater flow.

Table 3.3: Three-Element Controller Variables

<i>Variable</i>	<i>Definition</i>
1. G_1	Gain factor of the first PI controller
2. G_2	Gain factor of the second PI controller
3. G_v	Gain factor feedwater valve system
4. C_l	Feedwater valve coefficient
5. L_{dw}	Water level in the UTSG
6. M	Flow signal to the controller element
7. P	Steam generator pressure
8. U	Control signal leaving the first PI controller
9. V	Level signal leaving the filter element
10. W	Control signal leaving the second PI controller
11. W_{fi}	Feedwater flow rate
12. τ	Filter time constant
13. τ_1	Time constant of the first PI controller
14. τ_2	Time constant of the second PI controller
15. ζ	Damping ratio of the feedwater valve system
16. ω_n	Natural frequency of the feedwater valve system

Table 3.4: Design Parameters of the Three-element Controller

1. Gain factor of the first PI controller, G_1	65.2
2. Gain factor of the second PI controller, G_2	1
3. Gain factor feedwater valve system, G_v	32.2
4. Time constant of the first PI controller, $\tau_1(sec)$	250
5. Time constant of the second PI controller, $\tau_1(sec)$	120
6. Filter time constant, $\tau(sec)$	5.0
7. Damping factor of the feedwater valve system, ζ	3.18
8. Natural frequency of the feedwater valve system, ω_n (rad/sec)	0.63

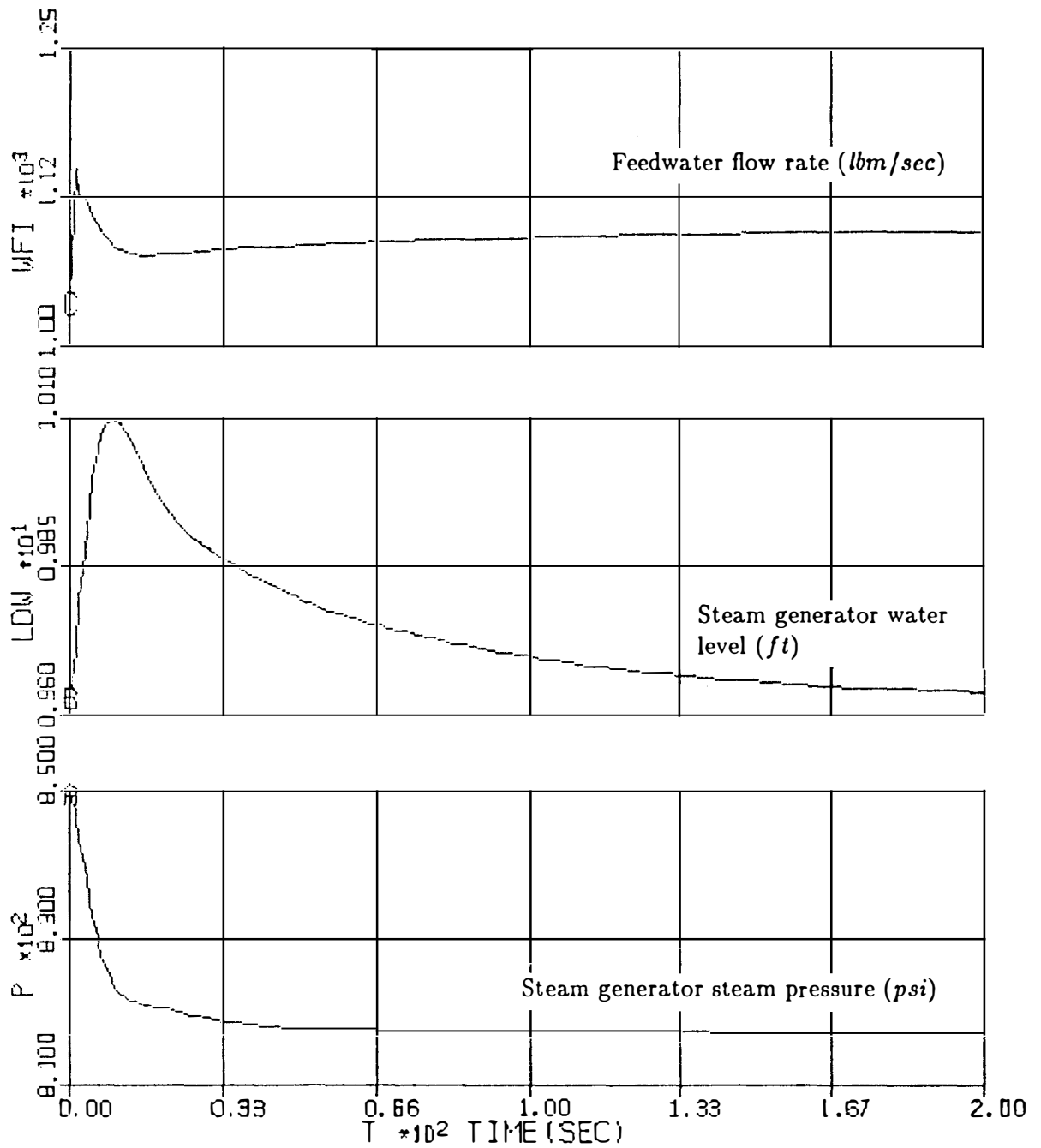


Figure 3.12: Typical responses of the steam generator nonlinear model, including the three-element controller, to a 10% step increase in the steam valve coefficient.

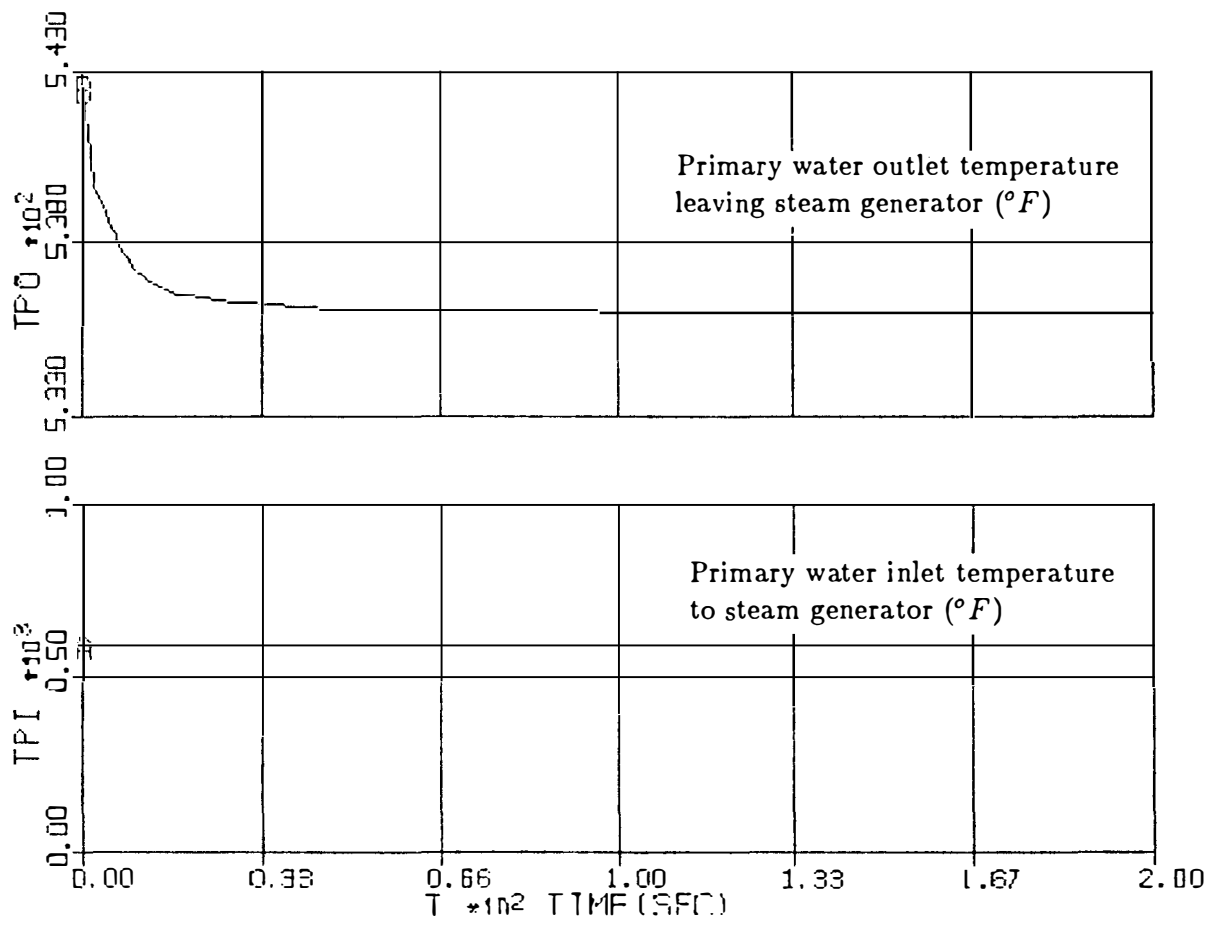


Fig. 3.12 (continued)

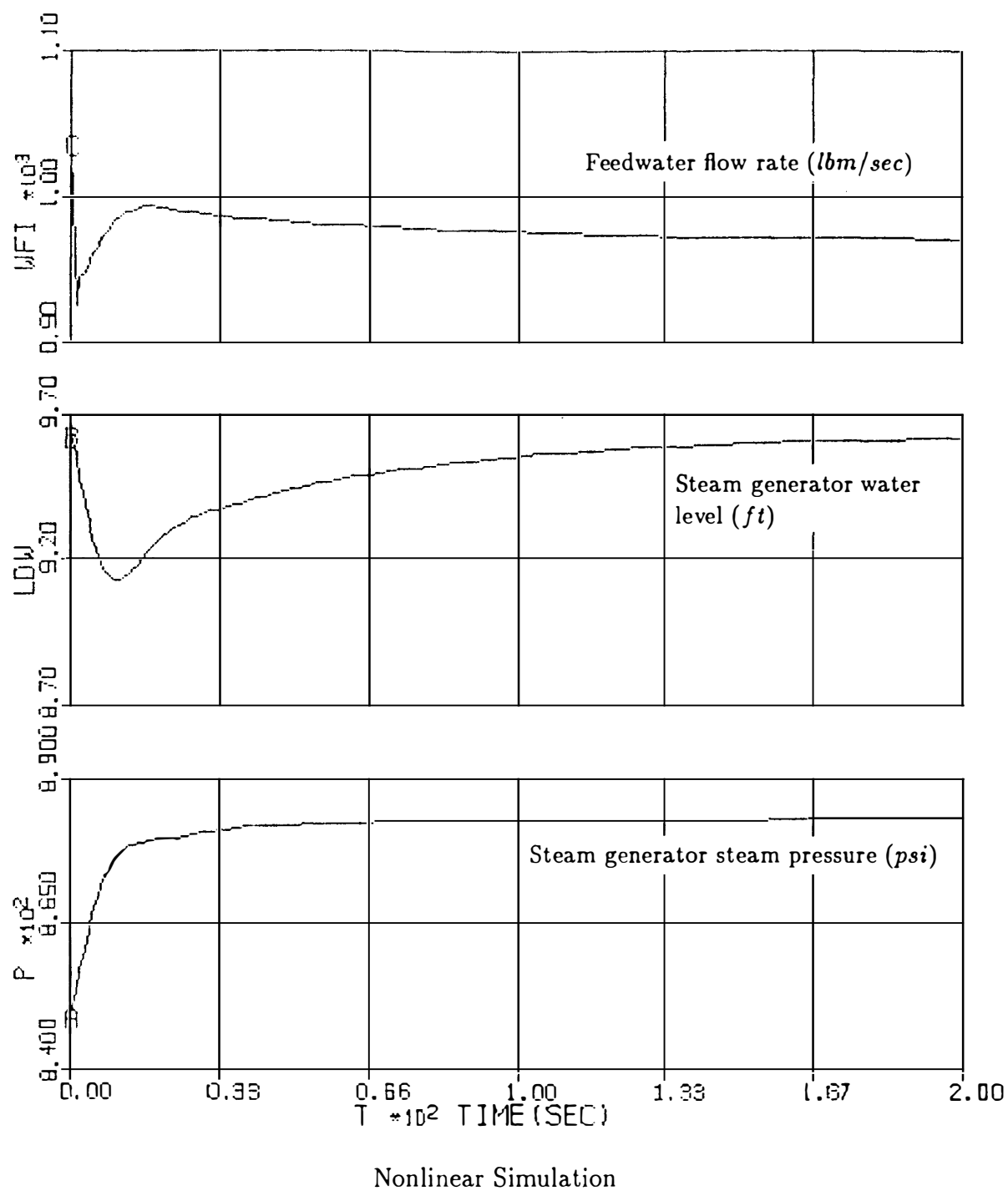
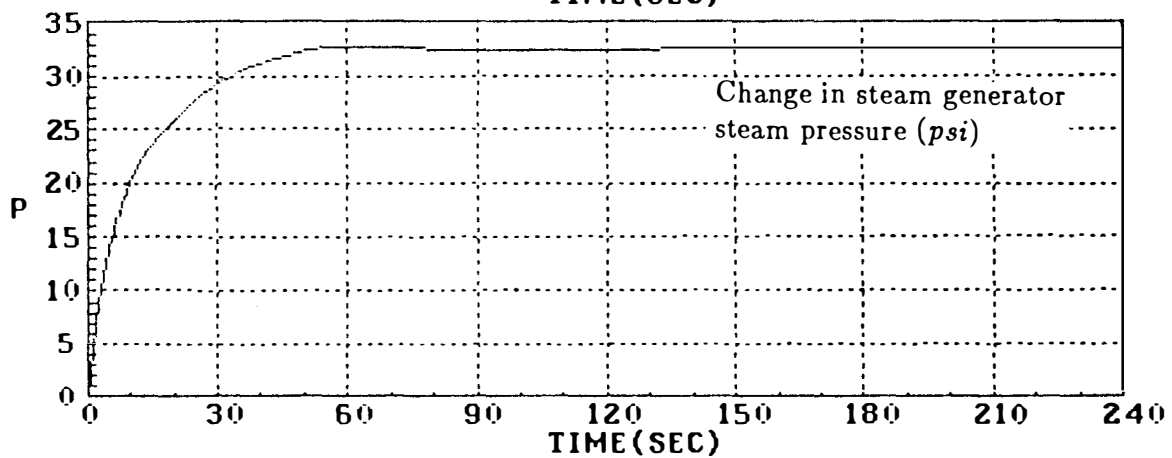
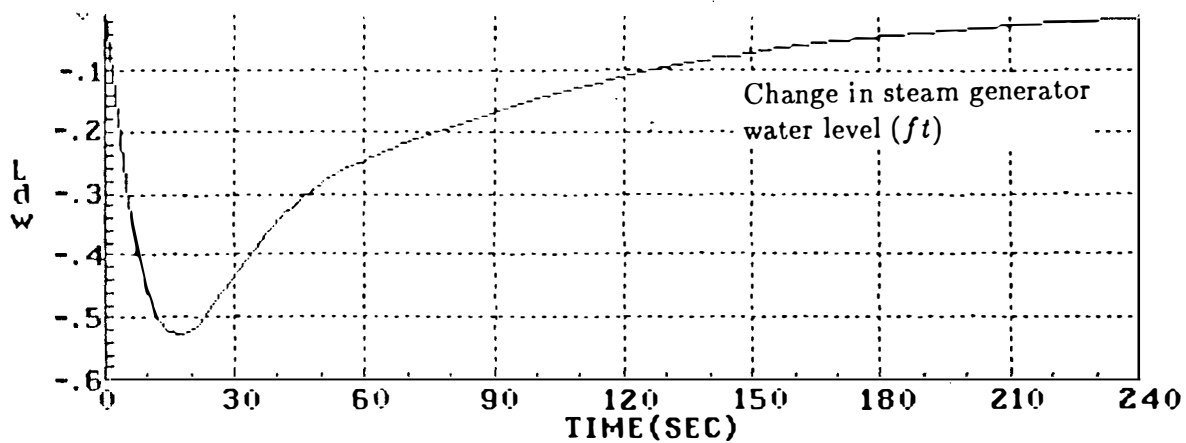
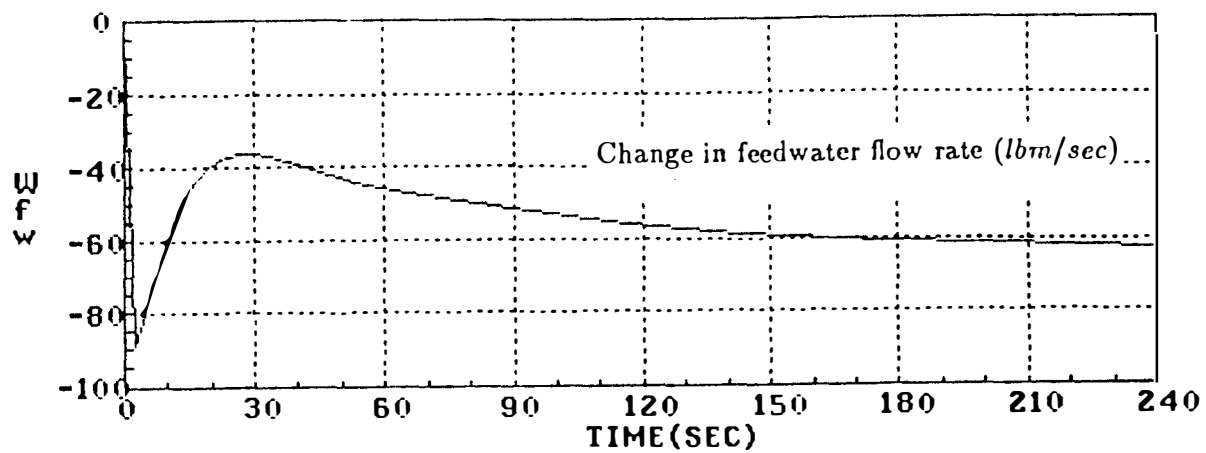
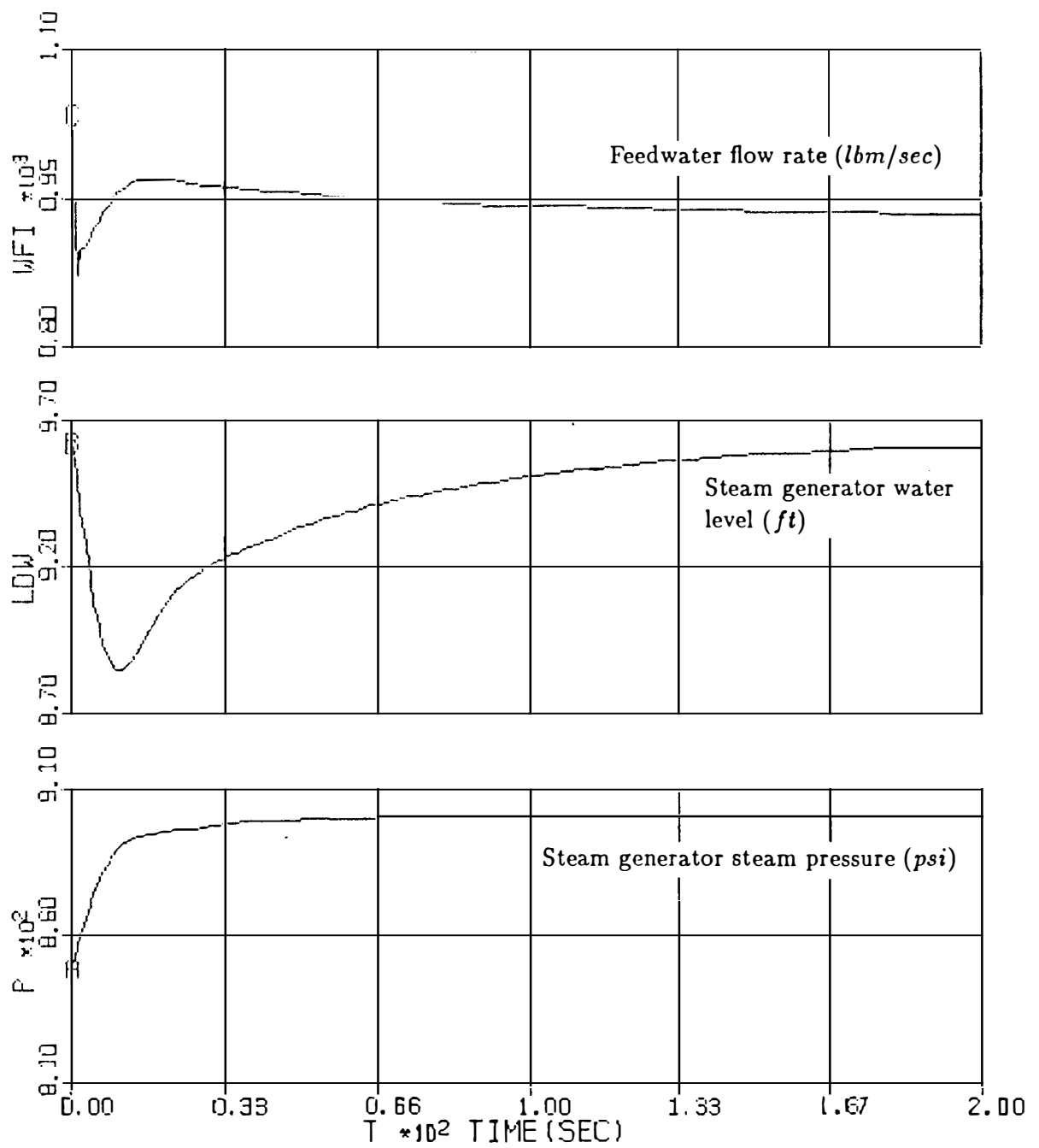


Figure 3.13: Dynamic responses of the linear and nonlinear simulation models of the steam generator to a 10% step decrease in the steam valve coefficient.



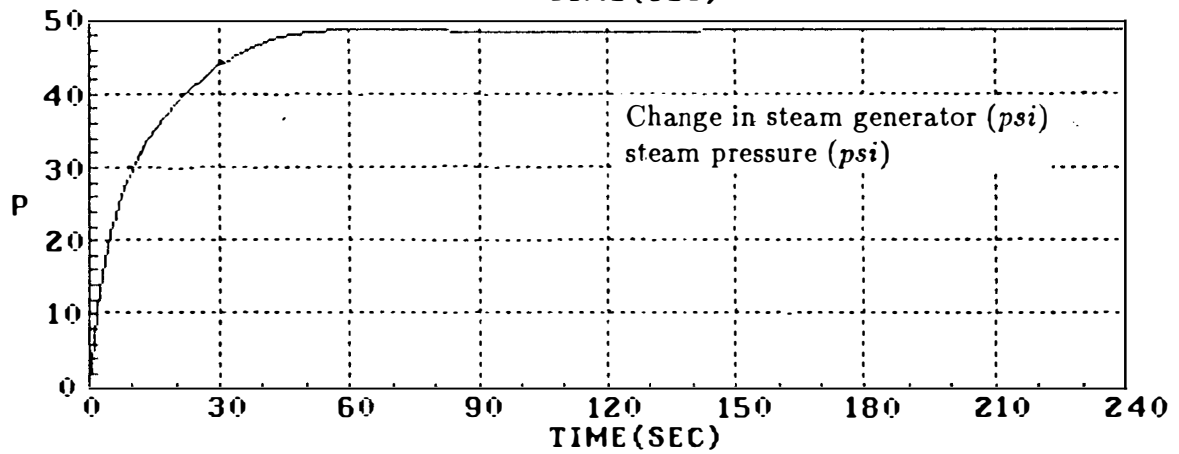
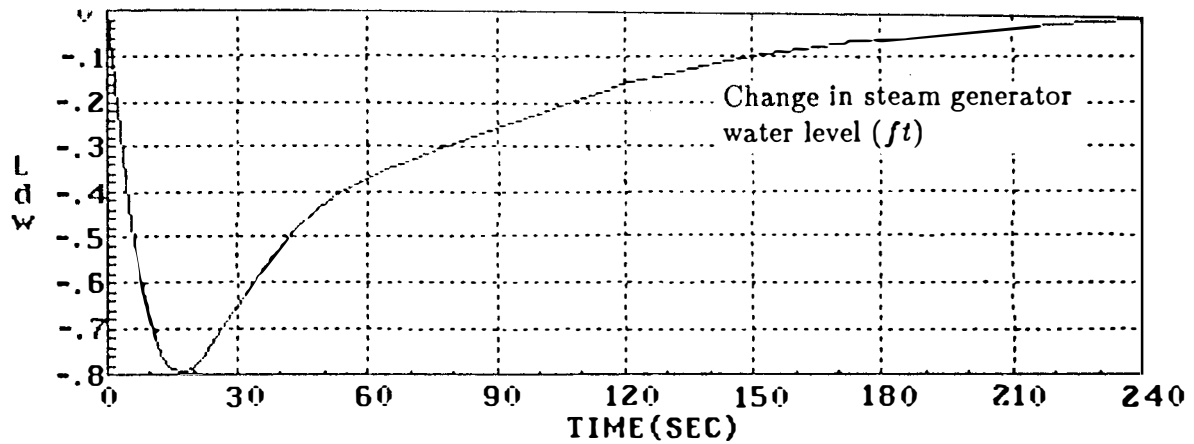
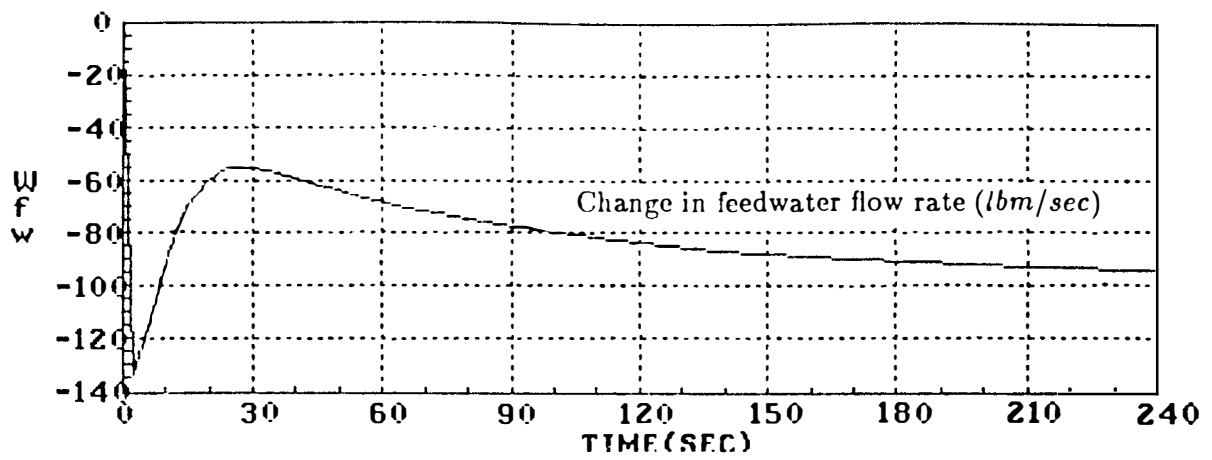
Linear Simulation

Fig. 3.13 (continued)



Nonlinear Simulation

Figure 3.14: Dynamic responses of the linear and nonlinear simulation models of the steam generator to a 15% step decrease in the steam valve coefficient.



Linear Simulation

Fig. 3.14 (continued)

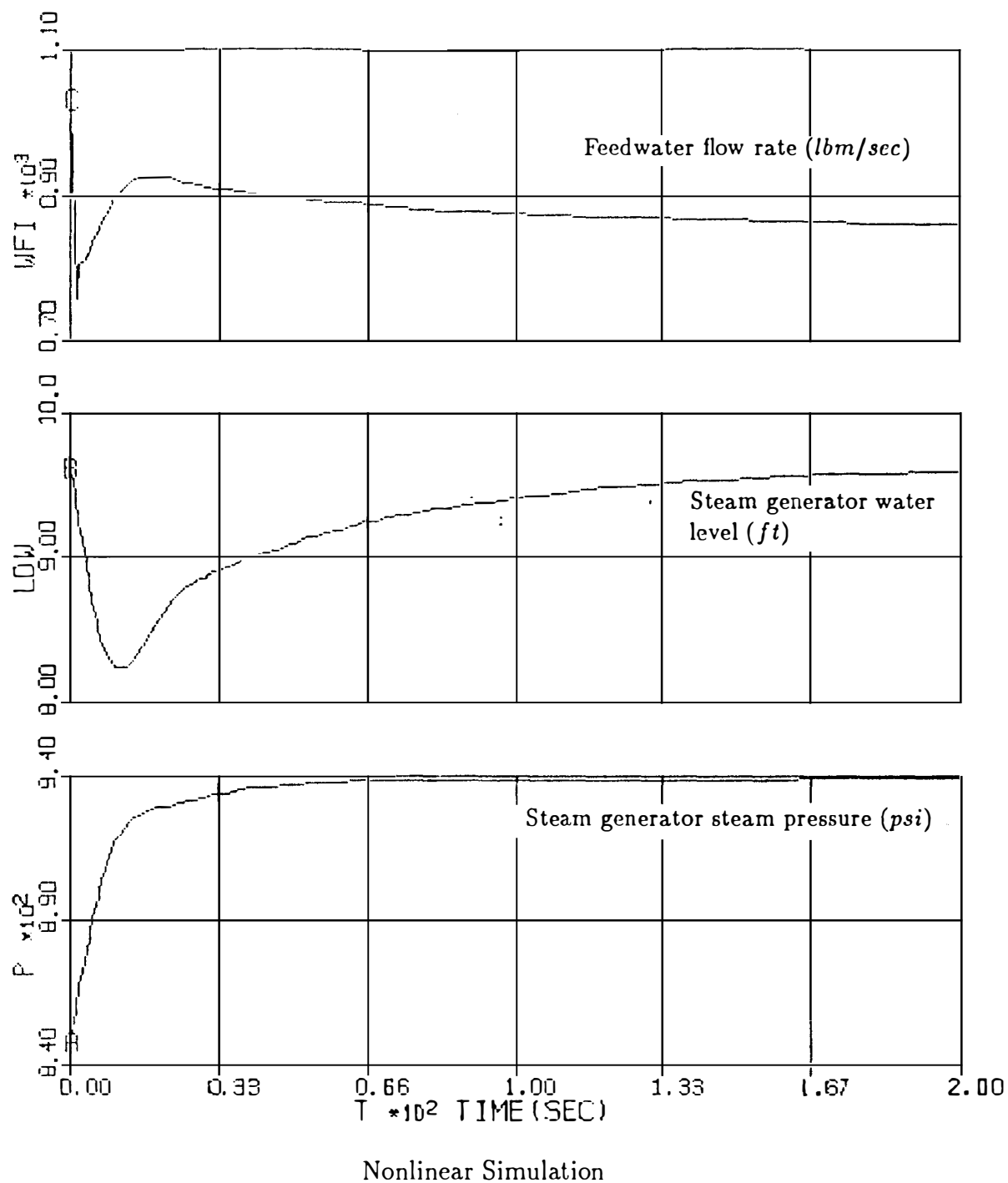
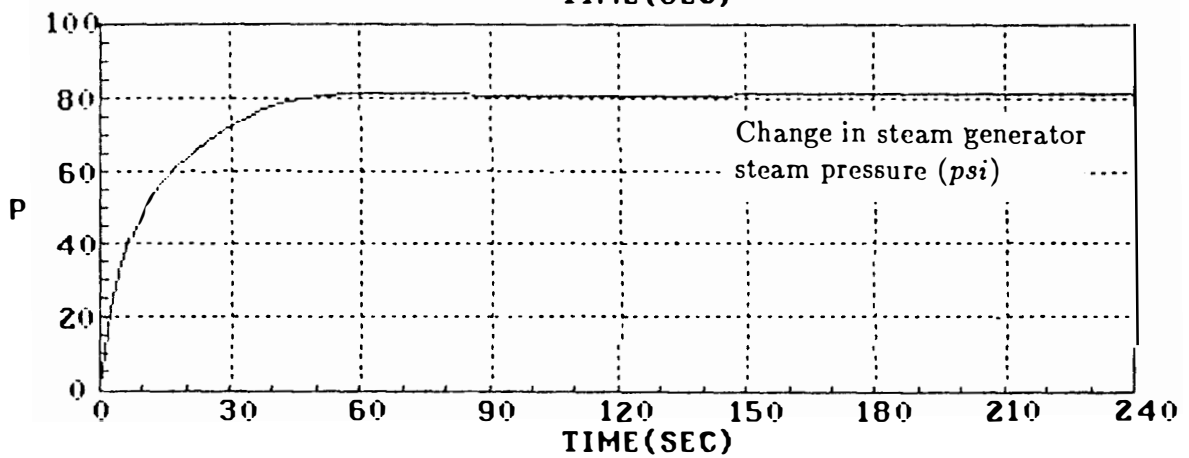
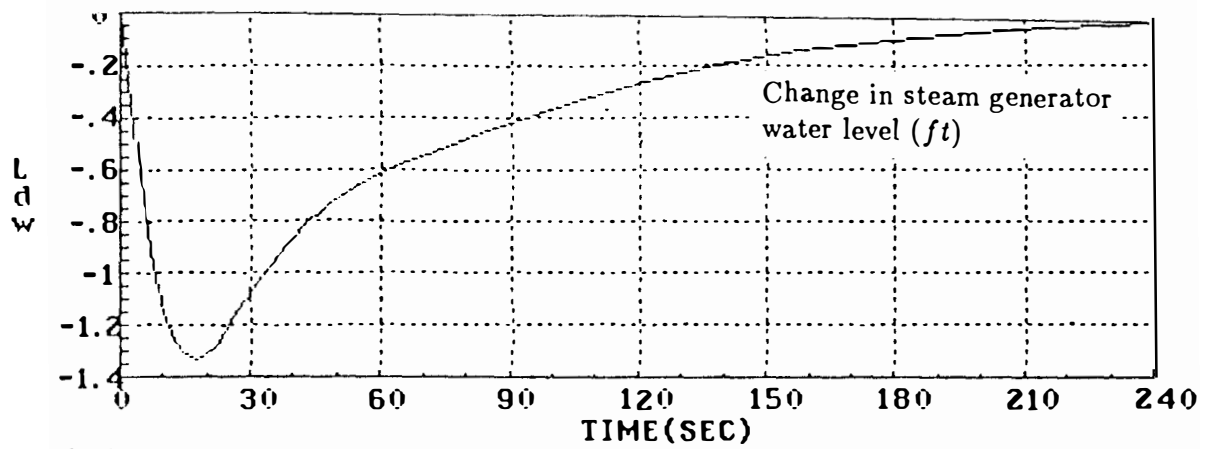
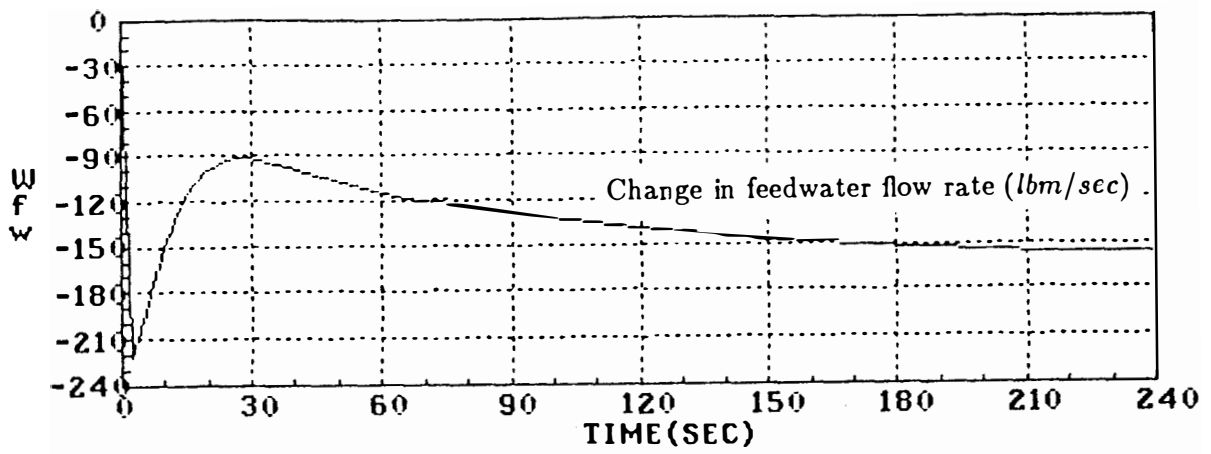


Figure 3.15: Dynamic responses of the linear and nonlinear simulation models of the steam generator to a 25% step decrease in the steam valve coefficient.



Linear Simulation

Fig. 3.15 (continued)

These variables are involved in nonlinear processes more than any other variables in the UTSG model. Therefore, they are used to compare the linear model with the nonlinear model for each case.

For the case of 10% perturbation, the linear model agrees with the nonlinear model (see Fig. 3.13). For the case of 15% perturbation, small differences are observed in the responses of feedwater flow and water level (see Fig. 3.14). In the linear model, the water level decreases by 0.2 *ft* of its set point and the feedwater flow decreases by 89 *lbm/sec* of its initial value. Whereas, in the nonlinear model, these values are 0.01 *ft* and 98 *lbm/sec* respectively. For the case of 25% perturbation, large discrepancies are observed between the responses of the two models (see Fig. 3.15). In the linear model, the water level decreases by 0.33 *ft* of its set point and the feedwater flow reduces by 155 *lbm/sec* of its initial value. While, in the nonlinear model, these values are 0.0133 *ft* and 174 *lbm/sec* respectively. The comparison results indicate that the linear model can not be used for more than 15% perturbations in the steam valve coefficient.

3.3 Pressurizer System

The pressurizer acts both as a control and as a safety component in a PWR plant. This device maintains a desired pressure in the reactor coolant system at steady-state conditions. The pressurizer can accommodate insurge or outsurge flows, about a prescribed pressure limit, during transient operating conditions of the plant.

A typical pressurizer is a vertical cylindrical vessel with two hemispherical heads at the top and bottom. The pressurizer is equipped with a set of electrical heater banks immersed at the bottom head and a spray nozzle and relief valves at the top head. The heaters are designed to be replaceable for the maintenance purposes. The pressurizer is installed in one of the hot leg pipings in the primary side of a PWR system. It usually contains 60% water and 40% steam at saturation conditions at full power operation. Typical design parameters of a pressurizer are shown in Table A.3 of Appendix A. A general schematic of the pressurizer is depicted in Fig. 3.16.

When a change of load occurs in a PWR plant, the coolant temperature in the primary loop will be changed. The temperature variations will result in a decrease or increase of the coolant volume. Therefore, there will be surges in the pressurizer volume until the system reaches a new steady-state condition. The surges will cause pressure variations in the system. They are controlled by either the pressurizer spray system or heater system. The spray system is actuated when the pressure exceeds a desired value. It condenses the steam by spraying the primary cold leg water into the steam space and thus decreases the pressure. The heater system is initiated when the pressure falls below a desired value. It produces additional water vapor in the pressurizer and thus increases the pressure. The relief valves will be actuated as safety devices when the excess pressure in the pressurizer cannot be controlled by the control system alone.

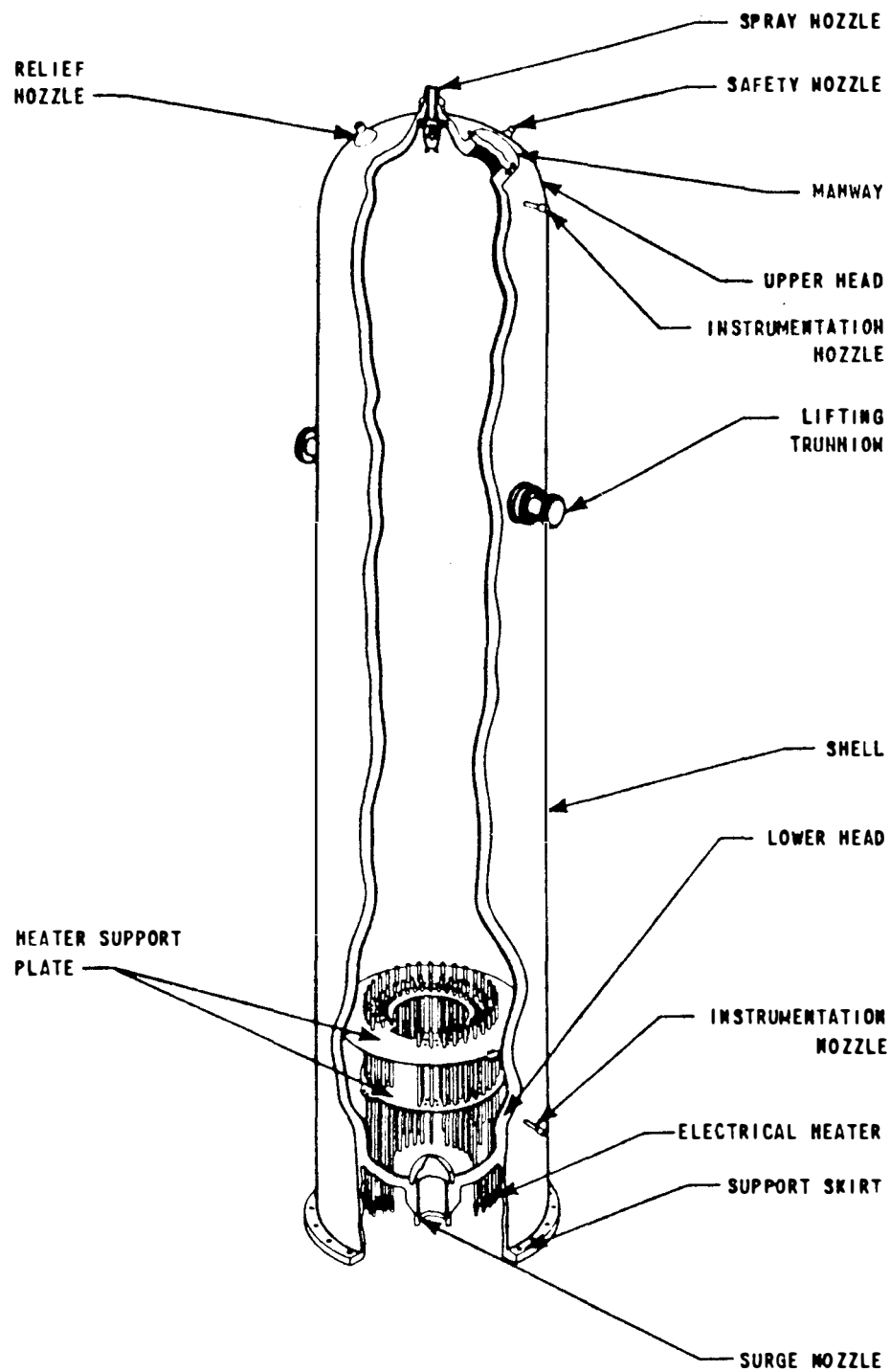


Figure 3.16: A general view of a typical pressurizer used in Westinghouse PWR systems [15].

3.3.1 Pressurizer Model

A theoretical model of a pressurizer, used in this study, has been previously developed by Thakkar [5]. The model can predict dynamic behavior of the pressurizer under steady-state and transient conditions. To improve the performance of the model, modifications are made by the introduction of steam compressibility as functions of thermodynamic properties of water and steam.

The pressurizer model is simulated as a two-phase equilibrium tank where the liquid and steam are considered to be saturated. The conservation equations of mass and energy are applied to the liquid and vapor phases. The governing equations (see Appendix C) are derived by using the following assumptions:

- Insurge flow mixes perfectly with the liquid inside the pressurizer.
- Steam condensation on the vessel wall and mass transfer at the steam-liquid interface is negligible.
- Water and steam properties are assumed to be a linear function of the pressurizer pressure for a range of ± 100 *psi* from the set point (2250 *psi*).
- The initial values of the spray flow rate and heater output do not have any effect on the model.
- Steam flow rate through the relief valves is assumed to be zero.

The pressure variations due to steam compressibility in the pressurizer is determined by taking a volume balance over the entire system.

$$V = V_s + V_w \tag{3.39}$$

where

V = Total volume of the pressurizer.

V_s = Volume of the steam region.

V_w = Volume of the water region.

Differentiating Equation (3.39) with respect to time gives

$$\frac{dV_s}{dt} + \frac{dV_w}{dt} = 0 \quad (3.40)$$

Define water and steam volumes as

$$V_s = M_s \nu_s \quad (3.41)$$

$$V_w = M_w \nu_w \quad (3.42)$$

where

M_s, M_w = Steam and water mass in each phase.

ν_s, ν_w = Specific volumes of the saturated steam and water.

Express the specific volumes as linear functions of the pressure:

$$\nu_s = X_{p1} + K_{p1} P_{pr} \quad (3.43)$$

$$\nu_w = X_{p2} + K_{p2} P_{pr} \quad (3.44)$$

where

X_{p1}, X_{p2} = Constant parameters of the equations.

$$K_{p1}, K_{p2} = \frac{\partial \nu_g}{\partial P_{pr}}, \frac{\partial \nu_f}{\partial P_{pr}}$$

Substituting Equations (3.41) through (3.44) into Equation (3.40) will result in the following equation.

$$\frac{d}{dt}[M_s(X_{p1} + K_{p1}P_{pr})] + \frac{d}{dt}[M_w(X_{p2} + K_{p2}P_{pr})] = 0 \quad (3.45)$$

Finally, the following equation, describing the pressurizer pressure due to the compressibility phenomenon, is extracted from the preceding equation as follows:

$$\frac{dP_{pr}}{dt} = -\frac{(X_{p1} + K_{p1}P_{pr})\frac{dM_s}{dt} + (X_{p2} + K_{p2}P_{pr})\frac{dM_w}{dt}}{M_sK_{p1} + M_wK_{p2}} \quad (3.46)$$

The compressibility equation which has been derived above describes the pressure variations more realistically than the compressibility equation obtained from the gas laws. This is due to the fact that saturated steam does not completely behave as a perfect gas.

The mathematical model of the pressurizer system is shown in Appendix C. It consists of two state variables and a few algebraic equations. The only forcing term in the model is the primary water surge flow.

3.3.2 Pressurizer Control System

A typical pressurizer in a PWR system requires two major control systems, level and pressure. The pressurizer level control system ensures sufficient water inventory for the reactor core coolant system. The pressure control system maintains the coolant pressure within a prescribed limit during steady-state and transient conditions of the plant. The dynamic behavior of the pressure control system will be investigated in this study.

A standard pressure control system has been designed for a pressurizer system by the Westinghouse Corporation [15]. The control system is a proportional-integral-derivative (PID) controller which initiates either the electric heater or spray system when deviations occur in the coolant pressure set point. The Westinghouse documentations [15] present a nonlinear program (see Fig. 3.17) for the gain factors of the PID controller. The program defines the gain factors for the heater and spray systems as a function of coolant pressure. The program indicates that the heater will be actuated when

$$-15 \text{ psi} \leq (P_{pr} - P_{ref}) \leq 15 \text{ psi},$$

and the spray system will be initiated when

$$25 \text{ psi} \leq (P_{pr} - P_{ref}) \leq 75 \text{ psi}.$$

The block diagram representation of the pressurizer control system is shown in Fig. 3.18. The time-domain equations of the PID controller are derived from Fig. 3.18 as follows:

$$Q = G_{he}[(P_{pr} - P_{pr0}) + \frac{D}{\tau_1} + \tau_2 \frac{dP_{pr}}{dt}] \quad (3.47)$$

$$W_{sp} = G_{sp}[(P_{pr} - P_{pr0}) + \frac{D}{\tau_3} + \tau_4 \frac{dP_{pr}}{dt}] \quad (3.48)$$

$$\frac{dD}{dt} = P_{pr} - P_{pr0} \quad (3.49)$$

where

$D_{1,2}$ = Dummy variables.

G_{he} = Gain factor of the heater PID controller.

G_{sp} = Gain factor of the spray PID controller.

Q = Heater output energy.

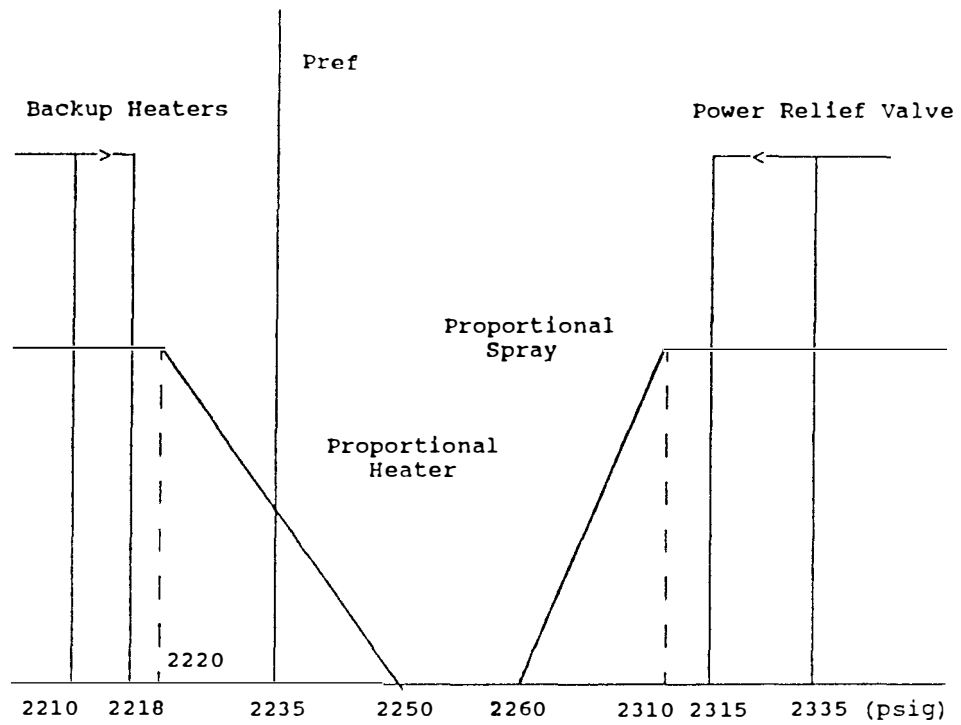


Figure 3.17: Pressurizer pressure control diagram [15].

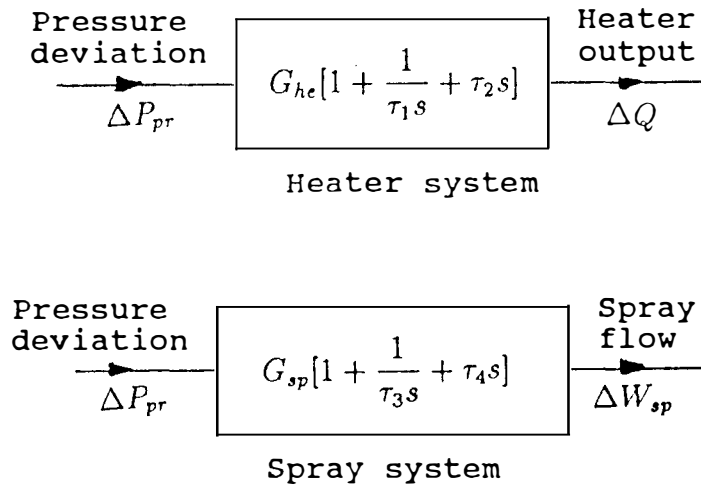


Figure 3.18: Block diagram representation of pressurizer pressure control system.

W_{sp} = Spray flow rate.

$\tau_{1,2}$ = Time constants of the heater PID controller.

$\tau_{3,4}$ = Time constants of the spray PID controller.

The design parameters for the PID controller are taken from Westinghouse documentation [15] and presented in Table A.3 of Appendix A.

The time responses of the pressurizer model, including the control system, due to perturbations in the surge flow are shown in Figs. 3.19-3.21.

For the case of +1 *lbm/sec* surge flow, pressurizer pressure is controlled by the heater control system. The pressure returns to the vicinity of its set point as the heater output reduces. For the case of +50 *lbm/sec* surge flow, the pressure first increases rapidly and then gradually returns to its set point as the spray control system is actuated. For the case of -1 *lbm/sec* surge flow, the pressure first drops below its set point and then returns to its set-point as the heater control system increases the heater output. In all the three cases, one observes that the pressure returns slowly to its set point. This is due to a large time constant (900 *sec*) in the pressurizer control system.

3.4 Reactor Coolant Pump

A large quantity of circulating water is required to remove the fission heat generated in the fuel rods of a PWR reactor core. This service is carried out by reactor coolant pumps, ensuring sufficient flow rate for a nonboiling heat transfer in the reactor vessel. The pumps must also compensate all the hydrodynamic

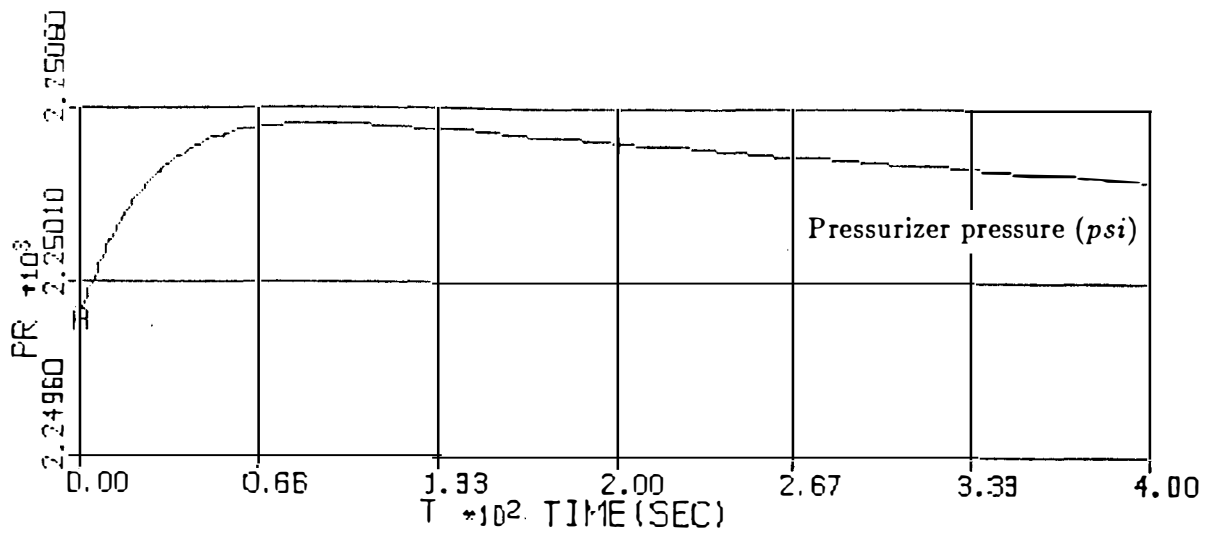


Figure 3.19: Response of the pressurizer nonlinear model to 1 *lbm/sec* surge flow.

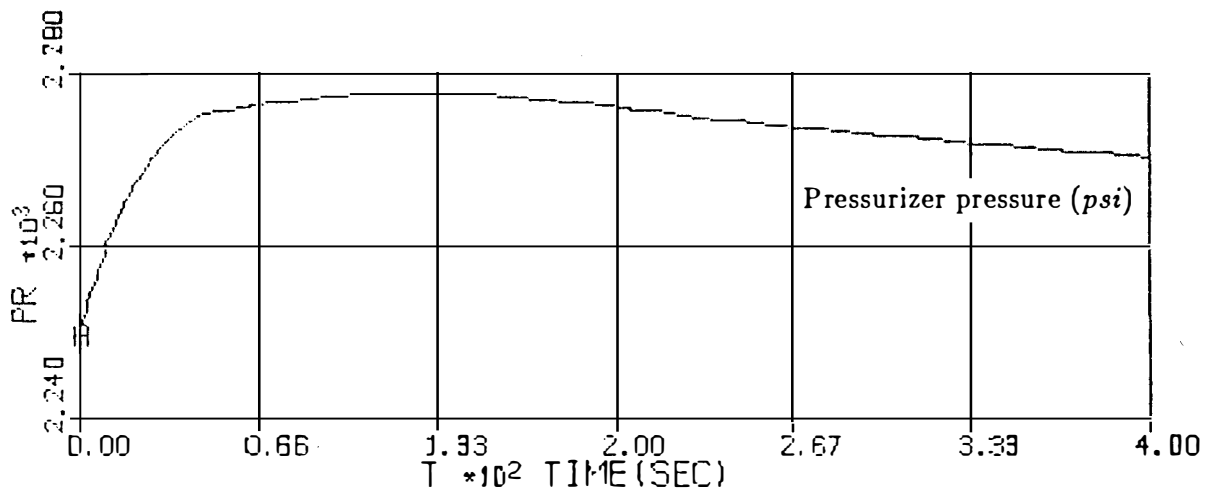


Figure 3.20: Response of the pressurizer nonlinear model to 50 *lbm/sec* surge flow.

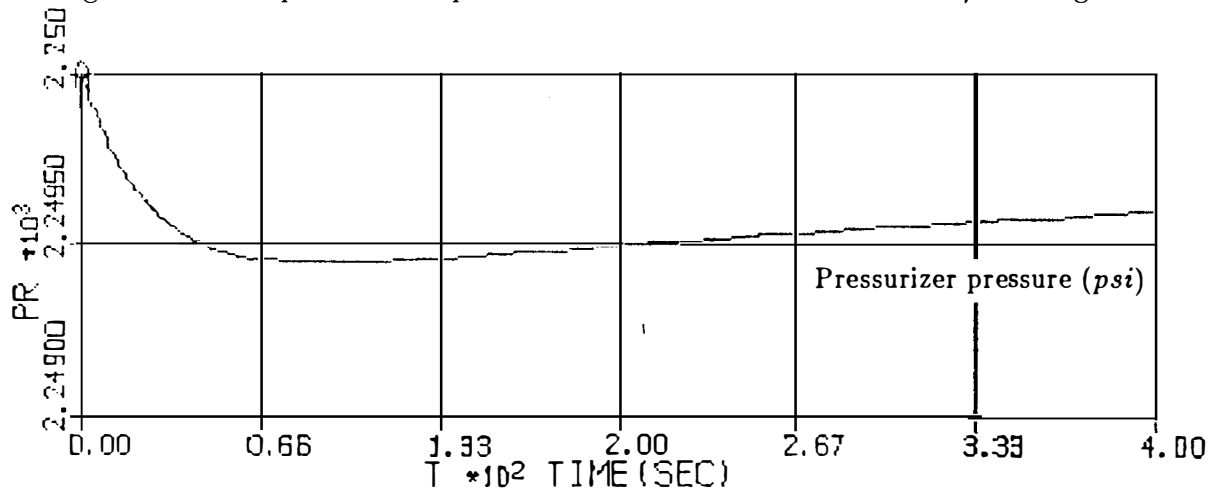


Figure 3.21: Response of the pressurizer linear model to -1 *lbm/sec* surge flow.

pressure drops due to water resistance in the primary loop system.

A typical reactor coolant pump, used in a Westinghouse PWR plant, is a vertical, centrifugal, and motor-driven pump. It is installed in the primary loop of the plant to circulate water in the system. The pump can function under high temperature and pressure with a constant speed. The hydrodynamic performance of the reactor coolant pump is characterized by the performance curve shown in Fig. 3.22. The mathematical description of the curve is used in the pump model.

3.4.1 Model Development of the Coolant Pump

A mathematical model of the reactor coolant pump is developed to predict the performance of the pump under steady-state and transient conditions. The model is simulated in a typical primary loop of a PWR system, in order to consider the effect of fluid inertia and system pressure drop on the model performance. Conservation of mass, momentum, and torque principals are applied to the pump simulation model. The performance curve of the pump for the developed head is expressed in a quadratic form for the pump flow rate. The homologous theory of pumps [17] is used to describe the developed head in terms of the pump speed and flow rate. The governing equations are derived using the following assumptions.

- Pump mechanical and volumetric efficiencies are assumed to be 100%.
- Water leakage is considered to be zero in the system.
- Turbulent flow exists in the system.

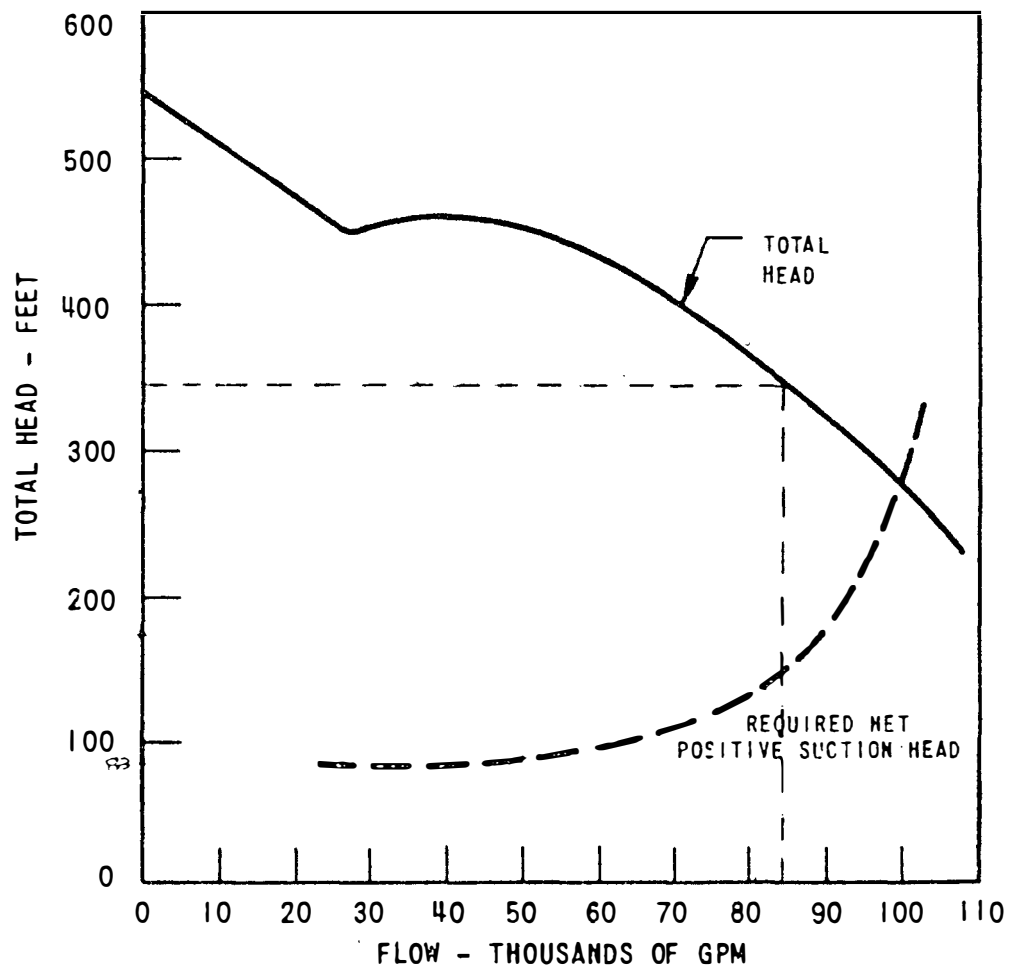


Figure 3.22: Reactor coolant pump characteristic curve [15].

The governing equations of the pump model are derived as follows.

Momentum Equation

$$\frac{d}{dt}(MV) = \rho g A_{ef}(H_p - \sum H_l) \quad (3.50)$$

where

$$M = \rho g L A_{ef} \quad (3.51)$$

$$V = \frac{\dot{Q}}{A} \quad (3.52)$$

$$\sum H_l = K \dot{Q}^2 \quad (3.53)$$

Substituting the above relations into Equation (3.50):

$$\frac{1}{g} \frac{L}{A_{ef}} \frac{d\dot{Q}}{dt} = H_p - K \dot{Q}^2 \quad (3.54)$$

Pump Characteristic Equation

The following fit is made to the curve in Fig. 3.22 ($30 \times 10^3 \text{ gpm} \leq \dot{Q} \leq 90 \times 10^3 \text{ gpm}$).

$$H_s(\dot{Q}) = A \dot{Q}_s^2 + B \dot{Q}_s + C \quad (3.55)$$

Pump Homologous Equations [17]

$$\frac{H_p}{H_s} = \left(\frac{N_p}{N_s}\right)^2 \quad (3.56)$$

$$\frac{\dot{Q}_p}{\dot{Q}_s} = \frac{N_p}{N_s} \quad (3.57)$$

Substituting Equations (3.56) and (3.57) into Equation (3.55)

$$H_p(\dot{Q}, N) = A \dot{Q}_p^2 + B \dot{Q}_p \left(\frac{N_p}{N_s}\right) + C \left(\frac{N_p}{N_s}\right)^2 \quad (3.58)$$

The preceding equation describes the hydrodynamic characteristic of the reactor coolant pump under different speeds and flow rates.

Pump Torque Equation

$$2\pi I \frac{dN_p}{dt} = T_d - T_h \quad (3.59)$$

where

$$T_d = \frac{P_d}{2\pi N_p} \quad (3.60)$$

$$T_h = \frac{\rho g Q_p H_p}{2\pi N_p} \quad (3.61)$$

Substituting the above equations into Equation (3.59):

$$\frac{dN_p}{dt} = \frac{P_d}{(2\pi)^2 N_p I} - \frac{\rho g Q_p H_p}{(2\pi)^2 N_p I} \quad (3.62)$$

Equations (3.54), (3.58) and (3.62) describe the mathematical model of the reactor coolant pump. The definitions of the variables used in the pump model equations are given in Table 3.5. The design parameters used in the pump model are shown in Table A.4 of Appendix A.

A typical response of the coolant pump model due to a 100% step decrease in the supplied power is shown in Fig. 3.23. The response curve shows that the pump flow rate is reduced by 83% of its initial value during 80 sec of the transient time. It also shows that the response characteristic is similar to the response of a first order system. Therefore, it is possible to evaluate a time constant for the

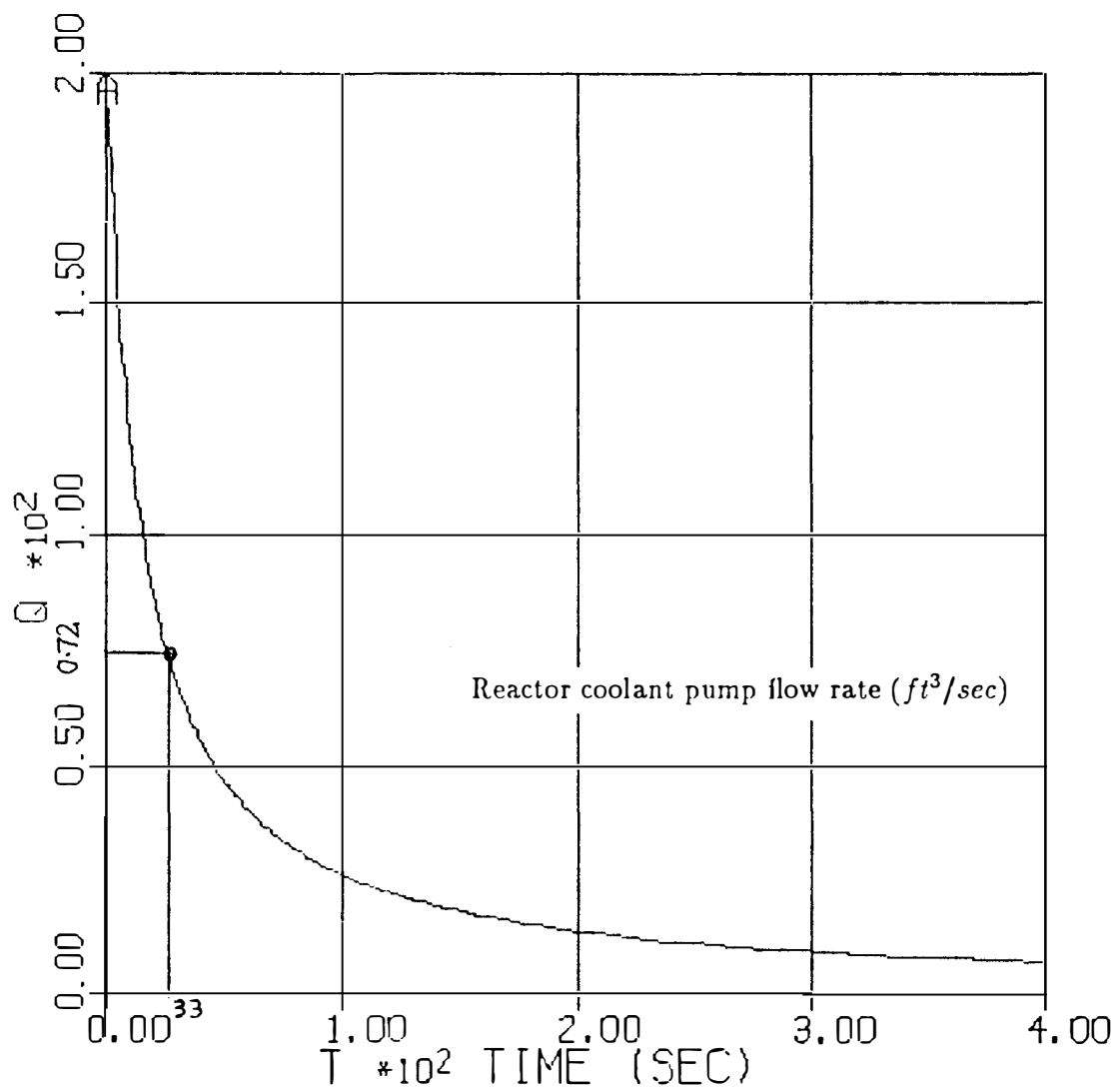


Figure 3.23: Dynamic response of the reactor coolant pump to a 100% step decrease in the supplied power.

pump system. Figure 3.23 shows that the time constant is approximately 33 sec which means that the large inertia of the pump-motor system is responsible for the large time constant.

3.5 Summary

The model development of the primary loop was presented in this chapter. This included models for reactor, steam generator, pressurizer, and reactor coolant pump. The models for the reactivity, steam generator water level (three-element controller), and pressurizer pressure control systems were also discussed.

The time responses of the nonlinear models of the primary loop components were also studied. The analysis of the responses showed the expected behavior during steady-state and transient conditions.

A comparison between linear and nonlinear models of both the reactor and steam generator systems was also made in this chapter. The comparison of results of the reactor core models proved the similarity of the responses using linear and nonlinear simulation. For the steam generator case, the comparison results indicated that linear model can not be used for more than 15% perturbations in the steam valve coefficient.

Table 3.5: Reactor Coolant Pump Variables

<i>Variable</i>	<i>Definition</i>
1. A, B, C	Constant parameters of the pump characteristic equation
2. A_{ef}	Effective area of the piping in the primary side
3. g	Acceleration due to gravity
4. H_t	Total hydrodynamic head losses in the primary side
5. H_p	Developed pump head
6. I	Pump-motor moment of inertia
7. L	Effective length of pipings in the primary loop
8. K	Friction factor coefficient
9. N_s	Nominal pump speed
10. N_p	Actual pump speed
11. \dot{Q}_p	Actual pump flow rate
12. Q_s	Nominal pump flow rate
13. P_d	Power delivered to the pump shaft
14. T_d	Torque delivered to the pump shaft
15. T_h	Hydrodynamic torque
16. ρ	Density of water

CHAPTER 4

MODEL DEVELOPMENT OF THE SECONDARY LOOP

The model development of the secondary side (Balance of Plant) components of a PWR plant is presented in this chapter. It describes models for turbine, condenser, and turbine speed control system. These models then are combined to construct the overall model of the secondary side system. The overall model is used to predict the behavior of the system in the time-domain. Typical responses of the secondary side simulation model are shown at the end of the chapter.

4.1 Steam Turbine System

A steam turbine, used in a steam power plant, is one in which the thermal energy of the supplied steam is converted to mechanical energy on the turbine shaft. High pressure and temperature steam, produced in the steam generator, is supplied to the steam turbine as a *working fluid*. The steam passing through the steam turbine is expanded and thus generates mechanical energy on the turbine shaft. The turbine drives an electric generator to produce electrical power.

A typical turbine system, used in a Westinghouse PWR plant, is applied in this study. The turbine consists of four major parts as follows:

- high pressure (HP) turbine,
- moisture separator,
- reheater, and
- low pressure (LP) turbine.

Four steam generators supply saturated steam to the main turbine. A portion of this steam is bypassed to a high pressure feedwater heater to improve the thermal efficiency of the turbine cycle.

The flow diagram representation of the turbine is depicted in Fig 4.1. The diagram is based on a typical regenerative turbine mass flow cycle of a Westinghouse [15] PWR system.

Steam enters the turbine at state 1. After expansion to state 2 in the high pressure turbine, a portion of the steam is extracted and passed to the high pressure feedwater heater. The remainder enters the moisture separator at state 3. As the steam passes through the moisture separator, the water is removed and fed to the high pressure feedwater system at state 4. The remaining steam is superheated in the steam heater to state 5. At this point, it enters the low pressure turbine where a portion of it is extracted for a low pressure feedwater heater (state 6). The remaining steam is expanded in the low pressure turbine and exhausted at state 7 to a condenser system. This describes the steam flow path in the turbine system.

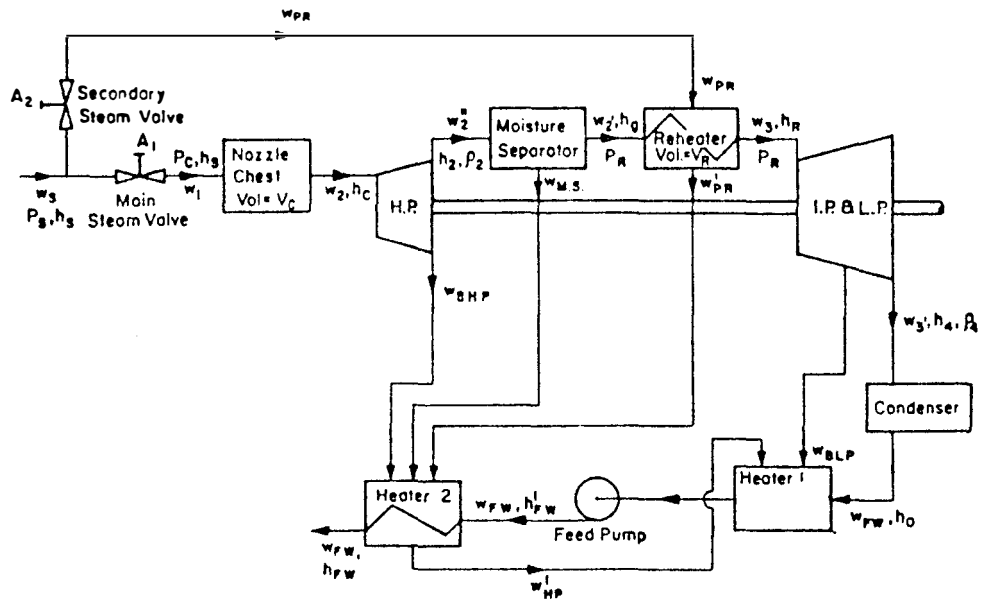


Figure 4.1: Flow diagram representation of a turbine cycle [6].

4.1.1 Turbine Model

A dynamic model of a turbine cycle has been developed previously by Shankar [6]. The turbine cycle model incorporates models for the nozzle chest, high pressure turbine, moisture separator, reheater, low pressure turbine, and low and high pressure feedwater heaters. The model development of the turbine system incorporates the following assumptions:

- Reversible adiabatic expansion process exists in the nozzle chest and moisture separator.
- Thermodynamic properties of the saturated steam and water are assumed to be linear functions of the steam pressure at each state.
- The bypass flow to the reheater is proportional to the main steam pressure and steam valve coefficient.
- Heat transfer coefficients for the reheater and feedwater heaters are assumed to be constant.
- Steam flow losses in the turbine system are considered to be zero.

To simplify the model complexity, modifications have been made for the evaluation of HP and LP turbine efficiencies. The efficiencies of high- and low-pressure turbines are considered to be constant within a range of ± 100 *psi* deviations in the exhaust pressure of the high pressure turbine from its initial value (at full power of operating condition of the plant). They are defined to be:

$$\eta_{hp} = \frac{h_c - h_2}{h_c - h'_2} \quad (4.1)$$

$$\eta_{lp} = \frac{h_r - h_4}{h_r - h'_4} \quad (4.2)$$

where

η_{hp} = High pressure turbine efficiency.

η_{lp} = Low pressure turbine efficiency.

h_2, h_4 = Steam enthalpy leaving the high-and low-pressure turbine
at points 2 and 4 respectively.

h'_2, h'_4 = Isentropic enthalpy at points 2 and 4.

h_c = Steam enthalpy leaving the nozzle chest.

The actual steam enthalpies at points 2 and 4 are derived from the preceding equations as follows.

$$h_2 = h_c - \eta_{hp}(h_c - h'_2) \quad (4.3)$$

$$h_4 = h_r - \eta_{lp}(h_r - h'_4) \quad (4.4)$$

The above relations are used to determine the output power of the turbine system. The governing equations of the turbine model are shown in Appendix D. The turbine design parameters are given in Table A.5 of Appendix A.

4.1.2 Main Condenser

A condenser is a large surface-type heat exchanger, which condenses steam from the exhaust of turbine by transferring steam latent heat to a circulating water inside the condenser. The condenser is desired to work under vacuum condition to obtain a maximum mechanical power from the turbine system.

A typical condenser, used in the Westinghouse [15] PWR systems, is applied for this study. The condenser is a surface type-heat exchanger with a single pass circulating water. Three hotwells, located at the bottom of the condenser, store the condensed water within a prescribed level limit. The main condenser is equipped with many auxiliary systems such as vacuum and hotwell pumps. The vacuum system maintains a constant pressure in the condenser for transient and steady-state conditions. The hotwell pumps and their control systems discharge the water to a low-pressure heater and control the water level in the hotwells.

A dynamic model of the main condenser is developed for this study. The model is used to predict the temperature variations of the condenser outlet water under transient and steady-state conditions.

4.1.3 Condenser Model Development

The main condenser is simulated as an equilibrium two-phase tank (see Fig 4.2). The space inside of the tank is divided into two independent control volumes, steam and water. They are assumed to be in thermal equilibrium during steady-state condition. Turbine exhaust flow enters the system at the condenser pressure. The water part of the flow falls into the hotwell region and mixes perfectly with the water already present there. The vapor part condenses on the outer surface of metal tubes through which the circulating water flows. The condensation process is associated with a time delay which is due to the dynamics of heat transfer between the vapor and the circulating water [22]. The following assumptions are made to simplify the mathematical model.

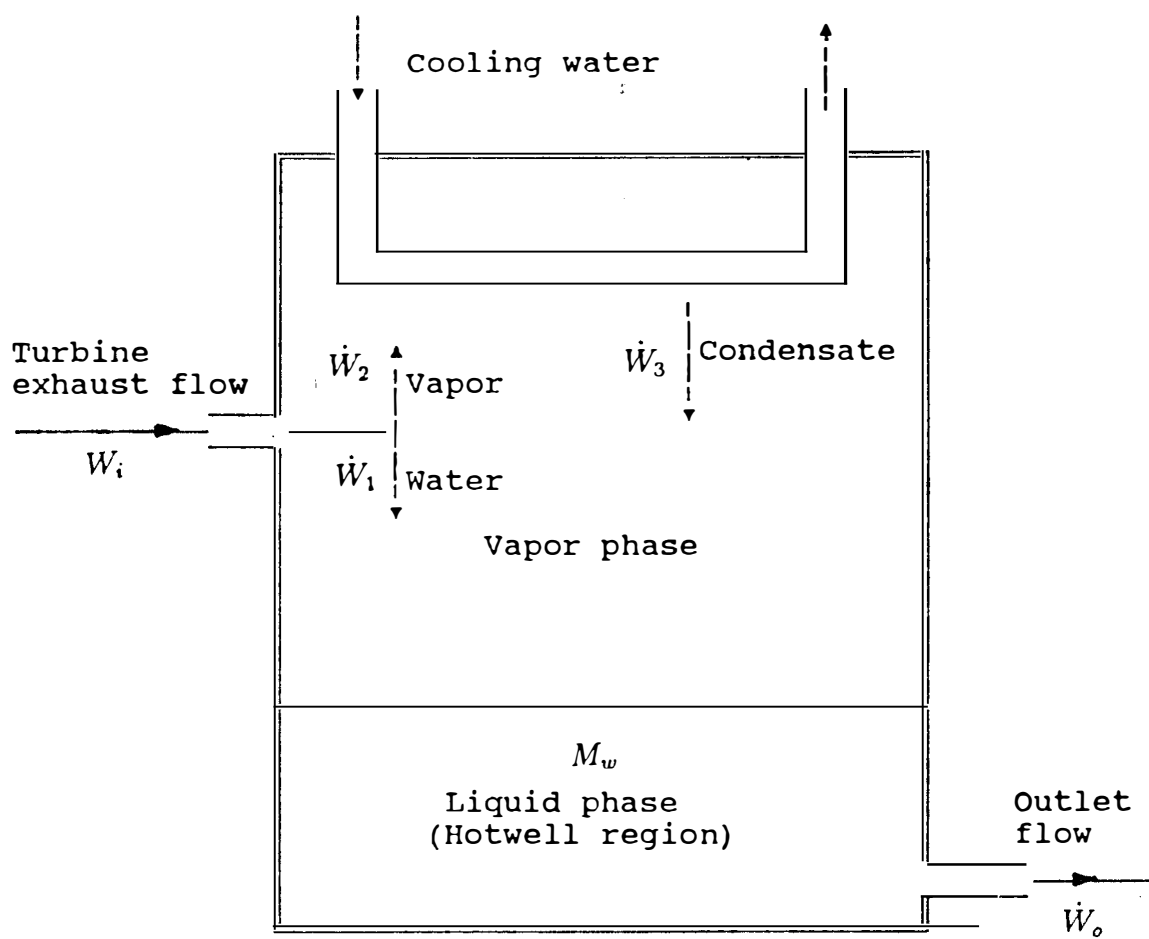


Figure 4.2: Schematic diagram of the turbine condenser model.

- Constant pressure exists in the condenser model.
- Mass transfer at steam-liquid interface is assumed to be negligible.
- Wall condensation is considered to be zero.

The describing equations of the model are derived based on the conservation of mass and energy equations at each phase. These equations are introduced below.

Mass Balance

Liquid phase

$$\frac{dM_w}{dt} = \dot{W}_1 + \dot{W}_3 - \dot{W}_o \quad (4.5)$$

where

M_w = Water mass inside the condenser.

\dot{W}_1 = Water droplet rate into the hotwells.

\dot{W}_3 = Water condensation flow rate.

\dot{W}_o = Outlet flow rate to the low pressure feedwater.

Vapor phase

$$\frac{d\dot{W}_3}{dt} = \frac{\dot{W}_2 - \dot{W}_3}{\tau_{co}} \quad (4.6)$$

where

\dot{W}_2 = Steam flow rate in the condenser.

τ_{co} = Time constant of the condensation process.

Energy Equation

$$\frac{d}{dt}(M_w h_o) = (\dot{W}_1 + \dot{W}_3)h_f - \dot{W}_o h_o \quad (4.7)$$

Or

$$h_o \frac{dM_w}{dt} + M_w \frac{dh_o}{dt} = (\dot{W}_1 + \dot{W}_3)h_f - \dot{W}_o h_o \quad (4.8)$$

where

h_f = Enthalpy of the saturated water.

h_o = Enthalpy of the outlet water.

Substituting Equation (4-5) into Equation (4-8)

$$\frac{dh_o}{dt} = \frac{(\dot{W}_1 + \dot{W}_3)(h_f - h_o)}{M_w} \quad (4.9)$$

Constitutive Relations

Mass Balance

$$\dot{W}_1 = \dot{W}_i - \dot{W}_2 \quad (4.10)$$

where

$$\dot{W}_2 = \dot{W}_i \frac{(h_i - h_f)}{h_{fg}} \quad (4.11)$$

\dot{W}_i = Entering flow rate to the condenser.

h_{fg} = Latent enthalpy of the water.

h_i = Enthalpy of the entering flow rate.

The preceding equations describe the mathematical model of the main condenser.

The design parameters of the model are shown in table A.5 of appendix A.

4.1.4 Turbine Speed Control System

The electrical generator coupled to the turbine system produces electricity at a constant frequency. The frequency stays constant if the turbine shaft speed remains constant. If a speed control system does not exist, the turbine speed will vary in accordance with the turbine load. Therefore, a speed control system is designed to maintain a constant turbine speed by regulating the amount of steam flow to the turbine.

Figure 4.3 shows a generalized block diagram of a typical speed control system for a steam turbine. The control system includes three major components: speed set point element, speed sensor, and a hydraulic PI controller. Initially, the speed is set at a reference value (3600 rpm). This value corresponds to the design frequency of the electrical generator. The speed sensor which is connected to the turbine shaft provides an actuating signal to the comparator device as the turbine speed deviates from its set point. The speed error signal (difference between speed set point and actual speed signals) initiates the hydraulic system to the action. The actuated hydraulic system provides sufficient power for rapid movement and accurate positioning of the steam valve system. Any changes at the steam valve position will be proportional to the turbine output torque which ultimately regulates the speed.

The block diagram representation of the speed control system is given in Fig. 4.4. The time-domain equations of the control system are derived from Fig. 4.4 as follows.

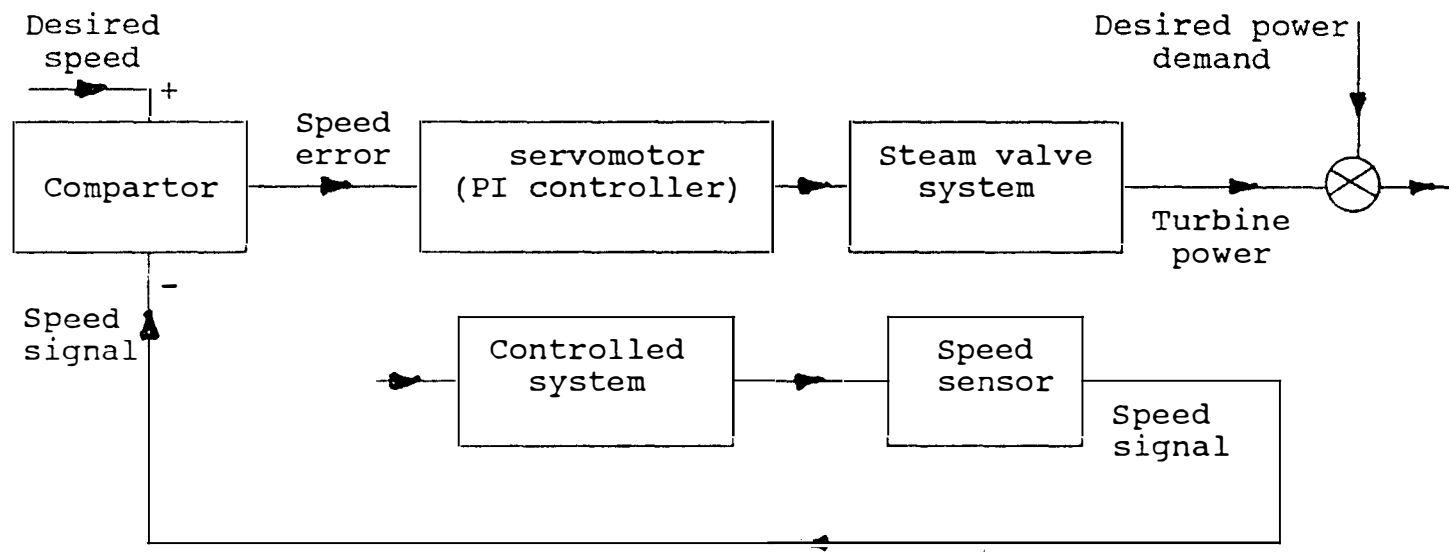


Figure 4.4: Block diagram representation of a turbine speed control system.

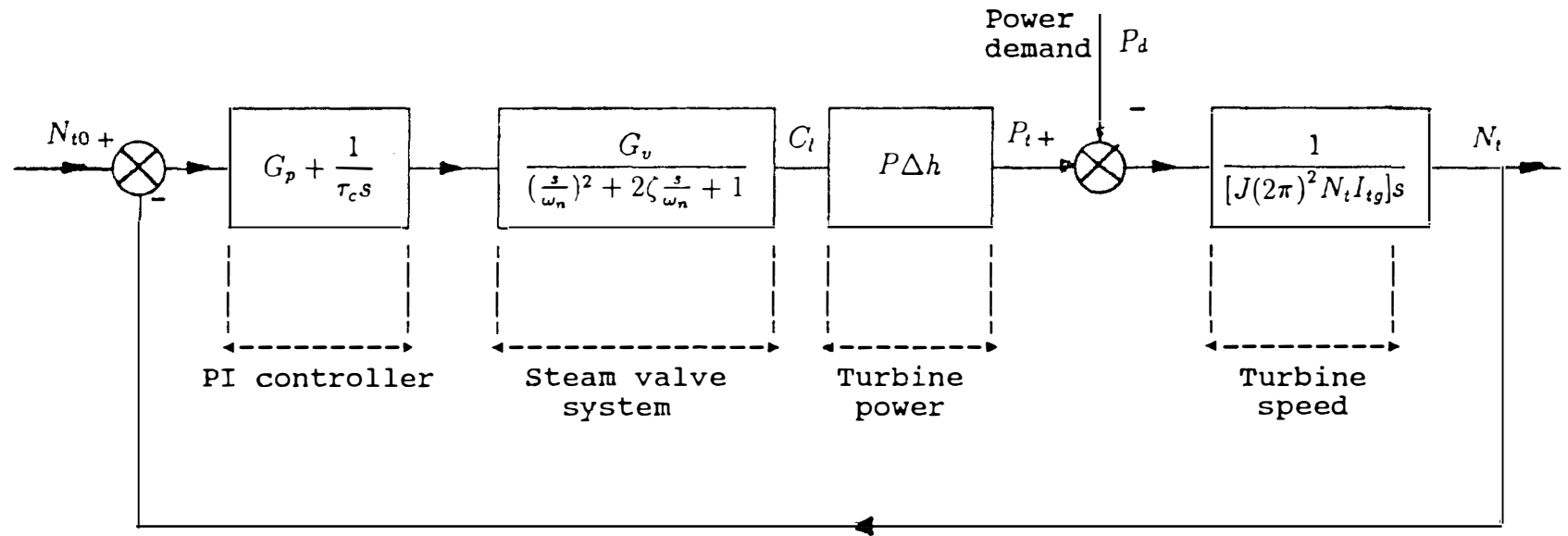


Figure 4.4: Block diagram representation of a turbine speed control system.

PI Controller Equation

$$\frac{dU}{dt} = G_p * \frac{dN_t}{dt} + \frac{N_t - N_{t0}}{\tau_c} \quad (4.12)$$

where

G_p = Gain factor of the PI controller.

N_t = Turbine speed.

U = Control signal.

τ_c = Time constant of the controller element.

Steam Valve Equation

$$\frac{d^2 C_l}{dt^2} + 2\zeta\omega_n \frac{dC_l}{dt} + \omega_n^2 (C_l - C_{l0}) = G_v \omega_n^2 U \quad (4.13)$$

where

C_l = Steam valve coefficient.

G_v = Gain factor of the steam valve system.

ω_n = Natural frequency of the steam valve system.

ζ = Damping ratio of the steam valve system.

Turbine Power Equation

$$P_t = C_l P \Delta h \quad (4.14)$$

where

P = Steam pressure of the steam generator.

P_t = Turbine output power.

Δh = Overall enthalpy drop in the turbine.

Turbine Inertia Equation

$$2\pi I_{tg} \frac{dN_t}{dt} = T_t - T_d = \frac{P_t - P_d}{2\pi N_t J} \quad (4.15)$$

$$\frac{dN_t}{dt} = \frac{P_t - P_d}{J(2\pi)^2 N_t I_{tg}} \quad (4.16)$$

where

J = Conversion factor of the equation.

I_{tg} = Moment of inertia of the turbine-generator.

P_d = Power demand.

T_d = Torque demand.

T_t = Turbine output torque.

The design parameters of the control system are optimized by a computer program in the balance of plant model. These parameters are shown in Table 4.1. Note that since the time constant of the governor is so small, it is considered as a part of the PI controller time constant.

Table 4.1: Design Parameters of the Turbine Speed Control System

1.	Gain factor of the PI controller, G_p	1.65
2.	Time constant of the controller element, $\tau_c(sec)$	4
3.	Gain factor of the steam valve system, G_v	1.5
4.	Natural frequency of the steam valve system, $\omega_n(rad/sec)$	9.75
5.	Damping ratio of the steam valve system, ζ	0.67

4.2 Balance of Plant Simulation Model

The overall simulation model of the balance of plant is developed by combining the individual models of turbine system, condenser, and speed control system. The model includes 12 state variables, 7 algebraic variables, and 1 forcing function. The forcing function is a power demand signal which perturbs the model variables.

Typical simulation results of the secondary side response system due to a 15% step decrease in the power demand are shown in Fig. 4.5.

The investigation of responses shows that as the power demand decreases, the turbine speed deviates from its set point momentarily (due to torque imbalance). This constitutes an error signal in the turbine speed control system which ultimately actuates the steam valve system. As a result of turbine speed control action, the steam valve coefficient reduces rapidly to $0.8 \text{ lbm/sec} - \text{psi}$ and then stabilizes at $1.09 \text{ lbm/sec} - \text{psi}$. This causes a steam flow rate reduction to the turbine system and thus a reduction in the turbine power. It also causes a reduction in the heat flow to the HP and LP feedwater heaters which consequently decreases the feedwater temperature. The analysis of the responses also indicates that the steam pressure at HP and LP turbine nozzles reduces to 725 psia and 128.5 psia , respectively.

4.3 Summary

In this chapter, the model development of the Balance of Plant (BOP) system has been described. The overall BOP model incorporates the subsystem models

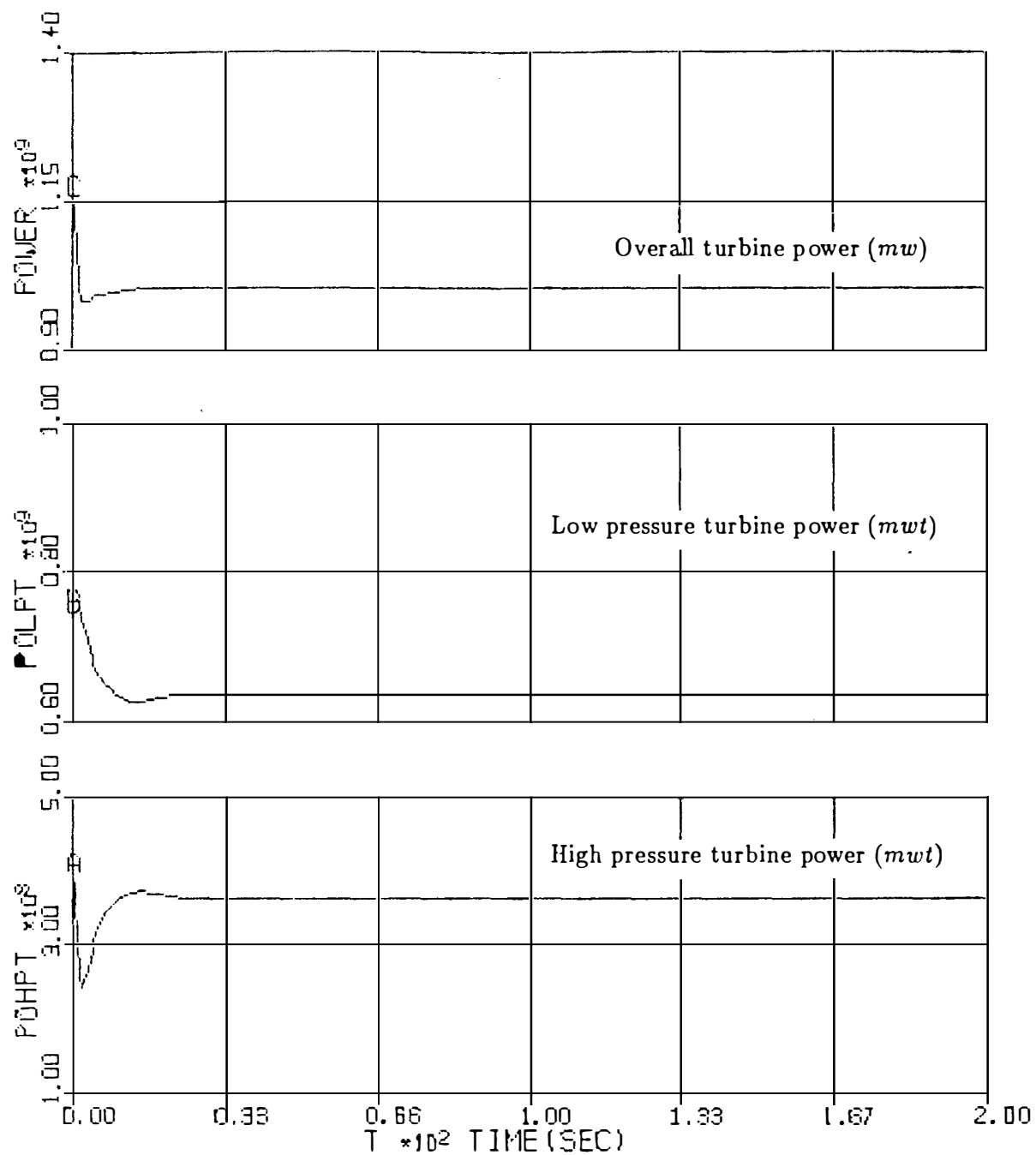


Figure 4.5: Typical responses of the secondary loop of the PWR system to a 15% step decrease in the power demand signal.

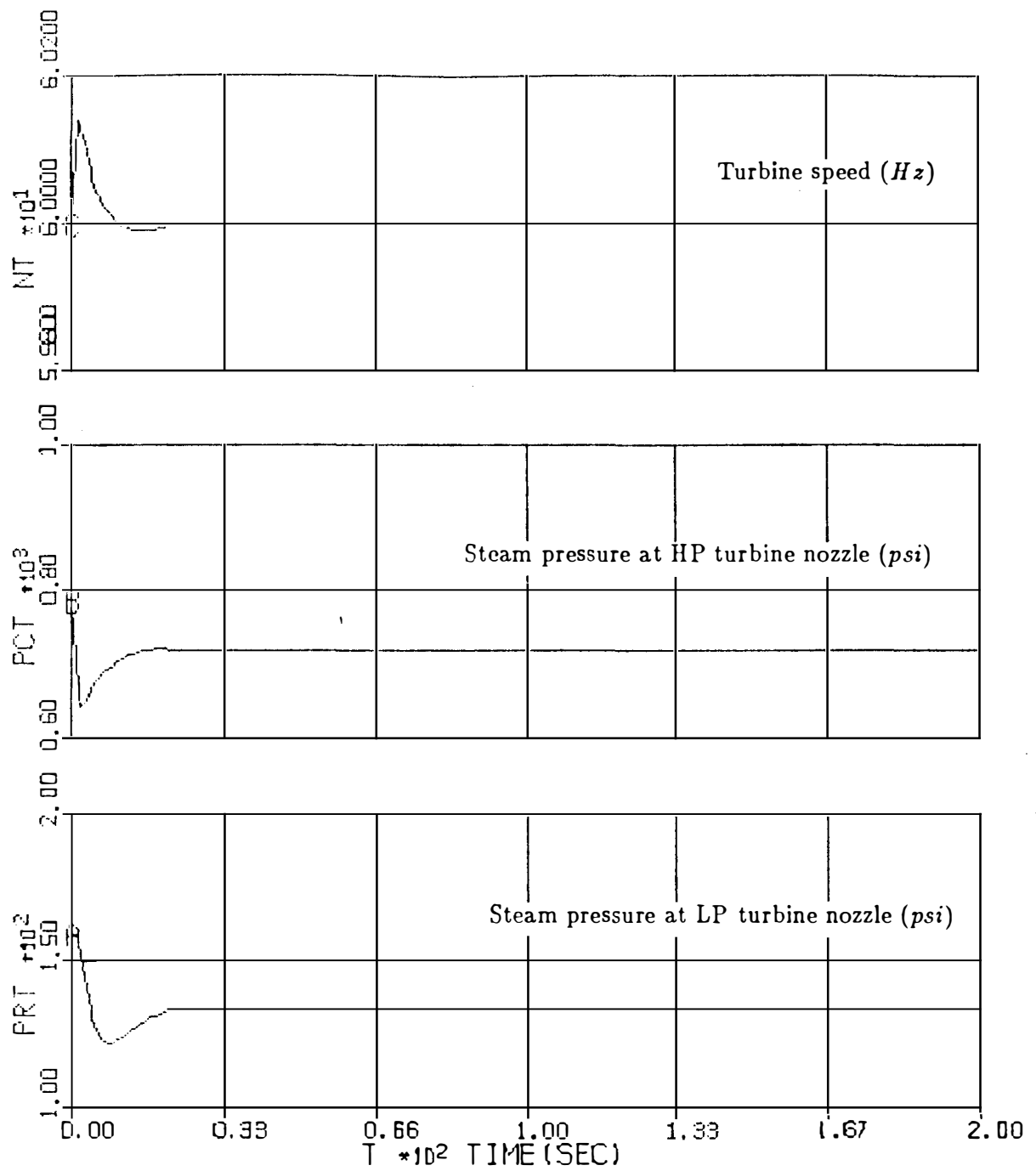


Fig. 4.5 (continued)

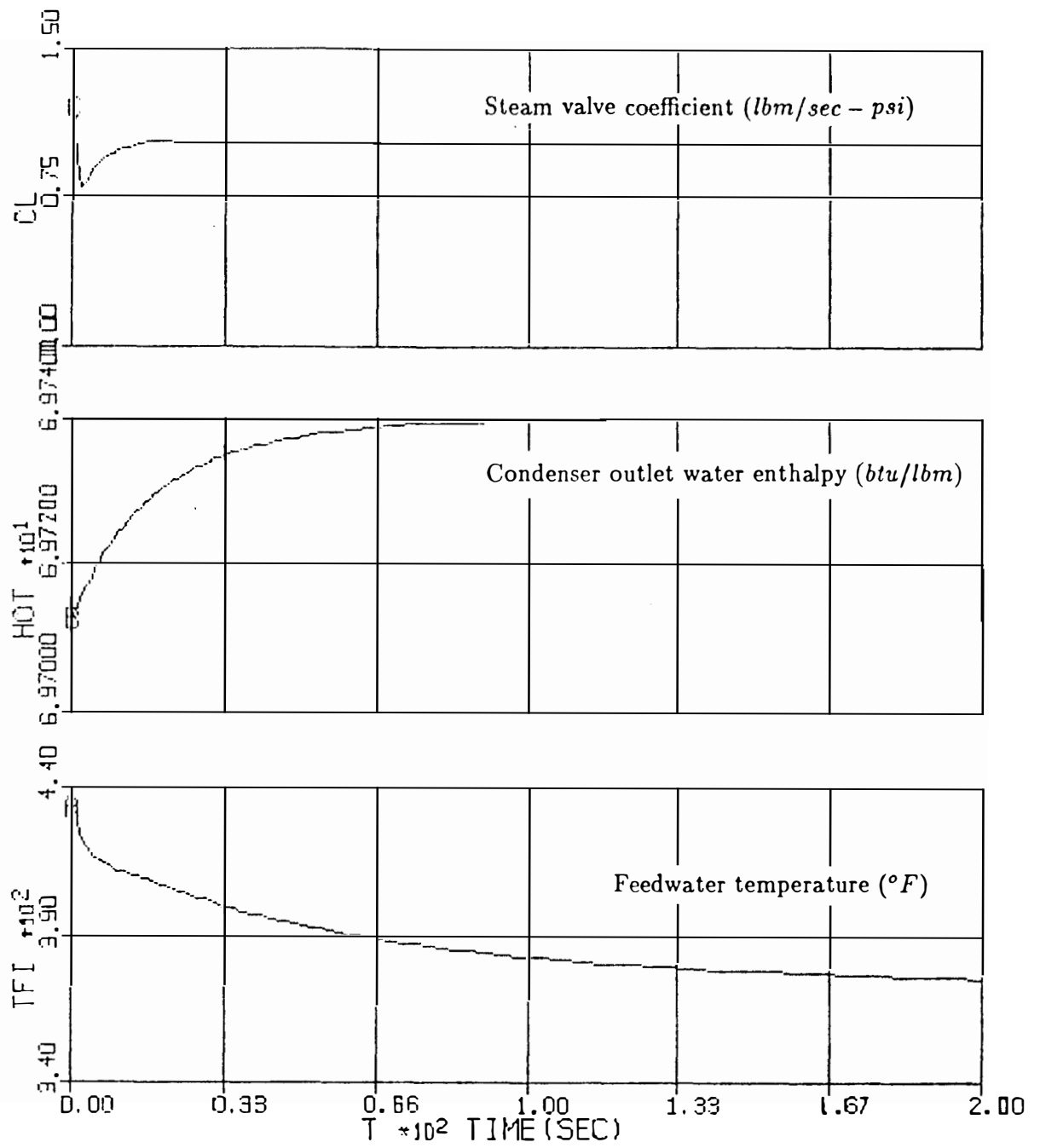


Fig. 4.5 (continued)

of the turbine, condenser, feedwater heaters, and turbine speed control system. The time responses of the BOP model have been examined and evaluated for a 15% step decrease in the turbine power demand. The analysis of the responses indicates that the turbine speed reaches its set point (60 Hz) in approximately 25 *sec*. It also shows that the steam valve coefficient decreases by 17.5% of its initial value.

CHAPTER 5

PRIMARY LOOP AND OVERALL SYSTEM SIMULATION

In the two preceding chapters the dynamic models of the PWR components were discussed. This chapter describes how these models are used for model simulations of the primary side and the overall plant systems.

5.1 Primary Side Simulation Model

The primary side of a PWR system (Westinghouse type) contains four major components: reactor, pressurizer, steam generator, and coolant pump. It also incorporates three main control systems; reactivity, steam generator water level (three-element controller), and pressurizer pressure. The primary side is sometimes called the “ Nuclear Steam Supply System (NSSS) ”.

A mathematical model is developed to simulate the dynamics of the primary side system. It includes reactor, steam generator, and pressurizer component models which have been previously described in Chapter 3. It also includes models for reactivity, steam generator water level, and pressurizer pressure control systems. The primary side model equations are obtained by combining the equations of its individual models. The only additional equation which needs to be derived is

the pressurizer surge flow. The surge flow is caused by temperature variations in the primary side coolant fluid during transient conditions. A simple relationship which expresses the pressurizer surge flow is given by

$$W_{sr} = \beta_{hl} V_{hs} \frac{dT_{hl}}{dt} + \beta_{cl} V_{cs} \frac{dT_{cl}}{dt} \quad (5.1)$$

where

W_{sr} = Pressurizer surge flow.

V_{cs} = Total volume of the cold leg piping, reactor core lower plenum, half of primary water in steam generator, and half of reactor core.

V_{hs} = Total volume of the hot leg piping, reactor core upper plenum, half of primary water in steam generator, half of core, and pressurizer water part.

T_{cl}, T_{hl} = Cold and hot leg temperatures, respectively.

β_{cl}, β_{hl} = Water density gradients evaluated at hot and cold leg temperatures, respectively.

The primary side model is described by 49 state variables and one forcing term. The only forcing term which perturbs the model is the steam valve coefficient.

Based on the primary side mathematical model, a computer code called “PRIMARY. CSL” has been developed using the ACSL [19] software package. This is used to study the dynamic performance of the primary side system under transient and steady-state conditions. Figure 5.1 shows typical responses of the primary side simulation code to a 15% step decrease in steam valve coefficient. The study of responses indicates that as the steam flow rate decreases the steam pressure

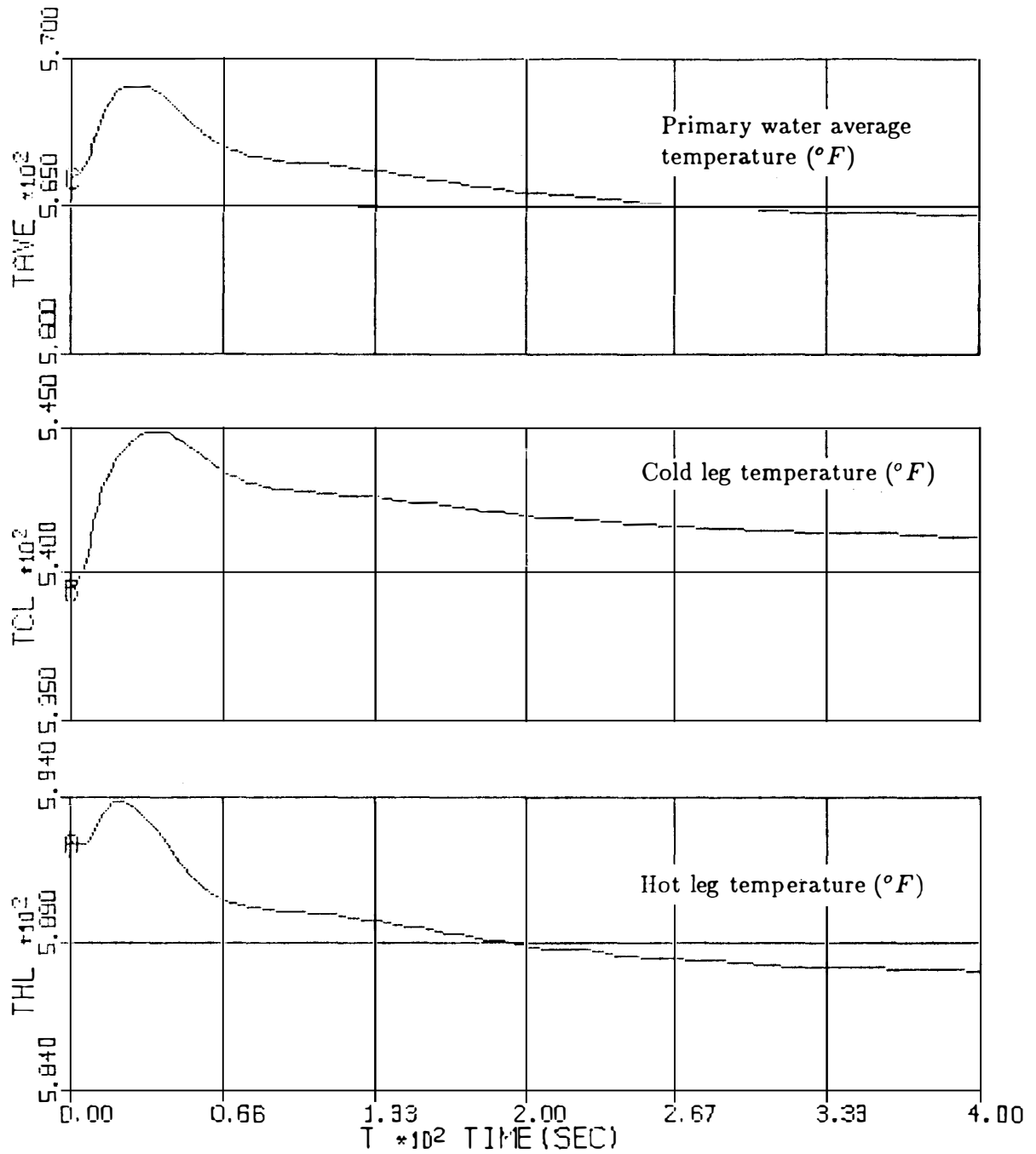


Figure 5.1: Typical responses of the PWR primary side to a 15% step decrease in steam valve coefficient.

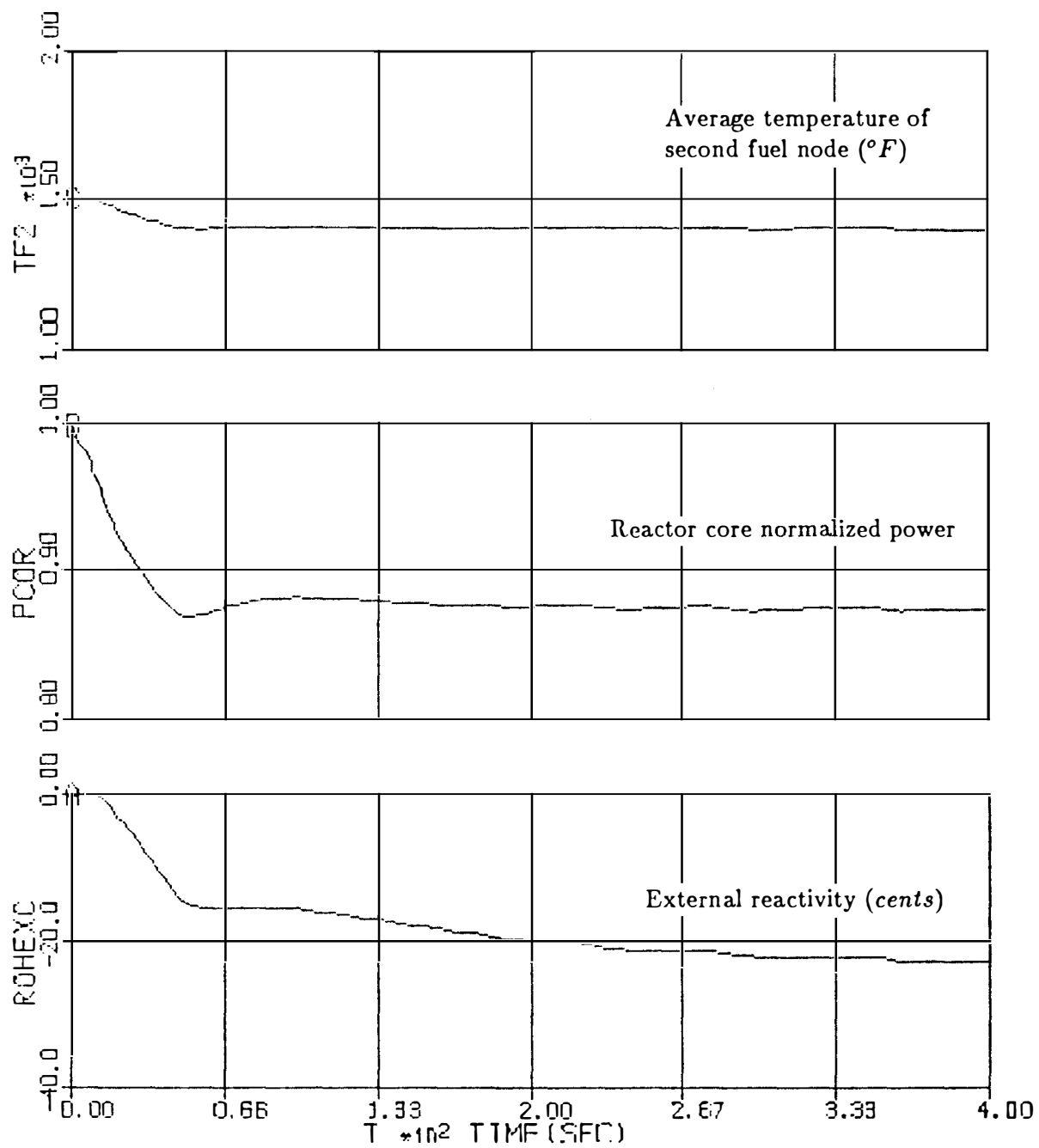


Fig. 5.1 (continued)

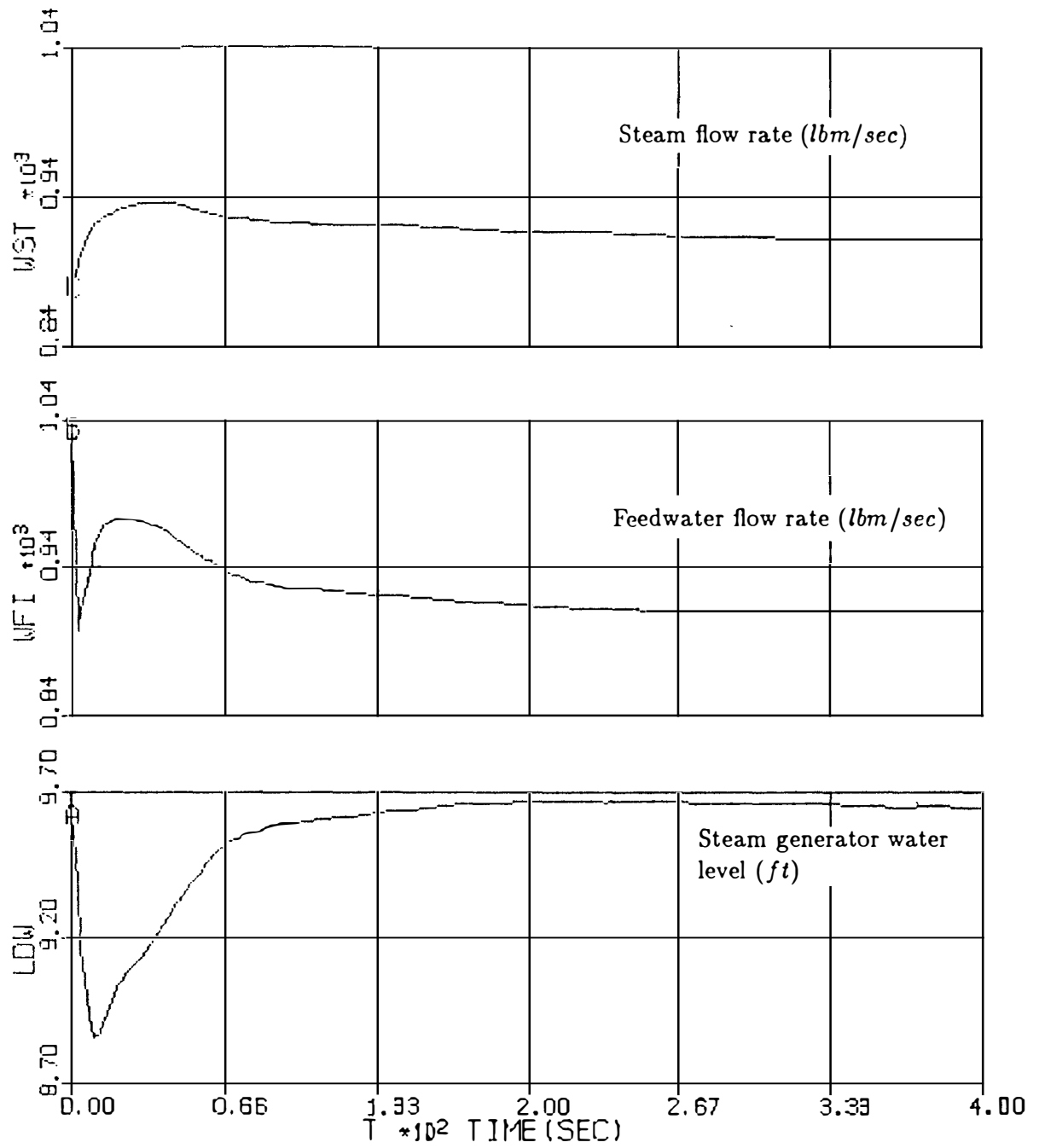


Fig. 5.1 (continued)

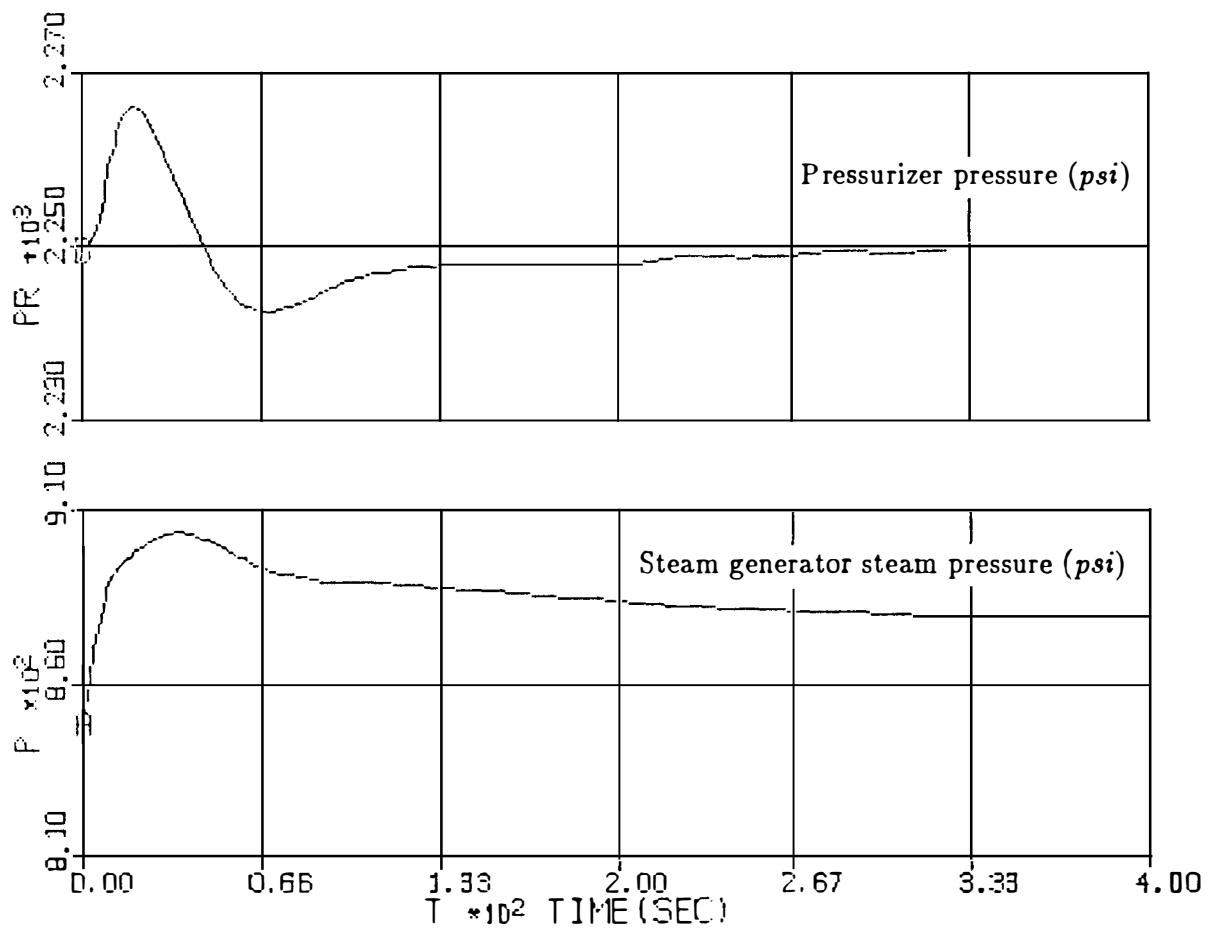


Fig. 5.1 (continued)

increases and consequently the water level in the steam generator falls below its set point (due to the shrink phenomenon). The three element- controller returns the level to its set point by adjusting the feedwater flow rate. The responses of the feedwater and the steam flow rates show that they reach the same flow rate at the steady state condition.

As the steam flow decreases, the reactor core normalized power reduces to 88% and the external reactivity decreases by 24 cents. The average temperature differs from its set point by less than $-1.0^{\circ}F$ at the steady state condition. This is due to the existence of a deadband zone in the control rod movement program. During a short period of transient time, the hot and cold leg temperatures are increased and cause an insurge flow to the pressurizer. The insurge flow rapidly increases the pressurizer pressure from its set point (2250 *psi*) to 2265 *psi*. At this point, the pressurizer pressure control system initiates the spray system and thus the pressure is reduced. Later on, an outsurge flow (due to the temperature reduction in hot and cold legs) decreases the pressure below its set point. This initiates the pressurizer heater system which builds up the pressure to its set point.

5.2 PWR Plant Simulation

A PWR plant consists of two main systems: the primary side and the secondary side. The primary side includes the reactor core, steam generator, pressurizer and reactor core coolant pump. The secondary side usually called “Balance of Plant (BOP)” contains turbine, moisture separator, steam reheater, condenser, and feedwater pump and heaters. In addition, the plant incorporates the con-

trol systems of reactivity, steam generator water level, pressurizer pressure, and turbine speed.

The plant model is obtained by combining the primary side and the secondary side models. The model is considered as an isolated system which is not affected by any external system (for example, an electric-generator). The plant model includes 67 state variables and 11 algebraic variables. The model is perturbed by a power demand signal which is the only forcing function to the system.

The computer codes of the primary and secondary sides are integrated into an overall plant simulation program. The program is written in ACSL [19] language and named "PLANT. CSL". This is utilized to analyze the behavior of the system under normal and abnormal conditions.

Figure 5.2 depicts the responses of the overall plant simulation program due to a 15% step decrease in the power demand signal. The analysis of the responses indicates that a sudden decrease in the power demand causes a momentary speed increase in the turbine shaft (due to torque imbalance). This constitutes an error signal in the speed control system which actuates the steam valve system. As the steam valve is activated, it sharply reduces the steam flow rate which consequently causes a sharp increase in the steam pressure (because of variations in the fluid inertia) and a sudden decrease in the the steam flow rate. A sudden increase in the steam pressure will result in a fast reduction in the steam generator water level (due to the shrink phenomenon). As the water level deviates from its set point, the three-element controller is activated and thus the feedwater flow is regulated. The exit pressure of the HP turbine decreases instantaneously due to

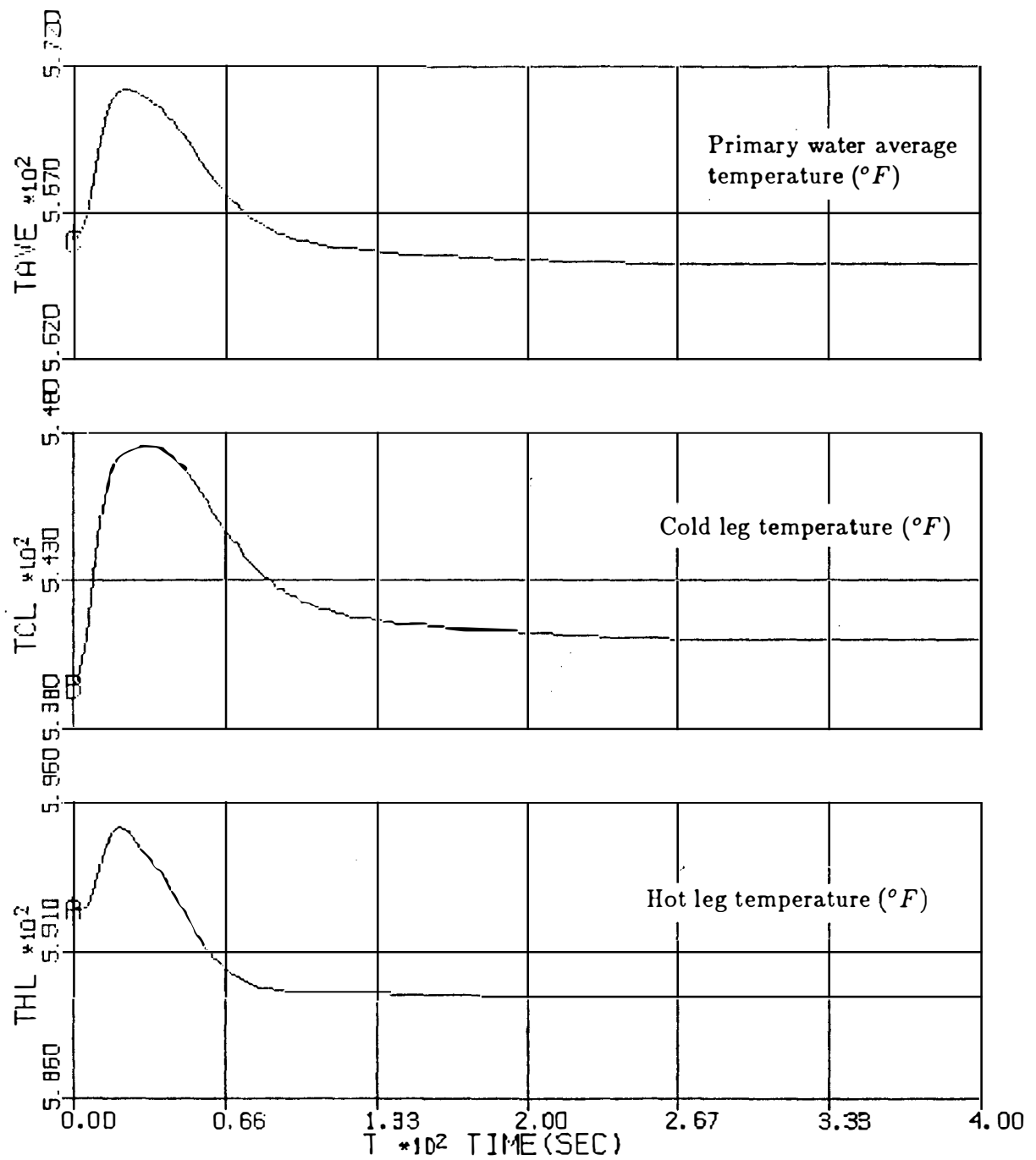


Figure 5.2: Typical responses of the overall PWR system to a 15% step decrease in power demand signal.

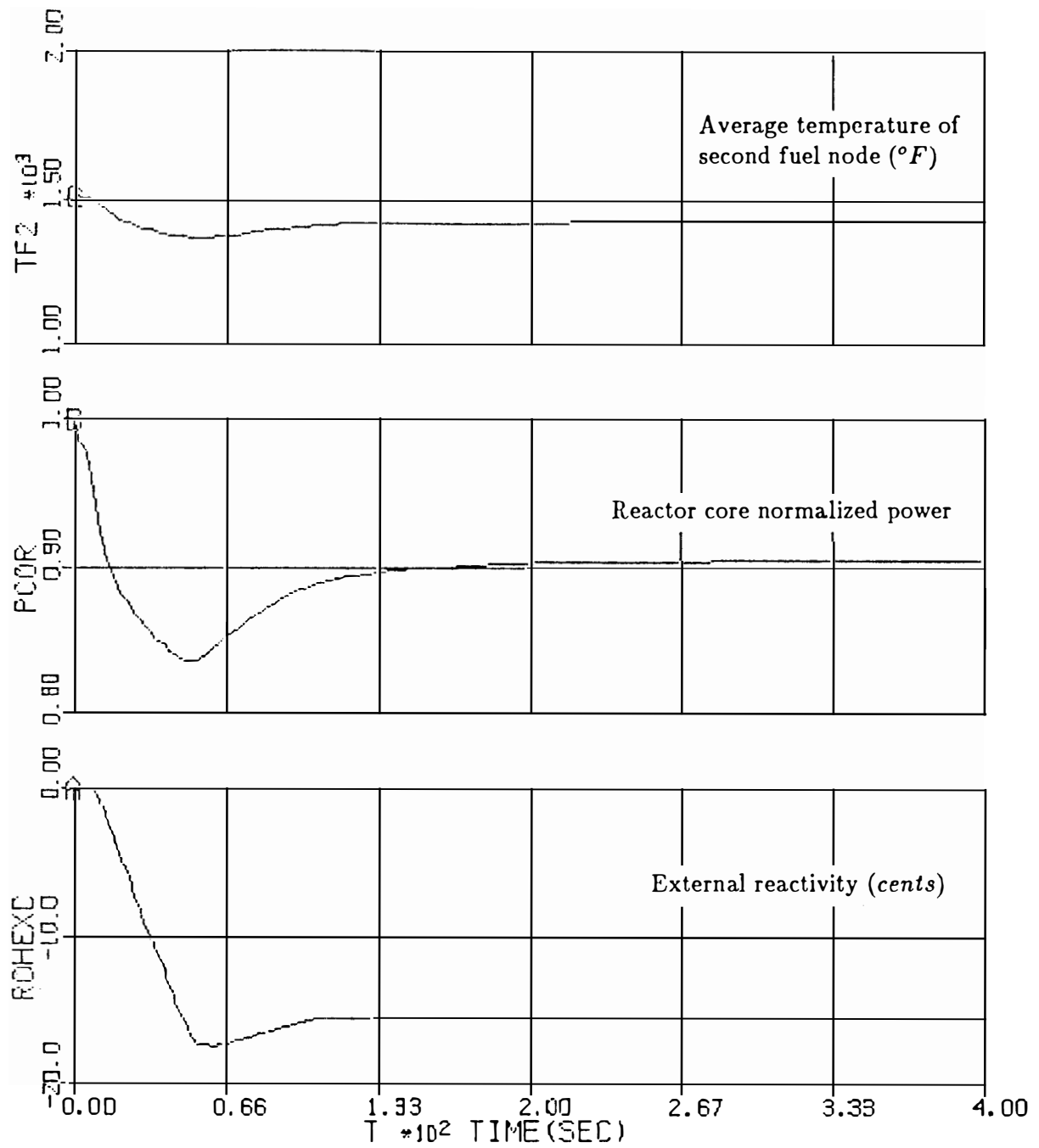


Fig. 5.2 (continued)

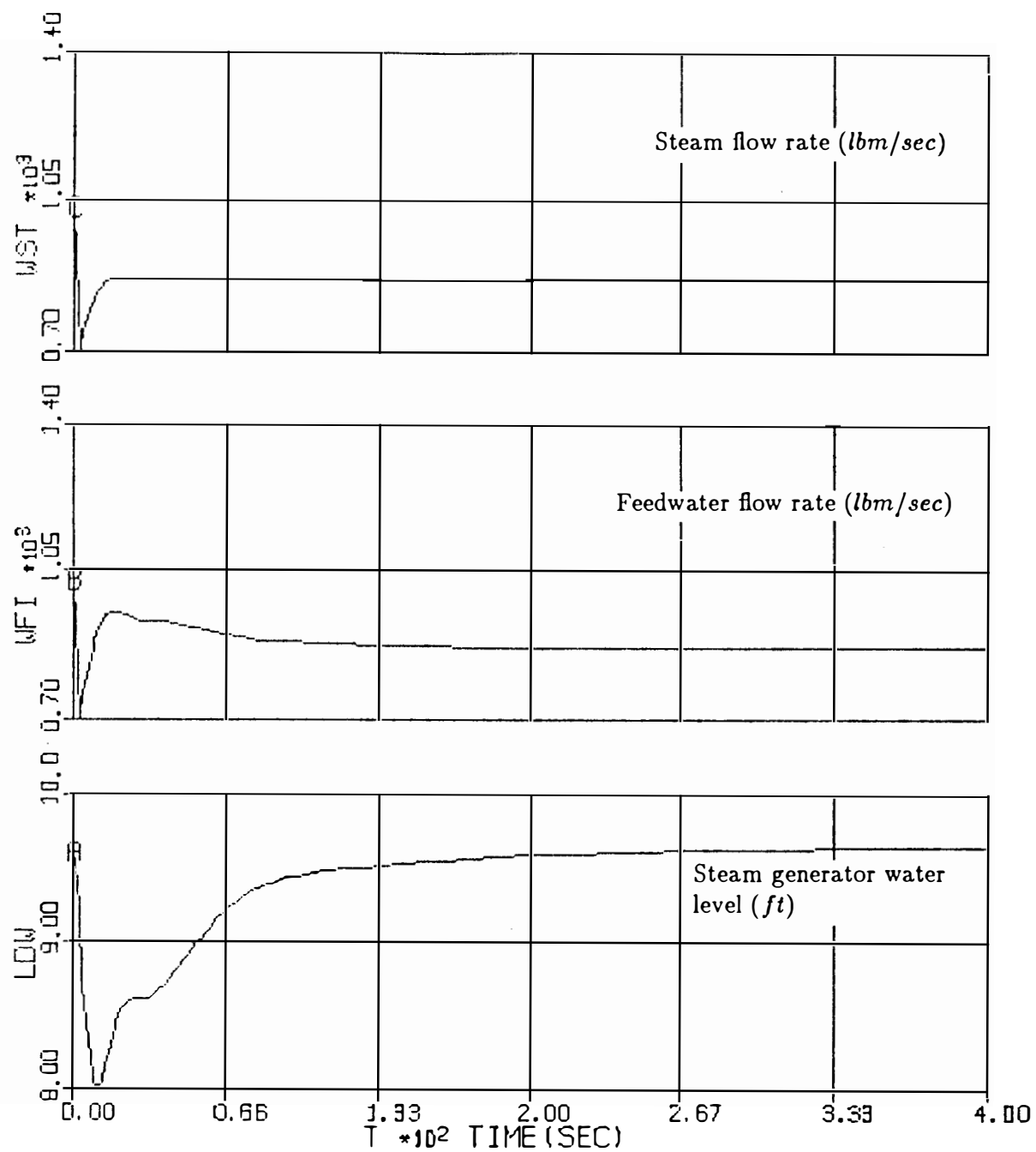


Fig. 5.2 (continued)

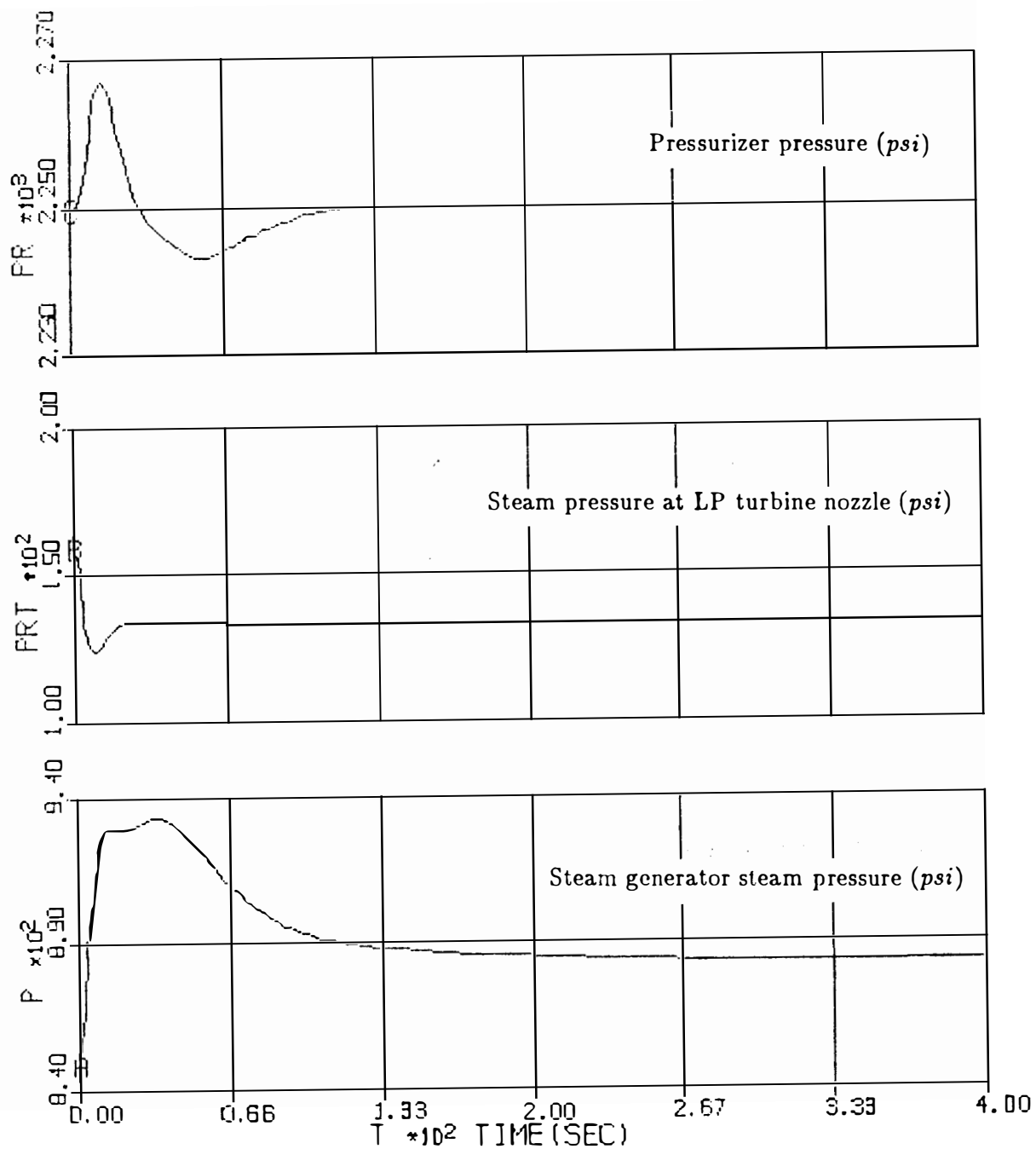


Fig. 5.2 (continued)

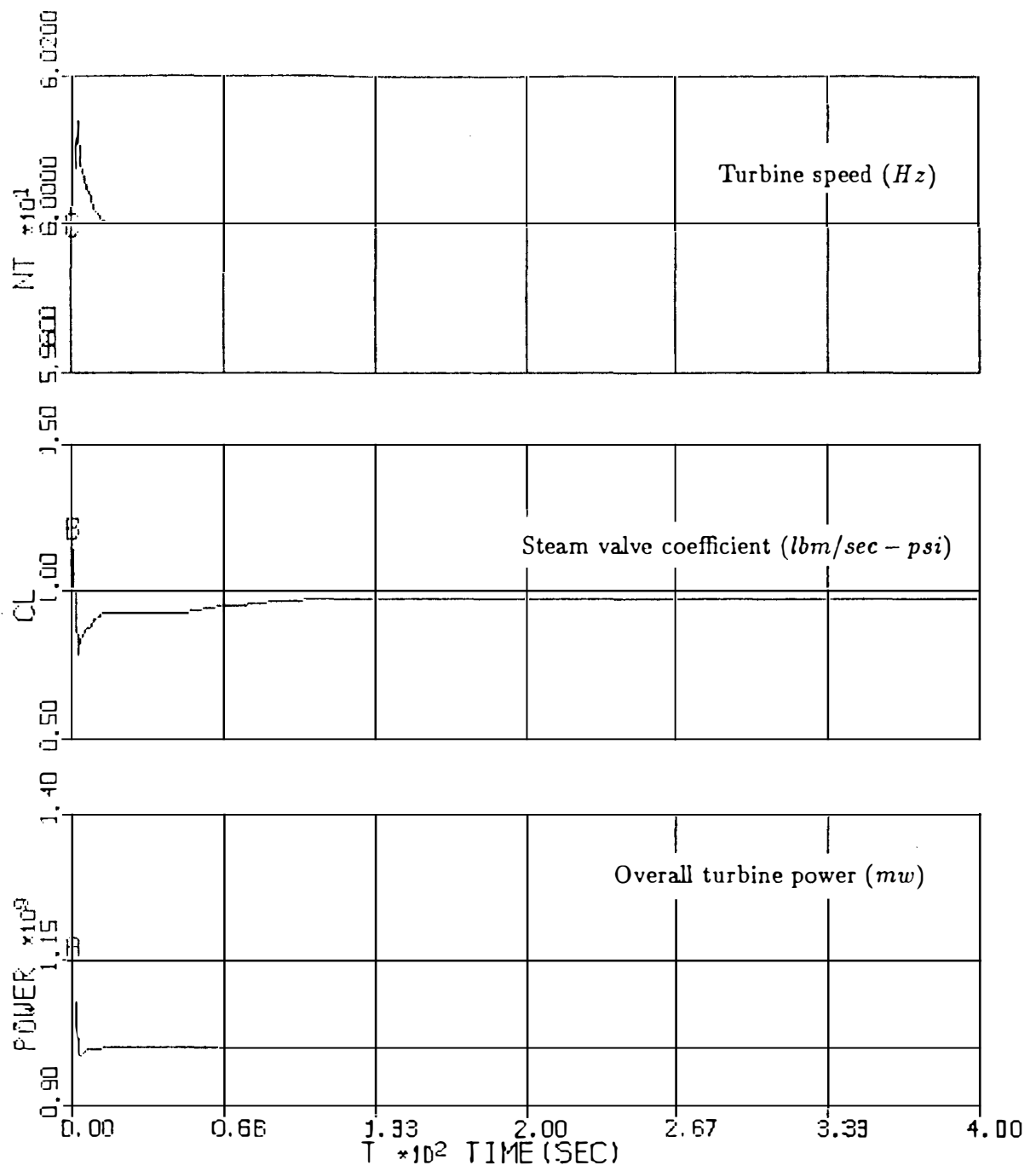


Fig. 5.2 (continued)

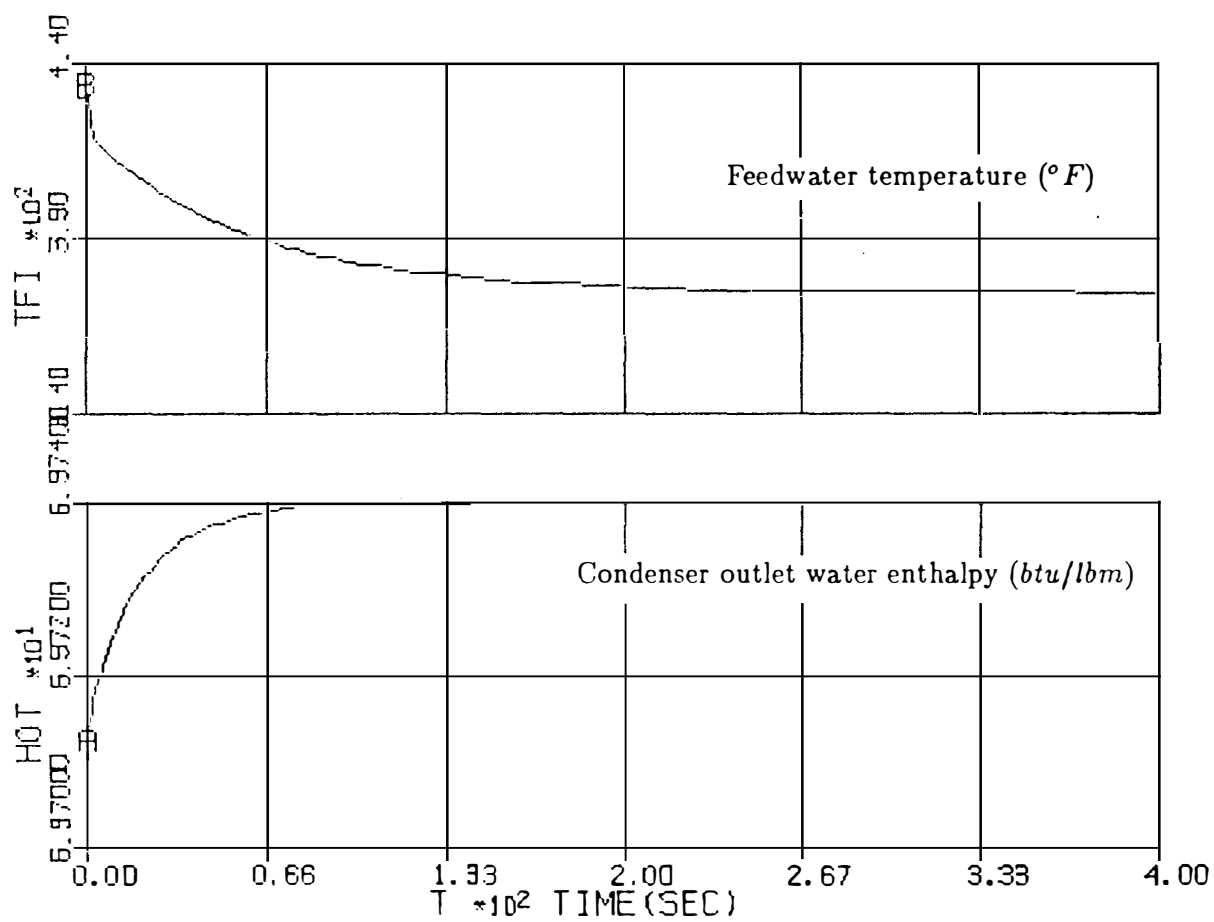


Fig. 5.2 (continued)

the steam flow reduction. This results in a reduction of the extracted steam flow to the feedwater heaters which decreases the feedwater temperature to the steam generator.

The effect of steam flow behavior can also be observed in the primary side variables. At the beginning, the average temperature of the primary water is increased due to the sudden reduction of heat removal in the steam generator, and then gradually decreases to the vicinity of its set point. The deviations between the average temperature and its set point constitutes an error signal in the reactor control system which ultimately determines the movement of control rods. The control rod motion decreases the external reactivity to a minimum (-17.5 cents) at the beginning of the transient; and then, increases it to -15 cents at steady state. As a result of control rod action, the reactor normalized power first drops to a minimum point of 84% and then is stabilized at 89%. The temperature variations in hot and cold leg piping cause pressure variations in the primary side. The pressurizer control system regulates the primary side pressure by actuating the spray and heater systems.

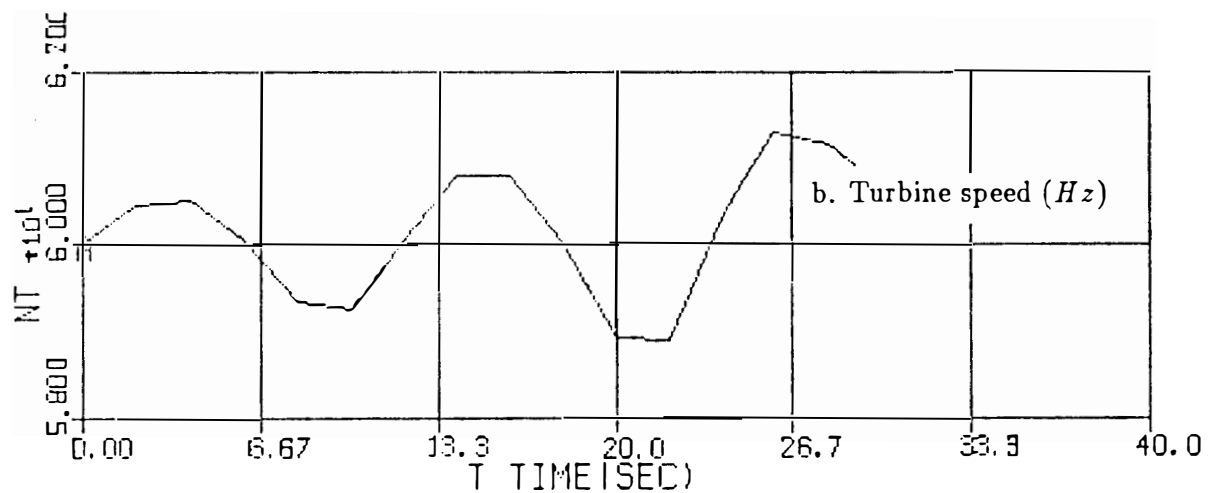
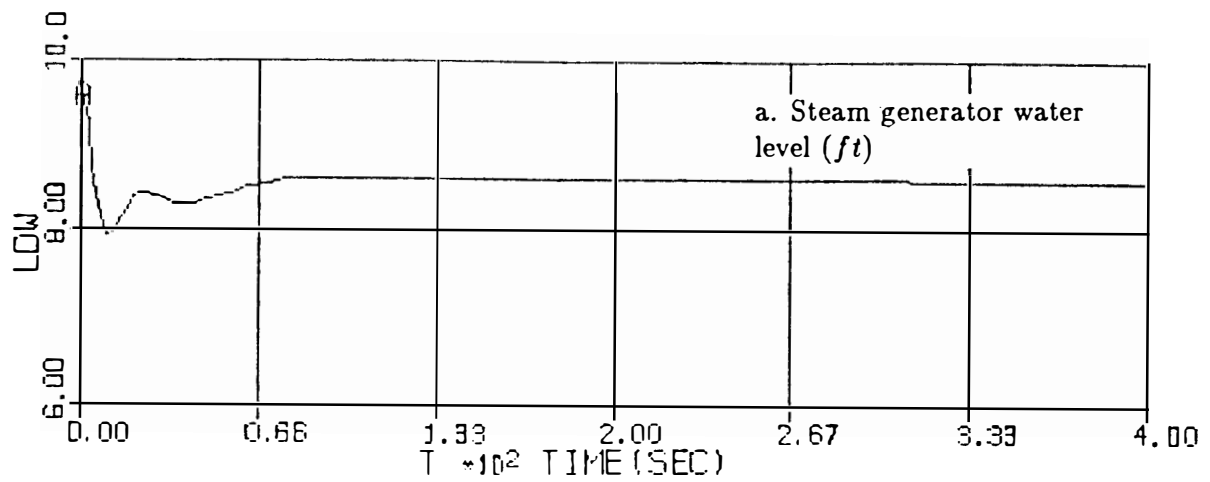
5.3 System Anomalies

The simulation program can also be used to identify the behavior of the measured process variables to anomalies in the plant components. The anomalies considered in the system are:

- Failure of a PI controller in the steam generator three-element controller due to a zero gain factor.
- Failure of speed control system as a result of a zero gain factor in the PI controller.
- Failure of spray system due to a zero gain factor in the spray PID controller of the pressurizer control system.
- Reduction of heat transfer area in the steam generator U-tubes as a result of blockage in 5% of the tubes.

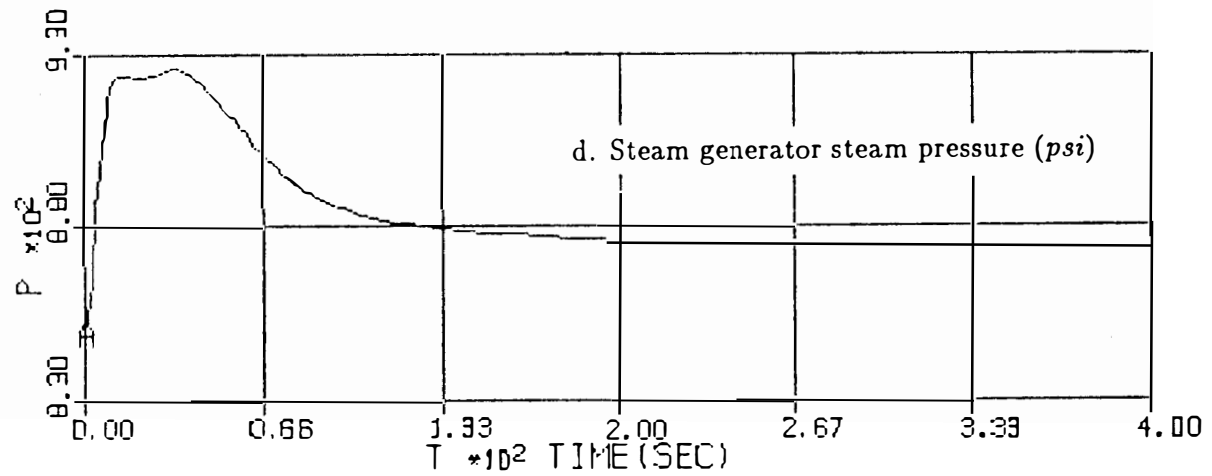
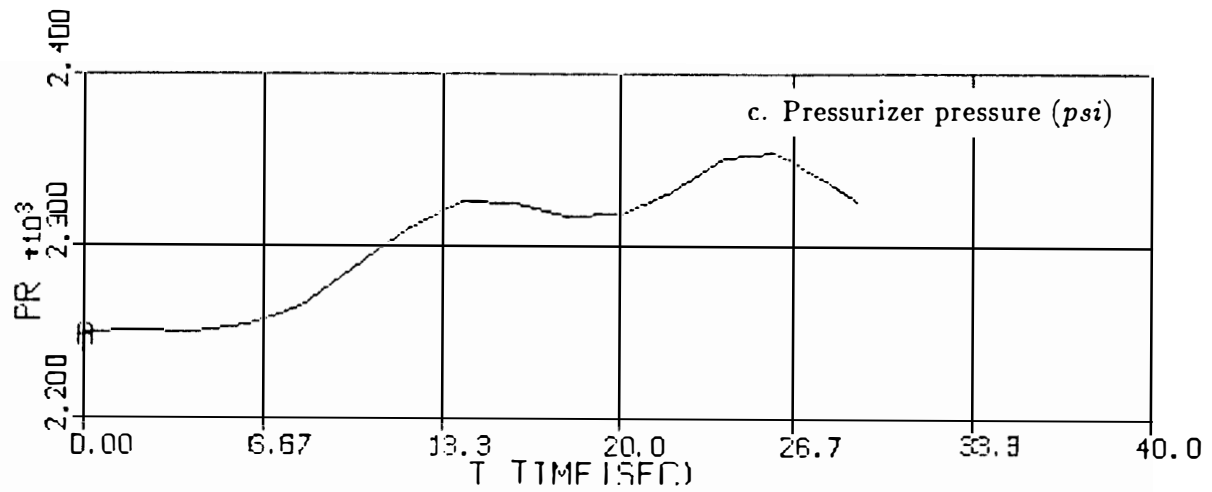
These anomalies are introduced to the system at 85% of the full power operating condition of the plant.

The effect of failure of a PI controller in the three-element controller is detected by the steam generator level signal. Figure 5.3.a shows that the level approximately falls down one foot below its set point. The failure of speed control system results in instability of the turbine speed. The turbine speed increases with time as shown in Fig. 5.3.b. The failure of the spray system causes a rapid increase in the primary side pressure during a short time (see Fig. 5.3.c). The pressure increases to 2350 *psi* in less than 30 seconds (note that in the real world, the safety valves are actuated when the pressure reaches 2315 *psi*). The effect of reduction in the U-tube heat transfer area is identified by steam generator pressure signal (see Fig. 5.3.d). The pressure decreases almost by 15 *psi* from its initial operating point (880 *psi*).



- a. Malfunction in PI controller element of the three-element controller.
- b. Malfunction in turbine speed control system.

Figure 5.3: Typical responses of the PWR system to anomalies at 85% of the full power operating conditions of the plant.



- c. Malfunction in spray system of the pressurizer control system.
- d. Reduction in heat transfer area of the steam generator U-tubes.

Fig. 5.3 (continued)

CHAPTER 6

FREQUENCY-DOMAIN ANALYSIS

This chapter deals with frequency-domain analysis of the primary side components in a PWR. It presents frequency responses using linear models of reactor core and steam generator components.

6.1 Introduction

Frequency-response method is used to investigate the behavior of a linear system under a sinusoidal input such as

$$F = F_0 \sin \omega t \quad (6.1)$$

where

F_0 = Initial amplitude.

t = Time.

ω = Angular velocity.

The response of a linear system to this input is characterized by a sinusoidal function with the same angular velocity as the input. The general form of the response is expressed by the following relationship.

$$Y = Y_0 \sin(\omega t + \phi) \quad (6.2)$$

where

Y_0 = Output amplitude.

ϕ = Phase angle.

Graphical representations of phase angle ϕ and amplitude ratio $|Y_0/F_0|$ versus angular velocity ω are used in the frequency-response analysis.

The phase angle and amplitude ratio (gain) can be determined by substituting $j\omega$ for s in the Laplace-domain transfer function of a system. Equation (6.3) shows a general operational form of a transfer function [11,21].

$$Y(s) = \frac{\sum_{m=1}^p a_m s^m}{\sum_{n=0}^q b_n s^n} = \frac{P(s)}{Q(s)} \quad (6.3)$$

and

$$Y(j\omega) = \frac{P(j\omega)}{Q(j\omega)} \quad (6.4)$$

where

$P(s)$ = an m rank polynomial with constant coefficients (a_m).

$Q(s)$ = an n rank polynomial with constant coefficients (b_n).

s = Laplace transform operator.

From the preceding equations, the gain factor and the phase angle are evaluated as follows:

$$G = \frac{Y_0}{F_0} = \left| \frac{P(j\omega)}{Q(j\omega)} \right| \quad (6.5)$$

$$\phi = \angle G(j\omega) = \tan^{-1} \left(\frac{I_m G(j\omega)}{R_e G(j\omega)} \right) \quad (6.6)$$

The graphical representation of ϕ and G quantities are usually plotted on semi-logarithmic coordinates with linear vertical scales and logarithmic horizon-

tal scales. The gain factor values are often determined in decibel units, as $20\log_{10}|Y(j\omega)|$, and placed on the linear vertical scale. The phase angle values are obtained in degrees and proportionally entered on the vertical scale. Both the gain and phase diagrams have logarithmic horizontal scales for frequency values. The phase diagram is usually sketched under the gain curve for the same frequency values.

6.2 Frequency-Response Analysis

A frequency-response analysis is performed for the reactor core and steam generator linear models. The frequency response functions of the reactor model are shown in Fig. 6.1. The responses are obtained in decibel units (db) in a frequency range of 0.001 to 100 (*rad/sec*). They include hot leg temperature, fuel temperature, and normalized core power. The analysis of responses indicates the following results:

- Both hot leg and fuel temperatures have a break frequency of about 1 (*rad/sec*).
- The core power gain factor increases from -28 to -18 db in the frequency range 0.1 to 3 *rad/sec* and remains almost constant at -18 db in the frequency range 3 to 100 *rad/sec*.

The frequency response functions of the steam generator model which incorporates the three-element controller are given in Fig. 6.2. The responses include steam pressure, water level, and feedwater flow rate. The study of these responses

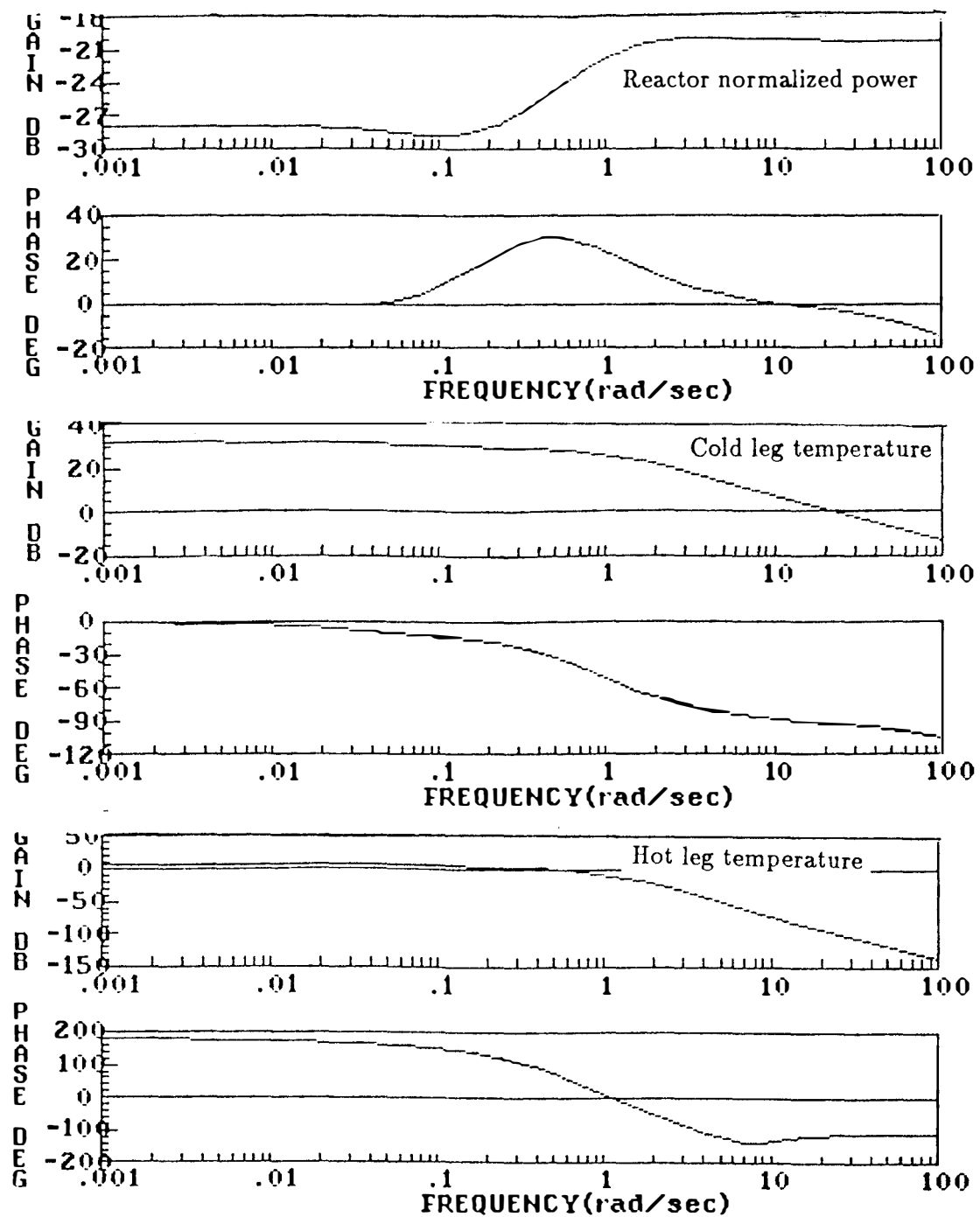


Figure 6.1: Frequency responses of the reactor core linear model.

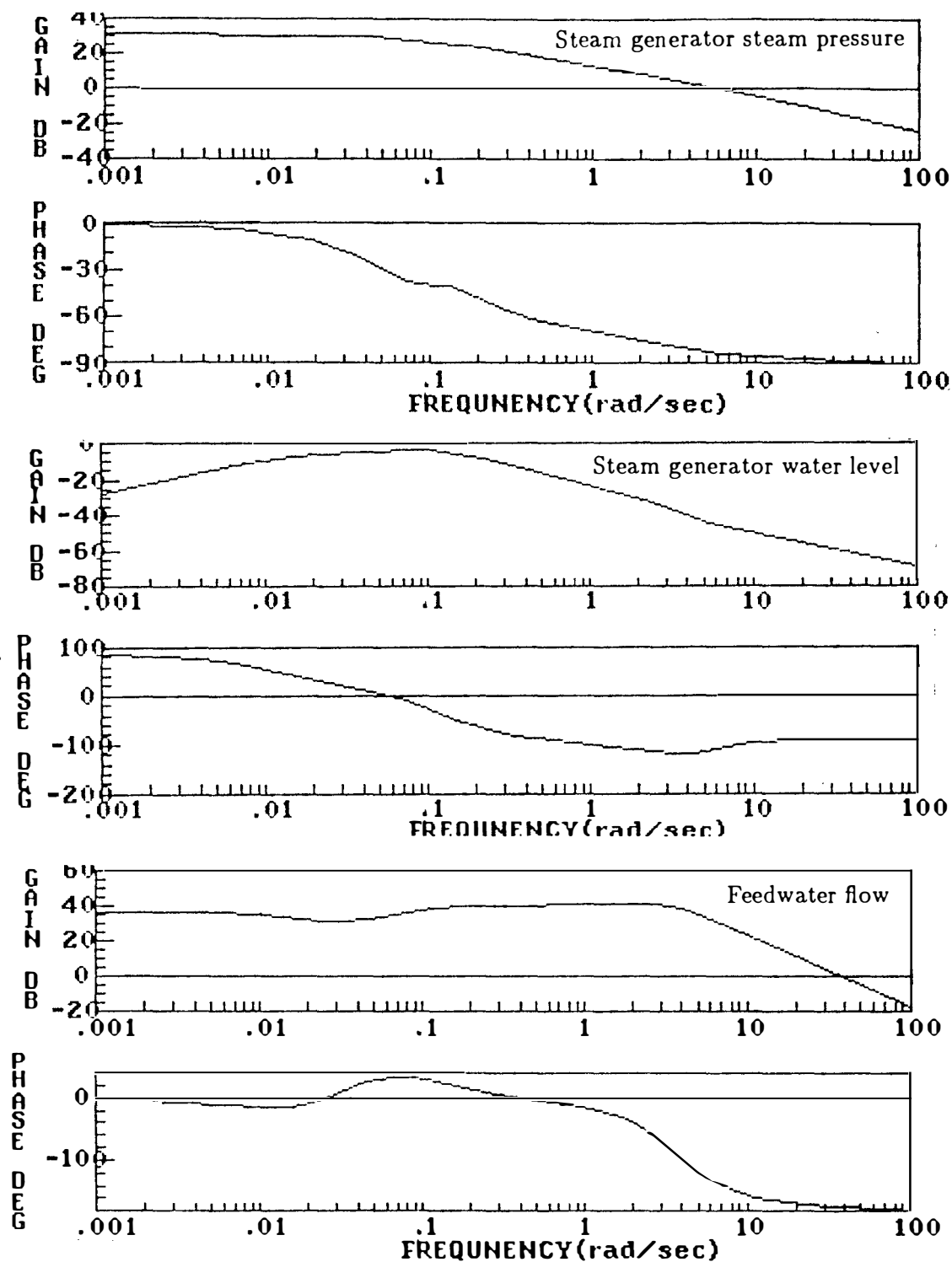


Figure 6.2: Frequency responses of the steam generator linear model.

shows that the steam pressure, feedwater flow, and steam generator water level have break frequencies of 0.07, 0.1, and 3 *rad/sec*, respectively.

From the preceding analysis, it is established that the reactor core and steam generator models have a stable behavior as indicated by the frequency-domain signatures.

CHAPTER 7

CONCLUSIONS AND FUTURE WORK

7.1 Conclusions

A nonlinear simulation, based on a lumped parameter modeling of a 1200 *MWe* Westinghouse PWR plant has been developed. The overall plant simulation model has been implemented in a computer workstation by combining individual models of the plant components. Based on theoretical models of the PWR plant and its components, computer codes have been developed to predict and evaluate response characteristics of the models under steady-state and transient conditions. These codes have been written in ACSL [19] simulation language and can be executed on a VAX workstation or a personal computer.

The dynamic responses of the individual models of a PWR are studied in Chapters 3 and 4. The simulation results indicate expected behavior and the steady-state values are similar to the results obtained by Freels [1], Mneimneh [2], and Cherng [4].

The overall simulation responses are investigated in Chapter 5. The analysis of the responses indicates that as the power demand signal decreases from 100% to 85%, the reactor normalized power reduces from 100% to 89%. This is due to the fact that steam flow rate decreases as a nonlinear function of the reactor

power. The feedwater temperature and steam pressure leaving the high pressure turbine decrease as load decreases.

The performances of the various control systems are studied in the overall plant simulation model (see Chapter 5). The steam generator three-element controller perfectly stabilizes the steam generator water level at its set point value. However, this results in relatively large transients in steam generator pressure and feedwater flow. The response of the primary water average temperature at 85% of full power operating conditions of the plant shows that the average temperature differs from its set point by less than $-1.0^{\circ}F$. This is due to the existence of a deadband zone in the reactor control rod speed program. The responses of the turbine speed and feedwater valve coefficients indicate that a rapid control of the turbine speed will result in a sudden change of feedwater valve coefficient during transient conditions. From the responses of the controlled variables, it is concluded that the optimized parameters of the control systems at 100% power conditions are also suitable for 85% power.

The overall PWR simulation model has been applied to study the effect of anomalies in the plant variables at 85% power conditions. This has been used to detect measurable signals which are sensitive to anomalies. It is concluded that anomalies in the speed control system can result in instability in the system.

The simulation results of the reactor and steam generator (including three-element controller) linear models are compared with the results of nonlinear models (see Chapter 3). These results indicate that the response characteristics of linear models are similar to those of nonlinear models for different perturbations.

However, for large perturbations, the steady-state responses of the linear models deviate from the nonlinear models significantly. For instance, a 25% perturbation in the steam valve coefficient causes a 20 *lbm/sec* difference in feedwater flow between the linear and nonlinear models.

Based on the results of this study, it is concluded that ACSL language [19] is quite suitable for nonlinear modeling and simulation. An important feature of ACSL is the capability of solving differential and algebraic equations simultaneously. It also has many good features of easy programming and graphical plotting.

7.2 Future Work

As an extension to the present study, it will be interesting to see the behavior of the PWR plant model under the following conditions:

- Developing additional plant component models such as feedwater pump, steam generator pressure, and pressurizer water level control systems into the overall plant model.
- Assuming non-constant heat transfer coefficients in reactor, steam generator, and turbine models during transient conditions.
- Deriving nonlinear relationships for thermodynamic properties of water and steam as a function of pressure.

- Considering mass transfer at steam-liquid interface of two phase flow phenomena.
- Taking a non-uniform heat flux distribution along the reactor core fuel elements.
- Programming a schedule for steam admission to the turbine system as a function of load demand. This can be simulated by a multi-steam valve model which regulates turbine steam flow rate.

Moreover, the overall nonlinear model of the PWR plant developed in this research can also be extended for safety and accident analyses. This requires more detailed models for critical components such as reactor and steam generator systems. For example, loss of coolant in the reactor or leak of primary water into the secondary fluid in the steam generator are problems which need additional model development.

The dynamic response characteristics derived from this model may be used to train diagnostic neural networks. This study will be useful in identifying incipient anomalies in plant components.

BIBLIOGRAPHY

BIBLIOGRAPHY

- [1] J. D. Freels, "Modeling for Long-Term Power System Dynamic Simulation," M.S. Thesis, Nuclear Engineering Department, The University of Tennessee, Knoxville, TN, 1978.
- [2] Mounir Janil Mneimneh, "Modular Modeling of a PWR System," Nuclear Engineering Department, M.S. Thesis, The University of Tennessee, Knoxville, TN, 1984.
- [3] M. R. A. Ali, "Lumped Parameter, State Variable Dynamic Models for U-Tube Recirculation Type Nuclear Steam Generators," Ph.D Dissertation, Nuclear Engineering Department, The University of Tennessee, Knoxville, TN, 1976.
- [4] J. C. Cherng, "An Investigation of Feedwater Control and Nonlinear Effects for a U-Tube Steam Generator Model," Nuclear Engineering Department, M.S. Thesis, The University of Tennessee, Knoxville, TN, December, 1978.
- [5] J. G. Thakkar, "Correlation of Theory and Experiment for the Dynamics of a Pressurized Water Reactor," Nuclear Engineering Department, M.S. Thesis, The University of Tennessee, Knoxville, TN, March, 1975.
- [6] Girija Shankar, "Simulation of a Nuclear Turbine," Journal of Nuclear Engineering and Design, Vol. 44, pp. 269-277, November, 1977.
- [7] P. Deshpande and P. Lu, "Main Condenser System," Proceedings of the Fifth Power Plant Dynamics, Control and Testing Symposium, Vol. 1, pp. 12.01-12.23, Knoxville, TN, March, 1983.
- [8] R. Moshe Heller, "Nuclear Simulation," Springer-Verlag Company, 1987.
- [9] James R. Rowland, "Modeling, Analysis, and Design," Wiley, New York, 1986,
- [10] Eugene M. Grabbe, "Handbook of Automation, Computation and Control," Wiley, New York, 1961.
- [11] Francis H. Raven, "Automatic Control Engineering," McGraw-Hill, New York, 1968.
- [12] Gordon J. Vanwylen, "Fundamentals of Classical Thermodynamics," Wiley, New York, 1981.
- [13] D. G. Walton, "Simulation for Nuclear Reactor Technology," Wiley, New York, 1987.
- [14] J. D. Holman, "Heat Transfer," McGraw-Hill, New York, 1981.

- [15] Westinghouse Electric Corporation, "Systems Manual Pressurized Water Reactors," Vol. 1-3, December, 1981.
- [16] W. J. Kearton, "Steam Turbine Theory and Practice," Sir Issac Pitman & Sons Ltd., 1964.
- [17] Robert L. Daugherty and Joseph B. Franzini, "Fluid Mechanics with Engineering Applications," McGraw-Hill, New York, 1977.
- [18] James R. Rowland, "Linear Control Systems, Modeling, Analysis, and Design," Wiley, New York, 1986,
- [19] ACSL (Advanced Continuos Simulation Language) User's Guide, Mitchel and Gauthier Associate, Edition 4.1, 1987.
- [20] MATRIXx User's Guide, Integrated Systems Inc., Version 5, 1985.
- [21] B. R. Upadhyaya, "An Introduction to Dynamics and Control," Department of Nuclear Engineering, The University of Tennessee, Vol. 1 & 2, 1988.
- [22] Donald Q. Kern, "Process Heat Transfer," McGraw-Hill, New York, 1960.
- [23] James H. Rust, "Nuclear Power Plant Engineering," Haralson Publishing Company, Georgia, 1979.
- [24] C. R. Wylie, "Advanced Engineering Mathematics," McGraw-Hill, New York, 1966.
- [25] William E. Boyce and Richard C. DiPrima, "Elementray Differential Equations and Boundary Value," Wiley, New York, 1986.
- [26] Y. Dayal, "Advanced Prism Plant Control Sytem," Proceedings of the Seventh Power Plant Dynamics, Control and Testing Symposium, Vol. 2, pp. 1.01-1.13, Knoxville, TN, May, 1983.

APPENDICES

APPENDIX A

DESIGN PARAMETERS OF A PWR SYSTEM

This appendix presents typical design parameters of a Westinghouse PWR plant. These parameters are used in plant modeling studies. The design parameters of the PWR components are organized into five tables. These tables include reactor core, steam generator, pressurizer, reactor coolant pump, and turbine cycle. The parameters have been mainly extracted from the Ref. [1], Westinghouse documentation [15], and water and steam thermodynamic tables.

Table A.1 : Reactor Design Parameters

Parameter	Value
1. Core Diameter (<i>inches</i>)	119.7
2. Core Height (<i>inches</i>)	144
3. First Delay Neutron Group Fraction	0.000209
4. Second Delay Neutron Group Fraction	0.001414
5. Third Delay Neutron Group Fraction	0.001309
6. Fourth Delay Neutron Group Fraction	0.002727
7. Fifth Delay Neutron Group Fraction	0.000925
8. Sixth Delay Neutron Group Fraction	0.006898
9. Total Delayed Neutron Group Fraction	0.006898
10. First Group Decay Constant (1/sec)	0.0125
11. Second Group Decay Constant (1/sec)	0.0308
12. Third Group Decay Constant (1/sec)	0.1140
13. Fourth Group Decay Constant (1/sec)	0.307
14. Fifth Group Decay Constant (1/sec)	1.19
15. Sixth Group Decay Constant (1/sec)	3.19
16. Moderator Coefficient of Reactivity (1/oF)	-2.0×10^{-4}
17. Fuel Coefficient of Reactivity (1/oF)	-1.1×10^{-5}
18. Prompt Neutron Generation Time (sec)	1.79×10^{-5}
19. Nominal Power Output (mwt)	3436
20. Fraction of Total Power Generated in Fuel	0.974
21. Coolant Volume in Upper Plenum (ft^3)	1376
22. Coolant Volume in Lower Plenum (ft^3)	1791
23. Coolant Volume in Hot Leg Pipings (ft^3)	1000
24. Coolant Volume in Cold Leg Pipings (ft^3)	2000
25. Coolant Volume in Core (ft^3)	540
26. Mass of Fuel (lbm)	222739
27. Total Coolant Mass Flow Rate (lbm/hr)	1.5×10^8
28. Effective Heat Transfer Area (ft^2)	59900
29. Specific Heat Capacity of Fuel (btu/lbm – oF)	0.059
30. Specific Heat Capacity of Moderator (btu/lbm – oF)	1.39
31. Average Overall Heat Transfer Coefficient (btu/lbm – ft^2)	200

Table A.2 : Steam Generator Design Parameters

Parameter	Value
1. Number of U-tubes	3388
2. Tube Outside Diameter (<i>inches</i>)	0.875
3. Tube Metal Thickness (<i>inches</i>)	0.05
4. Height of U-tubes (<i>ft</i>)	35.54
5. Total Height of Steam Generator (<i>ft</i>)	67.67
6. Effective Flow Area in Tube Region (<i>ft</i> ²)	60.87
7. Effective Flow Area in Downcomer Region (<i>ft</i> ²)	32
8. Effective Flow Area in Riser Region (<i>ft</i> ²)	48.7
9. Effective Flow Area in Drum Section (<i>ft</i> ²)	110.74
10. Riser Height (<i>ft</i>)	9.63
11. Primary Water Mass Flow Rate (<i>lbm/hr</i>)	3.939×10^7
12. Volume of Primary Water in Steam Generator (<i>ft</i> ³)	1077
13. Specific Heat Capacity of Primary Water (<i>btu/lbm - oF</i>)	1.39
14. Inlet Temperature of Primary Water (<i>oF</i>)	592.5
15. Outlet Temperature of Primary Water (<i>oF</i>)	542.5
16. Average Pressure in the Primary Side (<i>psia</i>)	2250
17. Average Density of Primary Water (<i>lbm/ft</i> ³)	45.710
18. Outlet Steam Flow Rate (<i>lbm/ft</i> ³)	3.731×10^6
19. Steam Pressure (<i>psia</i>)	849.7
20. Steam Temperature at Saturation Pressure (<i>oF</i>)	521.9
21. Inlet Temperature of Feedwater (<i>oF</i>)	434.3
22. Average Density of Secondary Subcooled Water (<i>lbm/ft</i> ³)	52.32
23. Effective Heat Transfer Area (<i>ft</i> ²)	51500
24. Film Heat Transfer Coefficient of Primary Water in Tubes (<i>btu/lbm - hr</i> ² - <i>oF</i>)	4500
25. Film Heat Transfer Coefficient of Secondary Subcooled Water (<i>btu/lbm - hr</i> ² - <i>oF</i>)	1972
26. Film Heat Transfer Coefficient of Secondary Boiling Water (<i>btu/lbm - hr</i> ² - <i>oF</i>)	6000
27. Metal Tube Conductivity (<i>btu/lbm - hr - oF</i>)	15

Table A.3 : Pressurizer Design Parameters

Parameter	Value
1. Operating Pressure of the Primary Side System (<i>psia</i>)	2250
2. Saturation Temperature (<i>oF</i>)	653
3. Steam Volume at Full Power (<i>ft</i> ³)	720
4. Water Volume at Full Power (<i>ft</i> ³)	1080
5. Initial Water Level (<i>ft</i>)	28.06
6. Effective Cross Section Area (<i>ft</i>)	38.48
7. Average Density of Water (<i>lbm/ft</i> ³)	37.06
8. Steam Density (<i>lbm/ft</i> ³)	6.45
9. Electric Heater Output (<i>kwt</i>)	1800
10. Continuous Spray Flow Rate (<i>gpm</i>)	1.0
11. Specific Heat Capacity of Saturated Water (<i>btu/lbm – oF</i>)	2.12
12. Gain Factor of the Heater PID Controller (<i>kwt/psi</i>)	-250
13. Time Constant of the Heater PID Controller (<i>sec</i>)	900

Table A.4 : Coolant Pump Design Parameters

Parameter	Value
1. Design Operating Pressure (<i>psig</i>)	2485/2235
2. Design Operating Temperature (<i>oF</i>)	650
3. Pump Speed at Nameplate Rating (<i>RPM</i>)	1190
4. Water Suction Temperature (<i>oF</i>)	539
5. Volume Flow Rate Capacity (<i>gpm</i>)	87500
6. Pump-Motor Moment of Inertia (<i>lb – ft</i> ²)	82000
7. Input Power to the Pump (<i>hp</i>)	6000
8. Pump Water Volume Capacity (<i>ft</i> ³)	56
9. Developed Head at Full Power (<i>ft</i>)	282
10. Total Pressure Drop in the Primary Loop (<i>psi</i>)	91.5

Table A.5 : Turbine Cycle Design Parameters

Parameter	Value
1. Steam Flow Rate to the Nozzle Chest (<i>lbm/sec</i>)	3959.5
2. Steam Flow Rate Leaving the Reheater Shell Side (<i>lbm/sec</i>)	2852.8
3. Steam Flow Rate to the Reheater Tube Side (<i>lbm/sec</i>)	186.4
4. Drain Water Flow Rate from Moisture Separator (<i>lbm/sec</i>)	358.1
5. Total Feedwater Flow Rate (<i>lbm/sec</i>)	4145.9
6. Fraction of Steam Extracted from high Pressure Turbine to the High Pressure Feedwater Heater	0.1634
7. Fraction of Steam Extracted from Low Pressure Turbine to the Low Pressure Feedwater heater	0.2174
8. Fraction of Steam Bypassed from Main Steam Pipe to the Low Pressure Feedwater Heater	0.219
9. Heat Transfer Time Constant in the High Pressure Feedwater Heater (<i>sec</i>)	40
10. Heat Transfer Time Constant in the Low Pressure Feedwater Heater (<i>sec</i>)	100
11. Flow Time Constant in Low Pressure Turbine (<i>sec</i>)	10
12. Flow Time Constant in High Pressure Turbine (<i>sec</i>)	2
13. Flow Time Constant in Steam Reheater (<i>sec</i>)	3
14. Average Rate of Heat Transfer in High Pressure Feedwater Heater (<i>btu/lbm</i>)	1122.65
15. Average Rate of Heat Transfer in Low Pressure Feedwater Heater (<i>btu/lbm</i>)	863.76
16. Specific Heat Capacity of Steam in Steam Reheater (<i>btu/lbm – oF</i>)	21.6
17. Heat Transfer Rate in Reheater (<i>mwt</i>)	226.43
18. Total Volume of the Reheater Shell Side (<i>ft³</i>)	2000
19. Total Volume of the Nozzle Chest (<i>ft³</i>)	200
20. Low Pressure Turbine Efficiency	0.86
21. High Pressure Turbine Efficiency	0.86
22. Design Operating Pressure of Condenser (<i>psia</i>)	1.0
23. Condenser Hotwell Volume (<i>gal</i>)	15000
24. Turbine Shaft Speed (<i>rpm</i>)	3600

APPENDIX B

U-TUBE STEAM GENERATOR MODEL FORMULATION

This appendix presents the theoretical model of a U-tube steam generator. The model is based on Ali's detailed model for the U-tube steam generators [3]. The final form of the model equations are described in this appendix. For more details about the derivation of equations, the reader is referred to Ali's dissertation [3].

A schematic diagram of the model is shown in Fig B.1. The definitions of the model variables are presented in Table B.1.

Governing Equations of The U-Tube Steam Generator

Primary Side Equations

Inlet Plenum

$$\frac{dT_{pi}}{dt} = \frac{W_{pi}}{M_{pi}}(\theta_i - T_{pi}) \quad (B.1)$$

U-Tube Primary Lump Equations

First node

$$\frac{dT_{p1}}{dt} = \frac{W_{pi}}{\rho_{pi}A_pL_{s1}}(T_{pi} - T_{p1}) + \frac{U_{pm}S_{pm1}}{M_{p1}C_{p1}}(T_{m1} - T_{p1}) \quad (B.2)$$

Second node

$$\frac{dT_{p2}}{dt} = \frac{W_{pi}}{\rho_{pi}A_pL_{s2}}(T_{p1} - T_{p2}) + \frac{U_{pm}S_{pm2}}{M_{p1}C_{p1}}(T_{m2} - T_{p2}) + \frac{(T_{p2} - T_{p1})}{L_{s2}} \frac{dL_{s1}}{dt} \quad (B.3)$$

Third node

$$\frac{dT_{p3}}{dt} = \frac{W_{pi}}{\rho_{pi}A_pL_{s1}}(T_{p2} - T_{p3}) + \frac{U_{pm}S_{pm2}}{M_{p1}C_{p1}}(T_{m3} - T_{p3}) \quad (B.4)$$

Fourth node

$$\frac{dT_{p4}}{dt} = \frac{W_{pi}}{\rho_{pi}A_pL_{s2}}(T_{p1} - T_{p2}) + \frac{U_{pm}S_{pm1}}{M_{p1}C_{p1}}(T_{m4} - T_{p4}) + \frac{(T_{p3} - T_{p4})}{L_{s1}} \frac{dL_{s1}}{dt} \quad (B.5)$$

Outlet Plenum

$$\frac{dT_{po}}{dt} = \frac{W_{pi}}{M_{po}}(T_{p4} - T_{po}) \quad (B.6)$$

Metal Tube Equations

First node

$$\begin{aligned} \frac{dT_{m1}}{dt} = & \frac{U_{pm}S_{pm1}}{M_{m1}C_m}T_{p1} - \frac{U_{pm}S_{pm1} + U_{ms1}S_{ms1}}{M_{m1}C_m}T_{m1} + \\ & \frac{U_{ms1}S_{ms1}}{M_{m1}C_m} \frac{(T_d + T_{sat})}{2} + \frac{(T_{m2} - T_{m1})}{2L_{s1}} \frac{dL_{s1}}{dt} \end{aligned} \quad (B.7)$$

Second node

$$\begin{aligned} \frac{dT_{m2}}{dt} = & \frac{U_{pm}S_{pm2}}{M_{m2}C_m}T_{p2} - \frac{U_{pm}S_{pm2} + U_{ms2}S_{ms2}}{M_{m2}C_m}T_{m2} + \\ & \frac{U_{ms2}S_{ms2}}{M_{m2}C_m}T_{sat} + \frac{(T_{m2} - T_{m1})}{2L_{s2}} \frac{dL_{s1}}{dt} \end{aligned} \quad (B.8)$$

Third node

$$\begin{aligned} \frac{dT_{m3}}{dt} = & \frac{U_{pm}S_{pm2}}{M_{m2}C_m}T_{p3} - \frac{U_{pm}S_{pm2} + U_{ms2}S_{ms2}}{M_{m2}C_m}T_{m3} + \\ & \frac{U_{ms2}S_{ms2}}{M_{m2}C_m}T_{sat} + \frac{(T_{m3} - T_{m4})}{2L_{s2}} \frac{dL_{s1}}{dt} \end{aligned} \quad (B.9)$$

Fourth node

$$\begin{aligned} \frac{dT_{m4}}{dt} = & \frac{U_{pm}S_{pm1}}{M_{m1}C_m}T_{p4} - \frac{U_{pm}S_{pm1} + U_{ms1}S_{ms1}}{M_{m1}C_m}T_{m4} + \\ & \frac{U_{ms1}S_{ms1}}{M_{m1}C_m} \frac{(T_d + T_{sat})}{2} + \frac{(T_{m3} - T_{m4})}{2L_{s1}} \frac{dL_{s1}}{dt} \end{aligned} \quad (B.10)$$

Secondary Side Equations

Subcooled Region Equations

Mass balance

$$\frac{dL_{s1}}{dt} = \frac{(W_1 - W_2)}{\rho_{s1}A_{fs}} \quad (B.11)$$

Energy balance

$$\frac{d}{dt}[\rho_{s1}A_{fs}L_{s1}C_{p2} \frac{(T_d + T_{sat})}{2}] = U_{ms1}P_{r2}L_{s1}(T_{m1} + T_{m4} - T_d - T_{sat}) +$$

$$W_1 C_{p2} T_d - W_2 C_{p2} T_{sat} \quad (B.12)$$

Boiling Region Equations

Mass balance

$$\frac{d}{dt}(\rho_b A_{fs} L_{s2}) = W_2 - W_3 \quad (B.13)$$

$$\frac{d\rho_b}{dt} = -\frac{(K_1 + K_2 \frac{X_e}{2})}{(V_f + \frac{X_e}{2} V_{fg})^2} \frac{dP}{dt} - \frac{V_{fg}}{2(V_f + \frac{X_e}{2} V_{fg})^2} \frac{dX_e}{dt} \quad (B.14)$$

Energy Balance

$$\begin{aligned} \frac{d}{dt}[\rho_b A_{fs} L_{s2}] &= U_{ms2} P_{r2} L_{s2} (T_{m2} - T_{sat}) + U_{ms2} P_{r2} L_{s2} (T_{m3} - T_{sat}) + \\ &W_2 h_f - W_3 h_{ex} \end{aligned} \quad (B.15)$$

Drum Region Equations

Riser/Separator Volume

$$\frac{d}{dt}(V_r \rho_r) = W_3 - W_4 \quad (B.16)$$

$$\frac{d\rho_r}{dt} = -\frac{(K_1 + K_2 X_e)}{(V_f + X_e V_{fg})^2} \frac{dP}{dt} - \frac{V f_g}{(V_f + X_e V_{fg})^2} \frac{dX_e}{dt} \quad (B.17)$$

Drum Water Volume

Mass balance

$$\frac{d}{dt}(\rho_{dw} A_{dw} L_{dw}) = W_{fi} + (1 - X_e) W_4 - W_1 \quad (B.18)$$

Energy balance

$$\frac{d}{dt}(\rho_{dw} A_{dw} L_{dw} T_{dw}) = W_{fi} T_{fi} + (1 - X_e) W_4 T_{sat} - W_1 T_{dw} \quad (\text{B.19})$$

Drum Steam Volume

$$(V_{dr} - A_{dw} L_{dw}) \frac{d\rho_g}{dt} - (\rho_g A_{dw}) \frac{dL_{dw}}{dt} = X_e W_4 - C_l P \quad (\text{B.20})$$

Downcomer Region Equation

$$\frac{dT_d}{dt} = \frac{W_1}{M_d} (T_{dw} - T_d) \quad (\text{B.21})$$

Constitutive Relations

Thermodynamic Properties of Water and Steam

$$h_b = h_f + \frac{X_e}{2} h_{fg} \quad (\text{B.22})$$

$$h_{ex} = h_f + X_e h_{fg} \quad (\text{B.23})$$

$$h_f = X_3 + K_3 P \quad (\text{B.24})$$

$$h_{fg} = X_4 + K_4 P \quad (\text{B.25})$$

$$L_{s2} = L - L_{s1} \quad (\text{B.26})$$

$$T_{sat} = X_5 + K_5 P \quad (\text{B.27})$$

$$V_f = X_1 + K_1 P \quad (\text{B.28})$$

$$V_{fg} = X_2 + K_2 P \quad (\text{B.29})$$

$$W_{st} = C_l P \quad (\text{B.30})$$

$$\rho_b = \frac{1}{V_f + \frac{X_e}{2} V_{fg}} \quad (\text{B.31})$$

$$\rho_r = \frac{1}{V_f + X_e V_{fg}} \quad (\text{B.32})$$

$$\rho_g = X_6 + K_6 P \quad (\text{B.33})$$

Recirculation Loop Equation

$$W_1 = \frac{C_1}{12} [\rho_d (L_{dw} + L_d - L_{s1}) - L_r \rho_r]^{1/2} \quad (\text{B.34})$$

Based on the UTSG model, a computer code called “ UTSG.CSI ” has been developed to perform nonlinear analysis of the steam generator. The code is written in ACSL [19] language and run on a VAX workstation machine. Also, another code called “ UTSG.DAT ” has been developed for linear analysis of the steam generator. It is written in MATRIXx [20] language and run on a VAX workstation machine.

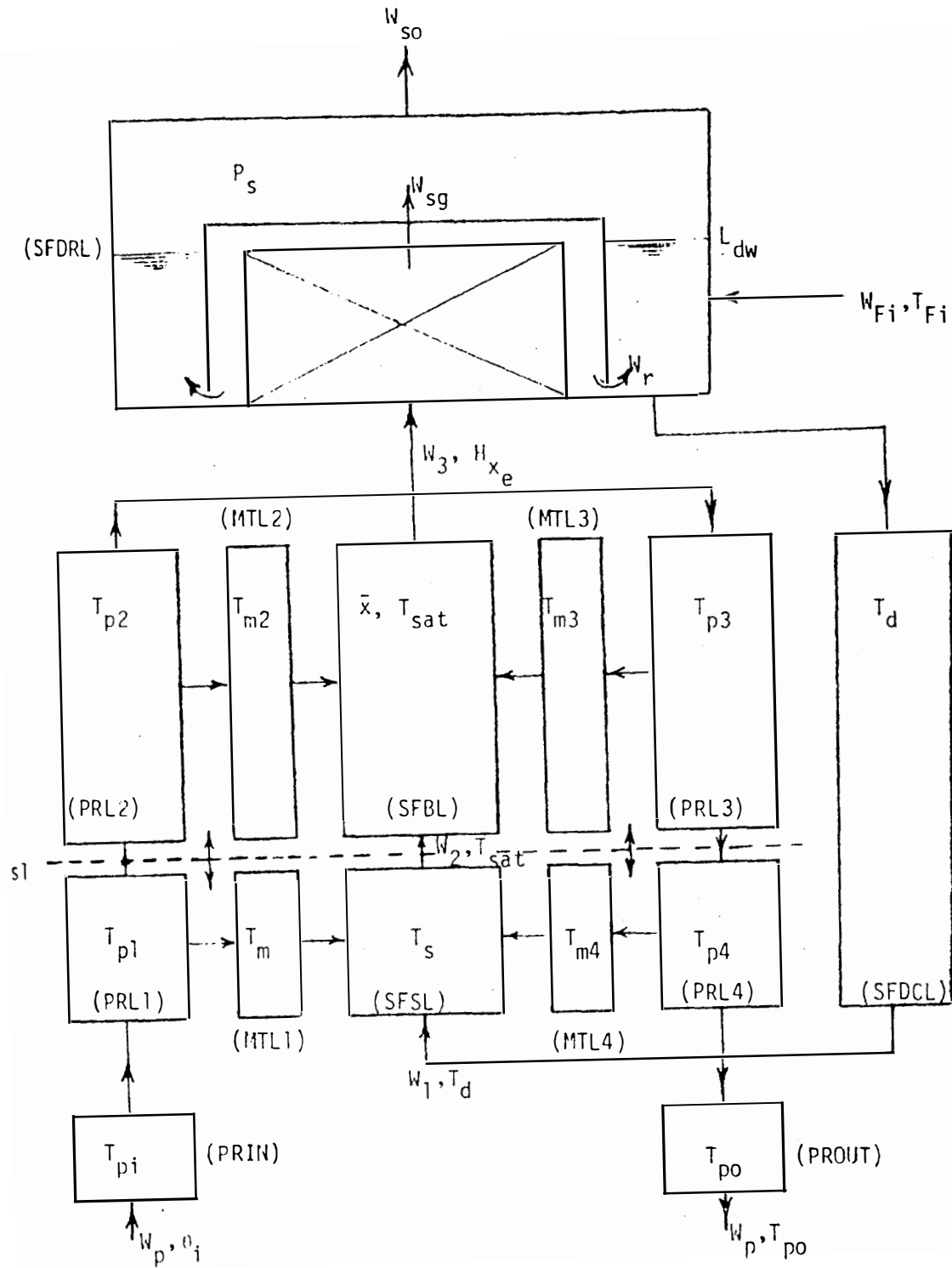


Figure B.1 : Schematic diagram of the steam generator model [3]

Table B.1 : Steam Generator Model Variables

Variable	Definition
1. A_{fs}	Secondary flow area in the U-tube region
2. A_{dw}	Effective area of the drum water section
3. C_1	Effective pressure drop coefficient in the recirculating loop
4. C_l	Steam valve coefficient
5. C_m	Specific heat capacity of the metal tubes
6. $C_{p1,2}$	Specific heat capacity of the primary fluid and subcooled region
7. h_b	Average enthalpy of the boiling region
8. $h_{f,fg}$	Saturated and latent enthalpies of the water
9. h_{ex}	Exit enthalpy of the boiling region
10. K_{1-6}	$\frac{\partial V_f}{\partial P}, \frac{\partial V_{fg}}{\partial P}, \frac{\partial h_f}{\partial P}, \frac{\partial h_{fg}}{\partial P}, \frac{\partial T_{sat}}{\partial P}, \frac{\partial \rho_g}{\partial P}$
11. L	Effective height of U-tubes
12. L_d	Downcomer length
13. L_{dw}	Water level in the steam generator(drum section)
14. $L_{s1,2}$	Subcooled and boiling lengths
15. $M_{m1,2}$	Metal mass in metal nodes (1,2)
16. M_{p1-4}	Mass of water in the the primary nodes (1-4)
17. M_{pi}	Mass of water in the inlet plenum
18. P	Steam generator pressure
19. $P_{r1,2}$	Inside and outside perimeters of the U-tubes
20. $S_{ms1,2}$	Heat transfer areas from the U-tubes to the secondary side in the subcooled and boiling regions respectively
21. $S_{pm1,2}$	Heat transfer areas from the primary side to the U-tubes in nodes (1,2)

Table B.1 (continued)

<i>Variable</i>	<i>Definition</i>
22. T_d	Downcomer temperature
23. T_{dw}	Drum water temperature
24. T_{m1-4}	Metal tube temperatures in nodes (1-4)
25. T_{p1-4}	Primary coolant temperatures in nodes (1-4)
26. T_{pi}	Coolant temperature in the inlet plenum
27. $T_{p\bullet}$	Coolant temperature in the outlet plenum
28. T_{sat}	Saturated temperature of the water and steam in the UTSG
29. U_{pm}	Heat transfer coefficient from the primary side to the metal side
30. $U_{ms1,2}$	Heat transfer coefficient from the metal side to the subcooled and boiling regions
31. V_{dr}	Volume of the drum section
32. $V_{f,g}$	Specific volume of the saturated water and steam
33. V_{fg}	$V_g - V_f$
34. V_r	Volume of the riser region
35. W_{st}	Steam flow rate
36. X_{1-6}	Constant parameters of the water property equations
37. X_e	Exit quality of the steam leaving the boiling region
38. ρ_{\bullet}	Average density of the fluid in the boiling region
39. ρ_g	Density of the saturated steam
40. ρ_r	Density of the fluid in the riser region

APPENDIX C

PRESSURIZER MODEL FORMULATION

The pressurizer model used in this study is similar to the model that Mounir Mneimneh [3] has applied for his work. However, the model is modified by the introduction of steam compressibility as functions of water and steam thermodynamic properties. The Mathematical formulations of the modified model are presented in this appendix. The schematic diagram of the model is shown in Fig. C.1; and definitions of the model variables are presented in Table C.1.

Mass Balance

Liquid Phase

$$\frac{dM_w}{dt} = W_{sg} + W_{sp} - W_{co} \quad (C.1)$$

Steam Phase

$$\frac{dM_s}{dt} = W_{co} \quad (C.2)$$

where

$$M_w = \rho_w A_{pr} L_w \quad (C.3)$$

$$M_s = \rho_s A_{pr} (L - L_w) \quad (C.4)$$

$$\rho_w = X_{p4} + K_{p4} P_{pr} \quad (C.5)$$

$$\rho_s = X_{p5} + K_{p5} P_{pr} \quad (C.6)$$

Equations (C.3-C.6) are substituted into Equations (C.1) and (C.2) in order to derive the following relationships for the water level L_w and condensation (or evaporation) rate (W_{co}).

$$\frac{dL_w}{dt} = \frac{1}{\rho_s A_{pr}} [(A_{pr}(L - L_w)K_{p5} - \frac{C_2}{C_1}) \frac{dP_{pr}}{dt} + \frac{W_{sr}}{C_1} + \frac{W_{co}}{C_1}] \quad (C.7)$$

$$W_{co} = \frac{1}{C_1} (C_2 \frac{dP_{pr}}{dt} - W_{sr} - W_{sp}) \quad (C.8)$$

where

$$C_1 = \frac{\rho_w}{\rho_s} - 1 \quad (C.9)$$

$$C_2 = [A_{pr}(L - L_w) \frac{\rho_w}{\rho_s} K_{p5} + A_{pr} L_w K_{p4}] \quad (C.10)$$

Energy Equation

Liquid Phase

$$\frac{dU_w}{dt} = Q + W_{sr} h_{sr} + W_{sp} h_{sp} - W_{co} h_{fg} - \frac{P_{pr}}{J} \frac{dV_w}{dt} \quad (C.11)$$

or

$$\frac{d}{dt} [M_w (h_f - P_{pr} \nu_f)] = Q + W_{sr} h_{sr} + W_{sp} h_{sp} - W_{co} h_{fg} - \frac{P_{pr}}{J} \frac{dV_w}{dt} \quad (C.12)$$

where

$$\nu_f = X_{p1} + K_{p1} P_{pr} \quad (C.13)$$

$$\nu_g = X_{p2} + K_{p2} P_{pr} \quad (C.14)$$

$$\nu_{fg} = X_{p3} + K_{p3} P_{pr} \quad (C.15)$$

$$h_f = X_{p6} + K_{p6} P_{pr} \quad (C.16)$$

$$h_{fg} = X_{p7} + K_{p7} P_{pr} \quad (C.17)$$

Compressibility Equation

From Section 3 of Chapter 3, we have the following equation:

$$\frac{dP_{pr}}{dt} = - \frac{(X_{p1} + K_{p1}P_{pr})\frac{dM_s}{dt} + (X_{p2} + K_{p2}P_{pr})\frac{dM_w}{dt}}{M_s K_{p1} + M_w K_{p2}} \quad (C.18)$$

Equations (C.13-C.18) are substituted into the equation (C.12) in order to extract a state equation for the pressurizer pressure as follows:

$$\frac{dP_{pr}}{dt} = \frac{NUM}{DEN} \quad (C.19)$$

where

$$NUM = Q + W_{sr} \left(\frac{P_{pr}}{J} \frac{\nu_g}{C_1} + \frac{h_{fg}}{C_1} \right) + W_{sp} \left[h_{sp} - h_f + \frac{h_{fg}}{C_1} + \frac{P_{pr}}{J} \frac{(\nu_g + \nu_{fg})}{C_1} \right] \quad (C.20)$$

$$DEN = M_w \left(K_{p6} + \frac{K_{p2}P_{pr}}{J} \right) + M_{sp} K_{p2} \frac{P_{pr}}{J} - \frac{V_w}{J} + \frac{C_2}{C_1} \left[h_{fg} + \frac{P_{pr}}{J} (\nu_f + \nu_{fg}) \right] \quad (C.21)$$

Therefore, the dynamic behavior of the pressurizer is characterized with two state variables which are pressure and level.

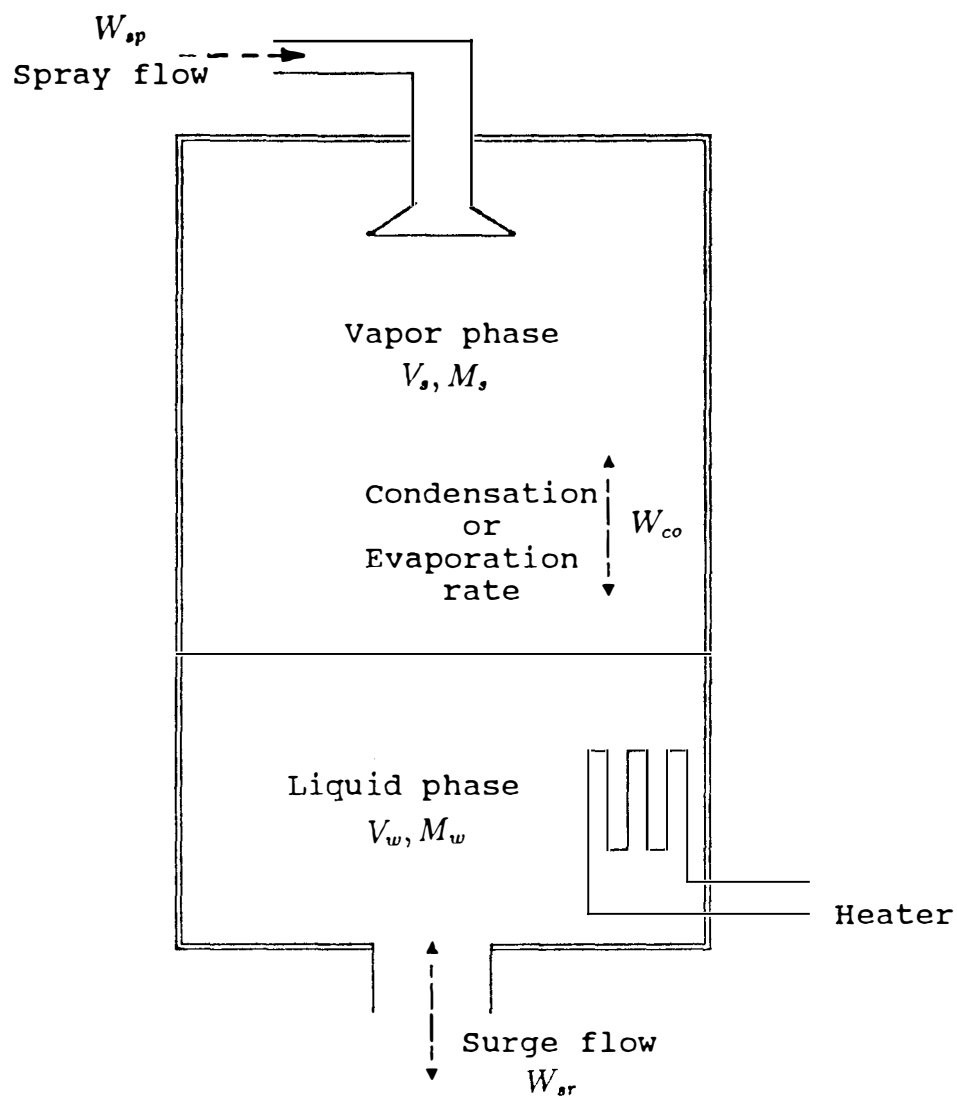


Figure C.1: Schematic diagram of the pressurizer model.

Table C.1: Pressurizer Model Variables.

<i>Variable</i>	<i>Definition</i>
1. A_{pr}	Cross-sectional area of the pressurizer
2. h_f	Saturated water enthalpy
3. h_{fg}	Latent heat of the vaporization
4. h_{sp}	Water enthalpy at the spray nozzle
5. J	Heat conversion factor
6. K_{p1-p6}	$\frac{\partial \nu_f}{\partial P_{pr}}, \frac{\partial \nu_g}{\partial P_{pr}}, \frac{\partial \nu_{fg}}{\partial P_{pr}}, \frac{\partial \rho_s}{\partial P_{pr}}, \frac{\partial \rho_w}{\partial P_{pr}}, \frac{\partial h_f}{\partial P_{pr}}, \frac{\partial h_{fg}}{\partial P_{pr}}$
7. L	Effective pressurizer length
8. L_w	Water level in the pressurizer
9. M_s	Mass of steam in the pressurizer
10. M_w	Mass of water in the pressurizer
11. P_{pr}	Pressurizer pressure
12. W_{co}	Condensation/Evaporation flow rate in the pressurizer
13. W_{sp}	Spray flow rate
14. W_{sr}	In/OutSurge flow rate
15. V_w	Water volume in the pressurizer
16. ν_f	Specific volume of the water
17. ν_g	Specific volume of the steam
18. ν_{fg}	$\nu_g - \nu_f$
19. ρ_s	Steam density in the pressurizer
20. ρ_w	Water density in the pressurizer

APPENDIX D

STEAM TURBINE MODEL FORMULATION

This appendix presents a dynamic model for a nuclear steam turbine cycle. The model has been previously developed by Shanakar [6]. It includes models for the nozzle chest, high pressure turbine, steam moisture separator, steam reheater, low pressure turbine, and high and low pressure feedwater heaters (see Fig 4.1 in Chapter 4). Modifications have been made to reduce the complexity of the model. The efficiencies of high and low pressure turbines have been considered to be constant during operating conditions of the turbine system. Note that the condenser model which has been developed in this study (see Chapter 4) is coupled to the turbine model. The final form of the model equations are given below. The definitions of the model variables are presented in Table D.1.

Governing Equations of the Turbine Model

Nozzle Chest Equations

Mass balance

$$\frac{d\rho_c}{dt} = \frac{W_1 - W_2}{V_c} \quad (\text{D.1})$$

Energy balance

$$\frac{dh_c}{dt} = \left[\frac{W_1 h_s - W_2 h_c}{\rho_c V_c} + \left(\frac{P_c}{J \rho_c^2} - \frac{h_c}{\rho_c} \right) \frac{d\rho_c}{dt} \right] \frac{1}{1 - \frac{k_1}{J}} \quad (\text{D.2})$$

High Pressure Turbine Equation

Mass balance

$$\frac{dW_2''}{dt} = \frac{W_2 - W_{bhp} - W_2''}{\tau_{hp}} \quad (D.3)$$

$$W_{bhp} = K_{bhp} W_2 \quad (D.4)$$

Moisture Separator Equations

$$W_{ms} = (W_2 - W_{bhp}) - W_2' \quad (D.5)$$

$$W_2' = \frac{h_2 - h_f}{h_{fg}} W_2'' \quad (D.6)$$

Reheater Equations

(a) *Main steam*

Mass balance

$$\frac{d\rho_r}{dt} = \frac{W_2' - W_3}{V_r} \quad (D.7)$$

Energy balance

$$\frac{dh_r}{dt} = \left[\frac{Q_R + W_2' h_g - W_3 h_r}{\rho_r V_r} + \left(\frac{P_r}{J \rho_r^2} - \frac{h_r}{\rho_r} \right) \frac{d\rho_r}{dt} \right] \frac{1}{1 - \frac{k_1}{J}} \quad (D.8)$$

(b) *Reheater steam*

Mass balance

$$\frac{dW_{pr1}}{dt} = \frac{W_{pr} - W_{pr1}}{\tau_{r1}} \quad (D.9)$$

Energy balance

$$\frac{dQ_R}{dt} = \frac{H_{et}(W_{pr} + W_{pr1})}{2\tau_{r2}} - \frac{Q_R}{\tau_{r2}} \quad (D.10)$$

Quantitative relations

$$P_R = \rho_r (K_1 h_r - K_2) \quad (D.11)$$

$$W_3 = K_3(P_R \rho_r)^{1/2} \quad (D.12)$$

$$W_{pr} = C_{lb} P_s \quad (D.13)$$

$$T_s = X_{6t} + K_{6t} P_s \quad (D.14)$$

$$T_r = \frac{K_{7t} P_R}{\rho_r} \quad (D.15)$$

Low Pressure Turbine

Mass balance

$$\frac{dW'_3}{dt} = \frac{W_3 - W_{blp} - W'_3}{\tau_{lp}} \quad (D.16)$$

$$W_{blp} = K_{blp} W_3 \quad (D.17)$$

Main Condenser Equations

Mass balance

$$\frac{dM_w}{dt} = W_{c\bullet 1} + W_{c\bullet 3} - W_\bullet \quad (D.18)$$

$$\frac{dW_{c\bullet 3}}{dt} = \frac{W_{c\bullet 2} - W_{c\bullet 3}}{\tau_{c\bullet}} \quad (D.19)$$

Energy balance

$$\frac{dh_o}{dt} = \frac{(W_{c\bullet 1} + W_{co3})(h_f - h_o)}{M_w} \quad (D.20)$$

$$W_{c\bullet 1} = W'_3 - W_{c\bullet 2} \quad (D.21)$$

$$W_{co2} = W'_3 \frac{(h_4 - h_{fco})}{h_{fgco}} \quad (D.22)$$

Feedwater Heater (1) Equation

Energy balance

$$\frac{dh_{fw1}}{dt} = \frac{Q_{h1}}{\tau_{h1} W_{fw}} + \frac{h_o - h_{fw1}}{\tau_{h1}} \quad (D.23)$$

Heat flow relation

$$Q_{h1} = H_{fw1}(W_{hp1} + W_{blp}) \quad (D.24)$$

Feedwater Heater(2) Equation

Mass balance

$$\frac{dW_{hp1}}{dt} = \frac{W_{bhp} + W_{ms} + W_{pr1} - W_{hp1}}{\tau_{h2}} \quad (D.25)$$

Energy balance

$$\frac{dh_{fw2}}{dt} = \frac{Q_{h2}}{\tau_{h1}W_{fw}} + \frac{h_{fw1} - h_{fw2}}{\tau_{h2}} \quad (D.26)$$

Heat flow relation

$$Q_{h2} = H_{fw2}(W_{blp} + W_{ms} + W_{pr1}) \quad (D.27)$$

Output Power Equations

$$h_2 = h_c - \eta_{hp}(h_c - h'_2) \quad (D.28)$$

$$h_4 = h_r - \eta_{lp}(h_r - h'_4) \quad (D.29)$$

$$POWER_{hp} = K_T W_2 (h_s - h_2) \quad (D.30)$$

$$POWER_{lp} = K_T \frac{(W_3 + W'_3)}{2} (h_s - h_4) \quad (D.31)$$

$$POWER_T = POWER_{hp} + POWER_{lp} \quad (D.32)$$

Auxiliary Equations

$$W_1 = C_l P \quad (D.33)$$

$$W_2 = K_a (P_c \rho_c - P_R \rho_2) \quad (D.34)$$

$$X_e = \frac{h_2 - h_f}{h_{fg}} \quad (D.35)$$

$$\rho_2 = \frac{1}{X_e \nu_g + (1 - X_e) \nu_f} \quad (D.36)$$

$$h_s = X_{1t} + K_{1t}P_s \quad (\text{D.37})$$

$$h_f = X_{2t} + K_{2t}P_R \quad (\text{D.38})$$

$$h_{fg} = X_{3t} + K_{3t}P_R \quad (\text{D.39})$$

$$h_g = X_{4t} + K_{4t}P_R \quad (\text{D.40})$$

$$\nu_g = X_{5t} + K_{6t}P_R \quad (\text{D.41})$$

$$P_c = \rho_c(K_1h_c - K_2) \quad (\text{D.42})$$

Callender's Equation

$$h'_2 = 1080.3 + 0.37(P_R - 200) - 0.0011(P_R - 200)^2 - 0.1(P_c - 1000) \quad (\text{D.43})$$

Based on the turbine model, a computer code called “ TURBINE.CSL ” has been developed to perform nonlinear analysis of the turbine cycle system. The code is written in ACSL [19] language and run on a Vax workstation machine.

Table D.1: Turbine Model Variables

Variable	Definition
1. $C_{l,lb}$	Main and bypassed steam valve coefficients.
2. h_2	Enthalpy of steam leaving high pressure turbine.
3. h'_2	Enthalpy of steam at isentropic end point from pressure P_c .
4. h_4	Enthalpy of steam leaving low pressure turbine.
5. h'_4	Enthalpy of steam at isentropic end point from pressure P_r .
6. h_c	Enthalpy of steam leaving nozzle chest.
7. h_f	Enthalpy of saturated water in reheater.
8. h_{fco}	Enthalpy of saturated water in condenser.
9. h_{fg}	Enthalpy of latent water in reheater.
10. h_{fgc}	Enthalpy of latent water in condenser.
11. h_r	Enthalpy of steam at reheater.
12. h_{fw1}	Enthalpy of water in high pressure feedwater heater (HPFH).
13. h_{fw2}	Enthalpy of water in low pressure feedwater heater (LPFH).
14. H_{fw1}	Constant parameter of heat flow in HPFH.
15. H_{fw2}	Constant parameter of heat flow in LPFH.
16. H_{et}	Constant parameter of heat flow in reheater.
17. J	Heat conversion factor.
18. $K_{1,2}$	Constant parameters of steam pressure equation.
19. K_{1t-6t}	Constant parameters of water and steam property equations.
20. K_{7t}	Constant parameter of reheater temperature equation.
21. K_T	Constant parameter of output power equation.
22. K_{bhp}	Fraction of steam extracted from H.P. to HPFH.
23. K_{blp}	Fraction of steam extracted from L.P. to LPFH.
24. Q_R	Heat transfer rate in reheater.
25. P_c	Pressure in nozzle chest.
26. P_r	Pressure in reheater.

Table D.1 (continued)

Variables	Definition
27. P_s	Steam pressure in steam generator.
28. T_R	Steam temperature in reheater.
29. V_c	Volume of nozzle chest.
30. V_r	Volume of reheater.
31. W_1	Steam flow rate passing through the main steam valve.
32. W_2	Steam flow rate leaving nozzle chest.
33. W'_2	Steam flow rate leaving moisture separator.
34. W''_2	Steam flow rate leaving high pressure turbine.
35. W_3	Steam flow rate leaving reheater.
36. W'_3	Steam flow rate leaving low pressure turbine.
37. W_{bhp}	bled steam from high pressure turbine to HPFH.
38. W_{blp}	bled steam from high pressure turbine to LPFH.
39. W_{co1}	Water droplet rate into the condenser hotwells.
40. W_{co2}	Water condensation flow rate.
41. W_{co3}	Steam flow rate in condenser.
42. W_{fw}	Feedwater flow rate.
43. W_{hp1}	Water flow rate from HPFH to LPFH.
44. W_o	Outlet flow rate from condenser to LPFH.
45. W_{pr}	Steam bypassed flow rate to reheater.
46. W_{pr1}	Water flow rate from reheater to HPFH.
47. X_{1t-6t}	Slope of water or steam properties with respect to pressure.
48. ρ_c	Density of steam at nozzle chest.
49. ρ_r	Density of steam at reheater.
50. τ_{co}	Time constant associated with main condenser.
51. $\tau_{h1,h2}$	Time constants associated with HPFH and LPFH respectively.
52. $\tau_{hp,lp}$	Time constant associated with high and low pressure turbines repectively.
53. $\tau_{r1,r2}$	Time constants associated with reheater.

APPENDIX E

COMPUTER PROGRAMS

Based on the models described in Chapters 3-5, the following computer codes have been developed on the ACSL language:

- “CORE.CSL” for the reactor core model
- “UTSG.CSL” for the UTSG model
- “PRESSURIZER.CSL” for the pressurizer model
- “PUMP.CSL” for the reactor coolant pump model
- “PRIMARY.CSL” for the primary loop model
- “SECONDARY.CSL” for the secondary loop model
- “PLANT.CSL” for the overall plant model

These codes have been used to simulate the nonlinear behavior of the above models under steady-state and transient conditions. They are integrated into a software system named “NSPWR”. The software is available at the University of Tennessee, Department of Nuclear Engineering.

For linear analyses of the reactor and UTSG models, two computer codes called “CORE.DAT” and “UTSG.DAT” have been developed respectively. These

codes are written in MATRIXx language and are executed on a VAX workstation machine.

The program “PLANT.CSL” is shown in this appendix. It is executed on a Vax workstation machine as a standrad ACSL code.

```

"*****"
"*****"
"* PROGRAMMER      : MASOUD NAGHEDOLFEIZI      *"
"* OPERATING SYSTEM : VAX WORKSTATION          *"
"* LANGUAGE        : SOFTWARE ACSL             *"
"*****"
"*
"* TITLE           : OVERALL SIMULATION OF A    *"
"*                               PWR PLANT      *"
"*
"* DESCRIPTION      :                          *"
"*
"*      This computer program simulates dynamics of a PWR      *"
"* model. It incorporates models for reactor core,pressurizer,*"
"* steam generator, turbine cycle and their control systems    *"
"* The program consists of 69 state variables and one forcing   *"
"* function (power demand signal). It is executed by the       *"
"* START command in the ACSL code.                             *"
"*
"*****"
"*****"

```

PROGRAM Nuclear PWR Power Plant Simulation

INITIAL

CONSTANT Tmax=400

"=====

```

"*****"
"*      CONSTANT PARAMETERS OF THE REACTOR MODEL      *"
"*****"

```

CONSTANT BETA1 = .000209,BETA2=.001414,BETA3=.001309, ...
 BETA4 = .002727,BETA5=.000925,BETA6=.000314

CONSTANT BETAt = .00689

CONSTANT LANDA1 = .0125,LANDA2 = .0308,LANDA3 = .114, ...
 LANDA4 = .307 ,LANDA5 = 1.19 ,LANDA6 = 3.19

CONSTANT C0 = 4625.71, NGT = 17.9E-6, ALPHAf = -1.1E-05

CONSTANT ALPHAc = -2.0E-04, ALPHAp = -1e-06, Mft = 222739
 CONSTANT Cpf = .059, FR = .974

```

CONSTANT Vup = 1376, Vlp = 1791, Vhl = 1000, Vcl = 2000
CONSTANT Vmo = 540 ,DENSMo = 45.71, Cpmo= 1.39

CONSTANT Bcl=-.0631,Bhl=-.0741

CONSTANT Tpo0=539.5,Tf10=1488.75,Tmo10=548.303,      ...
      Tmo20=557.106,Tf20=1506.38,      ...
      Tmo30=565.909,Tmo40=574.711,Tf30=1523.96,      ...
      Tmo50=583.514,Tmo60=592.5,      ...
      Th10=592.5,Tup0=592.5,Tlp0=539.5,Tcl0=539.5

CONSTANT ROHex0=0.,POWERi=691244.4199,Tset0=566,TOUset=30
CONSTANT Taves0=566,TOUla1=10,TOUla2=5,TOUle=80,AUXCD0=0
CONSTANT Tclp0=539.5,Thlp0=592.5,TOUrt0=4,React=.003375
CONSTANT Pcor0=1.,Pcor10=3.436e9,Wpth=1.57559e8

"END OF REACOTR CORE CONSTANTS"

"=====

"*****
"*          CONSTANT PARAMETERS OF THE UTSG MODEL          *"
"*****

CONSTANT DENSM=530., DENSW=45.710, DENSR0=7.94, DENSD=50.32
CONSTANT DENSDW=47.66, DENSG0=1.8325, DENSS=52.32,DENSB0=13.614

CONSTANT N=3388., Do=.875,Di=.775,L= 35.54,Ls10=3.4517
CONSTANT Ar=48.7, Adw=110.74,Ad=32,Afs=60.67,Lr=9.63,Ldw0=9.63
CONSTANT Ld=35.54,Vp= 1077,Vs= 3332.28,Vr= 468.981,Vdr=4398.706

CONSTANT Th10=592.5,Tpi0=592.5,Tp10=587.36,Tp20=557.4
CONSTANT Tp40=539.5,Tpo0=539.5,Tm10=553.49,Tm20=536.129
CONSTANT Tm40=527.38,Tdw0=504.7,Td0=504.7,Tsat0=521.9,Tfi=434.3
CONSTANT Tfw=434.3,Tp30=542.5,Tm30=529.38

CONSTANT p0= 849.7

CONSTANT Hf=515.2, Hfg=678.3, Vf= .02098,Vfg= .5247,Xe0= .2

CONSTANT K1=3.5e-06, K2=-7.135e-04, K3=.17, K4=-.2, K5=.14
CONSTANT K6=.14, K7=2.37e-03,K9=-.035

CONSTANT X1=402.94,X2=.018,X3=1.13096,X4=370.751,X5=850.04
CONSTANT X6=-.181289,X8=1225.85

```

```

CONSTANT hi= 1.25, hos= .87603, hob= 1.87, Kth= .0088275

CONSTANT Cp1=1.39, Cp2= 1.165, Cm= .11, Cpfw=1.2181

CONSTANT Wfi0=1036.39 , Wpi=10941.6 , W10=5181.95

CONSTANT Cl= 1.2195 , Cd= 4.101486234e-7

CONSTANT TOU = 5, TOU1 = 250, TOU2 = 120

CONSTANT G1 = 65.2, G2= 1.0

CONSTANT Gv=32.2, Wnv=.63, Ztv=3.18

CONSTANT v0=0, u0=0, w0=0, r0=0, m0=0

CONSTANT PI=3.1415

"END OF UTSG CONSTANTS"

"=====

"*****"
"*          CONSTANT PARAMETERS OF THE PRESSURIZER MODEL          *"
"*****"

CONSTANT Apr =38.484, Lwp0=28.06, Lsp0=18.7, Vsp0=720, ...
          Vwp0=1080, Mwp0=40029.65, Msp0=4588.33, ...
          Lp=46.76, Pr0=2250

CONSTANT Hwp0=701.1, Hfgp0=414.8, Hsp=574.36, Hwi0=672.84

CONSTANT ROUwp0=37.064, ROUsp0=6.37267, Vfp0=.02698, ...
          Vgp0=.15692

CONSTANT Kp1=-.008152, Kp2=.00470802, Kp3=.118, Kp4=-.2081, ...
          Kp5=5.9e-6, Kp6=-1.118e-4

CONSTANT Xwp=55.406, Xsp=-4.2203, Xfp=435.6, Xfgp=883.025, ...
          Xvfp=.013705, Xvgp=.40847

CONSTANT J=5.4027

CONSTANT Wsr0=0., Wsp=0.

```

```

CONSTANT Ghe=-250.,Ghe1=-250,TOU1pr=900,TOU2pr=2,AUXpr0=0

CONSTANT Gsp=0,Gsp1=75,TOU3pr=200,TOU4pr=2,AUX0=0

CONSTANT Kpr=0,Pr1=2265,Pr2=2275

"END OF PRESSURIZER CONSTANTS"

"=====

"*****
"*          CONSTANT PARAMETERS OF THE TURBINE MODEL          *"
"*****

CONSTANT  W1t0=3959.5,W2t0=3959.5,W3t0=3311.56,W4t0=2942.9,...
          W5t0=2942.9,W6t0=2303.,Wpr0=186.36,Wpr10=186.36,...
          Whp10=1217.8,Wfw=1036.39

CONSTANT  Kbhpr=.1634,Kblpr=.2174,COF=3.0326 ,LCOF=1.0143, ...
          Cl0=1.2195,Clb0=.219537,K3t=431.435

CONSTANT  TOUh1=65,TOUh2=22,TOU2p=10,TOUw2=2,TOUw3=10, ...
          TOUr2=10,TOUr1=3

CONSTANT  H4t0=1002.1,Hrt0=1269.7,Hct0=1196.1,Hfw10=280.4, ...
          H0t0=69.713,Hfw0=529.15,Vft=.018152,CPfw=1.218, ...
          Tfi0=434.3,H4p=958.4

CONSTANT  ROU2t0=.4,ROUct0=1.7337,ROUrt0=.291, ...
          ROU2p=.4045

CONSTANT  Prt0=160,Pct0=790,P=849.7

CONSTANT  K9=-.035,K10=.53,K11=-.45,K12=.1,K13=-.017, ...
          K14=.14,K15=.85612

CONSTANT  X8=1225.85,X9=251.36,X10=931.8,X11=1180,X12=5.556, ...
          X13=402.94

CONSTANT  HEfw1=475,HEfw2=863.76,Qrt0=216931,KTt=1.414, ...
          HEt=22.589

CONSTANT  K1c=1.27453,K2c=1068.8,J=5.404

```

```

CONSTANT  Vct=200,Vrt=20000,Tmax=200

CONSTANT  MLco=41422.9,  MVco=10360.5

CONSTANT  ETAhp=.861, ETA1p=.861

CONSTANT  K1co=37.74,K2co=32,K3co=1092.8,K4co=13,K5co=1054, ...
          K6co=-18.,K7co=.8833,K8co=.0166

CONSTANT  TOUco=7,Wco0=2072.5,Pco=1.0,Pco0=1.0

CONSTANT  Nt0=60,AUXt0=0,Vt0=0,Wnt=9.75,Zt=.67,Gvt=1.5,...
          G1t=1.65,POWco=1.531525e6,It=199642,TOU1t=4,PI=3.141

"*****"
"*          CALCULATION OF CONSTANT PARAMETERS          *"
"*          IN THE REACTOR CORE                          *"
"*****"

Pcor1  = (Pcor10*3.41)/(3600.*3.)
Hfm    = 200./3600.
Afm    = 59900./3.
Wpt    = Wpth/3600.

LANDA  = BETAt/(BETA1/LANDA1 + BETA2/LANDA2 + BETA3/LANDA3 + ...
          BETA4/LANDA4 + BETA5/LANDA5 + BETA6/LANDA6)

Mf=Mft/3.
Mmo=Vmo*DENSmo/3.
Mup=Vup*DENSmo
Mlp=Vlp*DENSmo
Mhl=Vhl*DENSmo
Mcl=Vcl*DENSmo

TOUmo  = Mmo/(2.*Wpt)
TOUup= Mup/Wpt
TOUlp= Mlp/Wpt
TOUhl= Mhl/Wpt
TOUcl= Mcl/Wpt

"END OF CORE PARAMETERS CALCULATIONS"

"===== "

"*****"

```

```

"*          CALCULATION OF THE CONSTANT PARAMETERS          *"
"*          IN THE UTSG                                     *"
"*****"

```

```

W20  = W10
W30  = W10
W40  = W10
Ls20 = L - Ls10
Mm   = DENSm*N*L*PI*(Do**2-Di**2)/(4*144)
Mm1  = Mm*Ls10/L
Mm4  = Mm1
Mm2  = Mm*(Ls20/L)
Mm3  = Mm2
Sm   = L*PI*Do*N/12
Sms1 = Sm*Ls10/L
Sms2 = Sm*(Ls20/L)
Sms3 = Sms2
Sms4 = Sms1
Spm1 = Sms1*Di/Do
Spm2 = Sms2*Di/Do
Spm3 = Spm2
Spm4 = Spm1
Pr1  = Spm1/Ls10
Pr2  = Sms2/Ls20
Dm   = (Di + Do)/2

Ap   = PI*Di**2*N/(4.*144.)
Mp   = DENSw*Ap*L
Mp1  = Mp*Ls10/L
Mp2  = Mp*Ls20/L
Mp3  = Mp2
Mp4  = Mp1
Ms1  = Afs*DENSs*Ls10

Upm  = 1./(1./hi + (Di*alog(Dm/Di))/(24*Kth) )
Ums1 = 1./(1./hos + (Do*alog(Do/Dm))/(24*Kth))
Ums2 = 1./(1./hob + (Do*alog(Do/Dm))/(24*Kth))

Vpi  = (Vp-Ap*2*L)/2
Mpi  = DENSw*Vpi
Mpo  = Mpi
Md   = DENSd*Ad*Ld

TOUpi = Mpi/Wpi

Hb0  = Hf + Xe0*Hfg/2

```

```

Hxe0 = Hf + Xe0*Hfg
DENSb0= 1/(Vf+Xe0*Vfg/2.)
Lb0   = Ls20

```

```

C1    = 1./SQRT(Cd)
Wr    = (1-Xe0)*W40

```

"END OF UTSG PARAMETERS CALCULATIONS"

"=====

CINTERVAL CINT=2

IALG = 2

END

"=====

```

"*****"
"*              EQUATIONS OF THE MODELS              *"
"*****"

```

DYNAMIC

DERIVATIVE

```

"*****"
"*              1. THE REACTOR MODEL EQUATIONS              *"
"*****"

```

```

ROH = ROHex + ALPHAf*( (Tf1-Tf10)+(Tf2-Tf20)+(Tf3-Tf30) )/3 ...
      + ALPHAac*( (Tmo1-Tmo10)+(Tmo2-Tmo20)+(Tmo3-Tmo30)+
      (Tmo4-Tmo40) + (Tmo5-Tmo50) + (Tmo6-Tmo60) )/6

```

DPcor =(ROH - BETAt)*Pcor/NGT + LANDA*C

DC = BETAt*Pcor/NGT - LANDA*C

DTf1 = (FR*Pcor1*Pcor)/(Mf*Cpf) + (Hfm*Afm)*(Tmo1-Tf1)/(Mf*Cpf)

DTmo1 = ((1-FR)*Pcor1*Pcor)/(Mmo*Cpmo) + (Hfm*Afm)*(Tf1-Tmo1)/ ...
 (Mmo*Cpmo) + (Tlp - Tmo1)/TOUmo

$$DTmo2 = ((1-FR)*Pcor1*Pcor)/(Mmo*Cpmo) + (Hfm*Afm)*(Tf1-Tmo1)/ \dots \\ (Mmo*Cpmo) + (Tmo1 - Tmo2)/TOUmo$$

$$DTf2 = (FR*Pcor1*Pcor)/(Mf*Cpf) + (Hfm*Afm)*(Tmo3-Tf2)/(Mf*Cpf)$$

$$DTmo3 = ((1-FR)*Pcor1*Pcor)/(Mmo*Cpmo) + (Hfm*Afm)*(Tf2-Tmo3)/ \dots \\ (Mmo*Cpmo) + (Tmo2 - Tmo3)/TOUmo$$

$$DTmo4 = ((1-FR)*Pcor1*Pcor)/(Mmo*Cpmo) + (Hfm*Afm)*(Tf2-Tmo3)/ \dots \\ (Mmo*Cpmo) + (Tmo3 - Tmo4)/TOUmo$$

$$DTf3 = (FR*Pcor1*Pcor)/(Mf*Cpf) + (Hfm*Afm)*(Tmo5-Tf3)/(Mf*Cpf)$$

$$DTmo5 = ((1-FR)*Pcor1*Pcor)/(Mmo*Cpmo) + (Hfm*Afm)*(Tf3-Tmo5)/ \dots \\ (Mmo*Cpmo) + (Tmo4 - Tmo5)/TOUmo$$

$$DTmo6 = ((1-FR)*Pcor1*Pcor)/(Mmo*Cpmo) + (Hfm*Afm)*(Tf3-Tmo5)/ \dots \\ (Mmo*Cpmo) + (Tmo5 - Tmo6)/TOUmo$$

$$DTup = (Tmo6-Tup)/TOUup$$

$$DTh1 = (Tup-Th1)/TOUh1$$

$$DTlp = (Tcl - Tlp)/TOUlp$$

$$DTcl = (Tpo - Tcl)/TOUcl$$

```

"*****"
"*      EQUATIONS OF THE REACTOR CORE CONTROL SYSTEM      *"
"*****"

```

$$Tave = (Tcl+Th1)/2.$$

$$DThlp = (Th1-Thlp)/TOUrt$$

$$DTclp = (Tcl-Tclp)/TOUrt$$

$$Tavep = (Thlp+Tclp)/2$$

$$Hst = X8+K9*P$$

$$POWERs = P*Cl*(Hst-CPfw*Tfi)$$

$$DTset = (.19*(POWERs*100./POWERi)+547.-Tset)/TOUset$$

$$DTaves = AUXco$$

$$DAUXco = (Tavep-Taves-(TOUla1+TOUla2)*AUXco+TOUle*...$$

$$(DTclp+DThlp)/2.)/(TOUla1*TOUla2)$$

```
"*****"
"*   SPEED ROD PROGRAM FOR THE REACTOR CORE CONTROL SYSTEM   *"
"*****"
```

PROCEDURAL

```
IF ( ABS(Tset-Taves) .LE. 1)DROHex=0
IF (    (Tset-Taves) .GE. 1)DROHex=8*React*.00689/60.
IF (    (Tset-Taves) .GE. 3)DROHex=React*.00689*...
( 32*(Tset-Taves)-88 )/60.
```

```
IF (    (Tset-Taves) .GE. 5)DROHex=72*React*.00689/60.
IF (    (Tset-Taves) .LE. -1)DROHex=-8*React*.00689/60.
IF (    (Tset-Taves) .LE. -3)DROHex=React*.00689*...
( 32*(Tset-Taves)+88 )/60.
IF (    (Tset-Taves) .LE. -5)DROHex=-72*React*.00689/60.
```

END

ROHexc= ROHex*100/.00689

```
"=====
"*****
"*           2. THE UTSG MODEL EQUATIONS           *"
"*****"
```

```
"*****
"* INLET PLENUM, PRIMARY WATER, METAL TUBE, AND OULET PLENUM *"
"*           EQUATIONS           *"
"*****"
```

$$DTpi = (1/TOUpi)*(Thl -Tpi)$$

$$DTp1 = Wpi*Tpi/(DENS*Ap*Ls1)-(Wpi/(DENS*Ap*Ls1) + \dots \\ (Upm*Spm1)/(Mp1*Cp1))*Tp1 \dots \\ +((Upm*Spm1)/(Mp1*Cp1))*Tm1$$

$$DTp2 = Wpi*(Tp1-Tp2)/(DENS*Ap*(L-Ls1)) \dots \\ -Upm*Spm2*(Tp2-Tm2)/(Mp2*Cp1) -(Tp1-Tp2)*AUX1/(L-Ls1)$$

$$DTp3 = Wpi*(Tp2-Tp3)/(DENS*Ap*(L-Ls1)) \dots \\ -Upm*Spm2*(Tp3-Tm3)/(Mp2*Cp1)$$

```

DTp4 = Wpi*(Tp3-Tp4)/(DENSs*Ap*Ls1) ...
      -Upm*Spm1*(Tp4-Tm4)/(Mp1*Cp1) -(Tp4-Tp3)*AUX1/Ls1

DTpo = (1/TOUpi)*(Tp4 -Tpo)

DTm1 = ( (Upm*Spm1)/(Mm1*Cm) )*Tp1+Td*Ums1*Sms1/(2*Mm1*Cm)...
      -( (Upm*Spm1 + Ums1*Sms1)/(Mm1*Cm) )*Tm1+( Ums1*Sms1/...
      (2*Mm1*Cm) )*(X1 + K5*P)- (Tm1-Tm2)*AUX1/(2*Ls1)

DTm2 = ( (Upm*Spm2)/(Mm2*Cm) )*Tp2-( (Upm*Spm2 + Ums2*Sms2)/...
      (Mm2*Cm) )*Tm2 + ( Ums2*Sms2/(Mm2*Cm) )*(X1 + K5*P)- ...
      (Tm1-Tm2)*AUX1/(2*(L-Ls1))

DTm3 = ( (Upm*Spm3)/(Mm3*Cm) )*Tp3 ...
      -( (Upm*Spm3 + Ums2*Sms3)/(Mm3*Cm) )*Tm3 ...
      +( Ums2*Sms3/(Mm3*Cm) )*(X1 + K5*P)- (Tm4-Tm3)*AUX1/(2*(L-Ls1))

DTm4 = ( (Upm*Spm4)/(Mm4*Cm) )*Tp4+Td*Ums1*Sms4/(2*Mm4*Cm) ...
      -( (Upm*Spm4 + Ums1*Sms4)/(Mm4*Cm) )*Tm4 ...
      +( Ums1*Sms4/(2*Mm4*Cm) )*(X1 + K5*P)- (Tm4-Tm3)*AUX1/(2*Ls1)

"*****"
"*      ALGEBRIC EQUATIONS FOR DECOUPLING THE DIFFERENTIAL      *"
"*      EQUATIONS IN THE SECONDARY SIDE                          *"
"*****"

DEN1  =  (Afs*DENSs*Cp2*(Td +X1+K5*P)/2.)

DEN2  =  (DENSb*Afs*(L-Ls1)*(X5+K4*P)/2.)

K01   =-(K1 + K2*Xe/2.)/(((X2+K1*P) + Xe*(X3 + K2*P)/2. )**2.)

K02   =-(X3+ P*K2)/2*(((X2+K1*P) + Xe*(X3 + K2*P)/2. )**2.)

K03   =-(K1 + K2*Xe)/(((X2+K1*P) + Xe*(X3 + K2*P) )**2.)

K04   =-(X3+P*K2)/( ( (X2+K1*P) + Xe*(X3 + K2*P) )**2.)

K05   =-DENSs*Afs

K06   =( Ums1*Pr2*Ls1*(Tm1+Tm4-Td-X1-K5*P)+W1*Cp2*Td- ...
      Afs*DENSs*Ls1*Cp2*AUX6/2.)/DEN1

K07   =-Cp2*(X1+K5*P)/DEN1

```

K08 $= -Afs * DENSs * Ls1 * Cp2 * K5 / DEN1$
 K09 $= -Afs * (L - Ls1)$
 K010 $= Afs * DENSb$
 K011 $= (Ums2 * Pr2 * (L - Ls1) * (Tm2 + Tm3 - 2 * (X1 + K5 * P))) / DEN2$
 K012 $= (X4 + K3 * P) / DEN2$
 K013 $= -(X4 + K3 * P + Xe * (X5 + K4 * P)) / DEN2$
 K014 $= -Afs * (L - Ls1) * (X4 + K3 * P + Xe * (X5 + K4 * P) / 2.) / DEN2$
 K015 $= Afs * DENSb * (X4 + K3 * P + Xe * (X5 + K4 * P) / 2.) / DEN2$
 K016 $= -Afs * (L - Ls1) * (K3 + Xe * K4 / 2.) / DEN2$
 K017 $= -Vr$
 K018 $= Wfi / (Adw * DENSdw)$
 K019 $= (1 - Xe) / (Adw * DENSdw)$
 K020 $= -W1 / (Adw * DENSdw)$
 K021 $= Wfi * Tfi / (Adw * DENSdw * Ldw)$
 K022 $= (1 - Xe) * (X1 + K5 * P) / (Adw * DENSdw * Ldw)$
 K023 $= -W1 * Td / (Adw * DENSdw * Ldw)$
 K024 $= -Td * DENSdw * Adw / (Adw * DENSdw * Ldw)$
 K025 $= Xe / (K7 * (Vdr - Adw * Ldw))$
 K026 $= -Cl * P / (K7 * (Vdr - Adw * Ldw))$
 K027 $= (X6 + K7 * P) * Adw / (K7 * (Vdr - Adw * Ldw))$
 P1 $= K018 + K019 * W1 + K020$
 P2 $= K019 * (K05 + K010)$
 P3 $= (K017 * K03 + K09 * K01) * K019$

$P4 = (K017 * K04 + K09 * K02) * K019$
 $P5 = K021 + K022 * W1 + K023 + K024 * P1$
 $P6 = K022 * (K05 + K010) + K024 * P2$
 $P7 = K022 * (K017 * K03 + K09 * K01) + K024 * P3$
 $P8 = (K017 * K04 + K09 * K02) * K022 + K024 * P4$
 $P9 = (K025 * W1 + K026 + K027 * P1) / (1 - (K017 * K03 + K09 * K01) * K025 - K027 * P3) \dots$
 $P10 = (K025 * (K05 + K010) + K027 * P2) / (1 - (K017 * K03 + K09 * K01) * K025 - K027 * P3) \dots$
 $P11 = ((K017 * K04 + K09 * K02) * K025 + K027 * P4) / (1 - (K017 * K03 + K09 * K01) * K025 - K027 * P3) \dots$
 $P12 = (K06 + K07 * W1) / (1 - K05 * K07)$
 $P13 = K08 / (1 - K05 * K07)$
 $P14 = (K011 + (K013 + K012) * W1) / (1 - (K02 * K09 * K013 + K014 * K02)) \dots$
 $P15 = (K012 * K05 + (K05 + K010) * K013 + K015) / (1 - (K02 * K09 * K013 + K014 * K02)) \dots$
 $P16 = (K01 * K09 * K013 + K014 * K01 + K016) / (1 - (K02 * K09 * K013 + K014 * K02)) \dots$

"*****"
 "* EQUATIONS OF THE SECONDARY WATER IN UTSG *"
 "*****"

$W1 = C1 * ((DENSd * (Ldw + Ld - Ls1) - (L - Ls1) * DENSb - Lr * DENSr) ** .5) / 12. \dots$
 $W2 = W1 - DENSs * Afs * AUX1$
 $W3 = W2 - Afs * (L - Ls1) * AUX7 + Afs * DENSb * AUX1$
 $W4 = W3 - Vr * AUX8$
 $DLs1 = AUX1$
 $AUX1 = (P12 + P13 * P9 + (P13 * P11 * (P14 + P16 * P9) / (1 - P16 * P11))) / \dots$

```

( (1-P10*P13)-(P13*P11*(P15+P16*P10) )/(1-P16*P11) )

DP      = AUX2

AUX2    = P9 +P10*AUX1 +P11*AUX3

DXe     = AUX3

AUX3    = (P14 +P16*P9 +(P15 + P16*P10)*AUX1)/(1-P16*P11)

DLdw    = AUX4

AUX4    = (Wfi + (1-Xe)*W4 -W1)/(DENSdw*Adw)

DTdw    = AUX5

AUX5    = P5 +P6*AUX1+P7*AUX2 + P8*AUX3

DTd     = AUX6

AUX6    = Md*(Tdw - Td )/W1

DDENSb  = AUX7

AUX7    = K01*AUX2 + K02*AUX3

DDENSr  = AUX8

AUX8    = K03*AUX2 + K04*AUX3

"*****"
"*      THE THREE-ELEMENT CONTROLLER EQUATIONS      *"
"*****"

Dv      = ( (Ldw0-Ldw)-v )/TOU

Du      = G1*( (Ldw0-Ldw)-v )/TOU + v/TOU1

Dw      = G2*(1/TOU1 - G1/TOU)*v + u/TOU2 + G1*G2*(Ldw0-Ldw)/TOU

Dm      = P*Cl-Wfi

Dr      = Gv*(Wnv**2)*(W-W0) + Gv*(Wnv**2)*(M-M0)/TOU2 - ...
          2*Ztv*Wnv*r-Wnv**2*(Wfi-Wfi0)+Gv*G2*Wnv**2*(Cl*P-Wfi)

```

$$DWfi = (r-r0)$$

"=====

"*****"
 "* EQUATIONS OF THE PRESSURIZER MODEL *"
 "*****"

$$ROUsp = Xsp + Kp2*Pr$$

$$ROUwp = Xwp + Kp1*Pr$$

$$Mwp = Lwp*Apr*ROUwp$$

$$Msp = (Lp-Lwp)*Apr*ROUsp$$

$$Vwp = Lwp*Apr$$

$$Hfsr = Xfp + Kp3*Pr$$

$$Hfgp = Xfgp + Kp4*Pr$$

$$Vfp = Xvfp + Kp5*Pr$$

$$Vgp = Xvgp + Kp6*Pr$$

$$Kp7 = (Kp1-ROUwp*Kp2/ROUsp)/ROUsp$$

$$C1p = ROUwp/ROUsp - 1$$

$$C2p = Apr*(Lp-Lwp)*Kp2*ROUwp/ROUsp + Apr*Lwp*Kp1$$

"*****"
 "* CALCULATION OF THE DIFFERENTIAL EQUATIONS (Pressurizer) *"
 "*****"

$$\begin{aligned} DPr = & (Ghe*(AUXpr/TOU1pr+(Pr-Pr0))+Kpr+ \dots \\ & Wsr*(Pr*Vfp/(C1p*J) + \dots \\ & Hfgp/C1p+(Vgp-Vfp)*Pr/C1p)+ \dots \\ & Gsp*(AUX/TOU3pr+(Pr-Pr0))*(Hsp-Hfsr + \dots \\ & Pr*Vgp/(C1p*J)+Hfgp/C1p+(Vgp-Vfp)*Pr/ \dots \\ & (J*C1p)))/(Mwp*(Kp3+Kp5*pr/J)+ \dots \\ & Msp*Kp6*Pr/J-Vwp/J+(C2p/C1p)*(Hfgp+Pr*Vfp/J- \dots \\ & (Vfp-Vgp)*Pr/J)-Ghe*TOU2pr-Gsp*TOU4pr*(Hsp-Hfsr \dots \\ & +Pr*Vgp/(C1p*J)+Hfgp/C1p+(Vgp-Vfp)*Pr/(J*C1p)) \end{aligned}$$

```
DLwp      = ( 1/(ROUsp*Apr) )*( (Apr*(Lp-Lwp)*Kp2-C2p/C1p)* ...
           Dpr + Wsr/C1p + Wsp/C1p )
```

```
"*****"
"*      EQUATIONS OF THE PRESSURIZER CONTROL SYSTEM      *"
"*****"
```

```
Wsp      = Gsp*( AUX/TOU3pr+(Pr-Pr0)+TOU4pr*DPr )
Qhe      = Ghe*( AUXpr/TOU1pr +(Pr-Pr0)+TOU2pr*Dpr )
```

```
DAUXpr   = Pr-Pr0
DAUX      = Pr-Pr0
```

PROCEDURAL

```
IF(Pr .LT. Pr1)GO TO N1
GO TO N4
N1..CONTINUE
Ghe=-250
Gsp=0
Kpr=0
N4..CONTINUE
IF(Pr .GE. Pr1)GO TO N2
GO TO N5
N2..CONTINUE
IF(Pr .GE. Pr2) GO TO N3
Kpr1=Ghe1*( AUXpr/TOU1pr +(pr-Pr0)+TOU2pr*Dpr )
Kpr=Kpr1
Ghe=0.
Gsp=0.
GO TO N6
N3..CONTINUE
Kpr=Kpr1
Ghe=0.
Gsp=Gsp1
N5..CONTINUE
N6..CONTINUE
Gsp2=0.
```

END

```
"*****"
"*      IN/OUT SURGE FLOW RATE EQUATION      *"
"*****"
```


$$Wsr = -(Bcl*(4*Vp/2.+Vcl+Vlp+Vmo/2.)*DTcl + \dots \\ Bh1*(4*Vp/2.+Vh1+Vup+Vmo/2.+Vwp0)*DTh1)$$

```
"*****"
"*          4. TURBINE MODEL EQUATIONS          *"
"*****"
```

$$Clb = .18*Cl$$

$$W1t = (Cl*4 - Clb)*P$$

```
"*****"
"*          NOZZLE CHEST EQUATIONS          *"
"*****"
```

$$W2t = COF*(Pct*ROUct - Prt*ROU2t)$$

$$DHct = ((W1t*Hst - W2t*Hct)/(ROUct*Vct) + \dots \\ ((W1t - W2t)/Vct) * (Pct/(J*(ROUct**2)) \dots \\ -Hct/ROUct))*(1/(1-K1c/J))$$

$$DROUct = (W1t - W2t)/Vct$$

$$Pct = ROUct*(K1c*Hct - K2c)$$

```
"*****"
"*          H.P. EQUATIONS          *"
"*****"
```

$$DW3t = (W2t - Wbhp - W3t)/TOUw2$$

$$Wbhp = Kbhp*W2t$$

```
"*****"
"*          MOSITURE SEPARATOR EQUATIONS          *"
"*****"
```

$$Wmst = (W2t - Kbhp*W2t) - W4t$$

$$W4t = (H2t - Hft)*W3t/Hfgt$$

$$Hft = X9 + K10*Prt$$

$$Hfgt = X10 + K11*Prt$$

$$Hgt = X11 + K12*Prt$$

$$X_{Et} = (H_{2t} - H_{ft}) / H_{fgt}$$

$$ROU_{2t} = 1. / (X_{Et} * V_{gt} + (1 - X_{Et}) * V_{ft})$$

$$V_{gt} = X_{12} + K_{13} * P_{rt}$$

```

"*****"
"*                REHEATER EQUATIONS                *"
"*****"

```

$$DROU_{rt} = (W_{4t} - W_{5t}) / V_{rt}$$

$$DH_{rt} = ((Q_{rt} + W_{4t} * H_{gt} - W_{5t} * H_{rt}) / (ROU_{rt} * V_{rt}) + \dots \\ ((W_{4t} - W_{5t}) / V_{rt}) * (P_{rt} / (J * (ROU_{rt} ** 2)) - H_{rt} / ROU_{rt})) \dots \\ *(1 / (1 - K_{1c} / J))$$

$$P_{rt} = ROU_{rt} * (K_{1c} * H_{rt} - K_{2c})$$

$$W_{5t} = K_{3t} * SQRT(P_{rt} * ROU_{rt})$$

$$DW_{pr1} = (W_{pr} - W_{pr1}) / TOU_{r1}$$

$$DQ_{rt} = H_{et} * (W_{pr} + W_{pr1}) * (T_{st} - T_{rt}) / (2 * TOU_{r2}) \dots \\ - Q_{rt} / TOU_{r2}$$

$$W_{pr} = C_{lb} * P$$

$$T_{st} = X_{13} + K_{14} * P$$

$$T_{rt} = K_{15} * P_{rt} / ROU_{rt}$$

```

"*****"
"*                L.P. EQUATIONS                *"
"*****"

```

$$DW_{6t} = ((1 - K_{b1p}) * W_{5t} - W_{6t}) / TOU_{w3}$$

$$W_{b1p} = K_{b1p} * W_{5t}$$

```

"*****"
"*                CONDENSER EQUATIONS                *"
"*****"

```

$$WV_{co} = W_{6t} * (H_{4t} - H_{fco}) / H_{fgco}$$

```

WLco      = W6t-Wvco

Hfco      = K1co+K2co*Pco

Hgco      = K3co +K4co*Pco

Hfgco     = K5co + K6co*Pco

XEco      = K7co + K8co*Pco

DWco      = (WVco-Wco)/TOUco

DH0t      =( (WLco + Wco )*(Hfco-H0t) )/MLco

"*****"
"*          FEEDWATER HEATER1 EQUATIONS          *"
"*****"

DHfw1     = Qh1/(TOUh1*Wfw*4) + (H0t-Hfw1)/TOUh1

Qh1       = HEfw1*( Whp1 + Wblp)

"*****"
"*          FEEDWATER HEATER2 EQUATIONS          *"
"*****"

DHfw      = Qh2/(TOUh2*Wfw*4) + (Hfw1-Hfw)/TOUh2

DTfi      = (Qh2/(TOUh2*Wfw*4) + (Hfw1-CPfw*Tfi)/TOUh2)/CPfw

Qh2       = HEfw2*(Wblp + Wmst + Wpr1)

DWhp1     = (Wbhp+Wmst+Wpr1-Whp1)/TOU2p

"*****"
"*          TURBINE POWER EQUATIONS              *"
"*****"

H2p       = 1080.3 +.37*(Prt-200)-.0011*(Prt-200)**2-    ...
           0.1*(Pct-1000)

H2t       = Hct-ETAhp*(Hct-H2p)

H4t       = Hrt-ETAlp*(Hrt-H4p)

```

```

POhpt    = KTt*W2t*(Hct-H2t)

POlpt    = KTt*( (W6t+W5t)/2 )*(Hrt- H4t)

POWER     = POhpt+POlpt

"*****"
"*          SPEED CONTROL SYSTEM EQUATIONS          *"
"*****"

DNt       = POWER*778/( ((2*PI)**2)*Nt*It )-...
           POWco*778/( ((2*PI)**2)*Nt*It )

DAUXt     = -G1t*DNt + (Nt0-Nt)/TOU1t

DVt       = (Wnt**2)*Gvt*AUXt-2*Zt*Wnt*Vt-(Wnt**2)*(c1-c10)

Dcl       = Vt

"*****"
"*          INTEGRATION ALGORITHM (Reactor Core)          *"
"*****"

Pcor      = INTVC(DPcor ,Pcor0 )
C         = INTVC(DC      ,C0      )
Tf1       = INTVC(DTf1   ,Tf10   )
Tmo1      = INTVC(DTmo1  ,Tmo10  )
Tmo2      = INTVC(DTmo2  ,Tmo20  )
Tf2       = INTVC(DTf2   ,Tf20   )
Tmo3      = INTVC(DTmo3  ,Tmo30  )
Tmo4      = INTVC(DTmo4  ,Tmo40  )
Tf3       = INTVC(DTf3   ,Tf30   )
Tmo5      = INTVC(DTmo5  ,Tmo50  )
Tmo6      = INTVC(DTmo6  ,Tmo60  )
Tup       = INTVC(DTup   ,Tup0   )
Th1       = INTVC(DTh1   ,Th10   )
Tlp       = INTVC(DTlp   ,Tlp0   )
Tcl       = INTVC(DTcl   ,Tcl0   )
Tclp      = INTVC(DTclp  ,Tclp0  )
Thlp      = INTVC(DThlp  ,Thlp0  )
Tset      = INTVC(DTset  ,Tset0  )
Taves     = INTVC(DTaves ,Taves0 )
AUXco     = INTVC(DAUXco ,AUXco0 )
ROHex     = INTVC(DROHex ,ROHex0 )

```

```

Tp1      = INTVC(DTp1,Tp10)
Tp1      = INTVC(DTp1,Tp10)
Tp2      = INTVC(DTp2,Tp20)
Tp3      = INTVC(DTp3,Tp30)
Tp4      = INTVC(DTp4,Tp40)
Tp0      = INTVC(DTp0,Tp00)
Tm1      = INTVC(DTm1,Tm10)
Tm2      = INTVC(DTm2,Tm20)
Tm3      = INTVC(DTm3,Tm30)
Tm4      = INTVC(DTm4,Tm40)
Ls1      = INTVC(DLs1,Ls10)
P         = INTVC(DP ,P0 )
Xe        = INTVC(DXe ,XE0 )
Ldw      = INTVC(DLdw,Ldw0)
Tdw      = INTVC(DTdw,Tdw0)
Td        = INTVC(DTd ,Td0 )
DENSb    = INTVC(DDENSb,DENSb0)
DENSr    = INTVC(DDENSr,DENSr0)
Wfi      = INTVC(DWfi ,Wfi0 )
v         = INTVC(Dv ,v0 )
u         = INTVC(Du ,u0 )
W         = INTVC(DW ,W0 )
M         =INTVC(DM ,M0 )
r         = INTVC(Dr ,r0 )

```

=====

```
Lwp      = INTVC(DLwp    ,Lwp0   )
Pr       = INTVC(DPr     ,Pr0    )
AUXpr    = INTVC(DAUXpr  ,AUXpr0 )
AUX      = INTVC(DAUX    ,AUX0   )
```

"END OF INTEGRATION PROCESS IN PRESSURIZER MODEL"

"=====

"*****

"* INTEGRATION ALGORITHM (Turbine cycle) *"

"*****

```
ROUct      = INTVC(DROUct ,ROUct0 )
ROUrt      = INTVC(DROUrt ,ROUrt0 )
Hct        = INTVC(DHct   ,Hct0   )
Hrt        = INTVC(DHrt   ,Hrt0   )
W3t        = INTVC(DW3t   ,W3t0   )
W6t        = INTVC(DW6t   ,W6t0   )
Wpr1       = INTVC(DWpr1  ,Wpr10  )
Whp1       = INTVC(DWhp1  ,Whp10  )
Qrt        = INTVC(DQrt   ,Qrt0   )
Hfw1       = INTVC(DHfw1  ,Hfw10  )
Hfw        = INTVC(DHfw   ,Hfw0   )
Tfi        = INTVC(DTfi   ,Tfi0   )
Wco        = INTVC(DWco   ,Wco0   )
H0t        = INTVC(DH0t   ,H0t0   )
Nt         = INTVC(DNt    ,Nt0     )
AUXt       = INTVC(DAUXt  ,AUXt0  )
Vt         = INTVC(DVt    ,Vt0     )
CL         = INTVC(DCL    ,CL0     )
```

END

"*****

"* TERMINATION COMMAND *"

"*****

TERMT(T .GE. Tmax)

END

END

VITA

Masoud Naghedolfeizi was born on May 4, 1961, in Tehran, Iran. He graduated from Tehran Science and Technology University, Tehran, Iran, in February, 1986 with a Bachelor of Science degree in Mechanical Engineering. After a year of employment in a private company, he left Iran for further studies. In August 1988, he entered The University of Tennessee, Nuclear Engineering Department, as a full-time graduate student. He received assistantship for two and half years during which he completed this thesis. In December 1990, he was awarded the Master of Science degree in Nuclear Engineering.